Third Annual Report
of the work of the
Bartol Research Foundation of the
Franklin Institute
Performed under Contract N6ori-144
Task Order 1 - "NR 026-021"
September 30, 1953

THIRD ANNUAL REPORT

of the Work of the

BARTOL RESEARCH FOUNDATION

OF THE FRANKLIN INSTITUTE

Performed Under Contract N6ori-144

Task Order 1 - "NR 026-021"

with the

OFFICE OF NAVAL RESEARCH

W. F. G. Swann, Director

Swarthmore, Pennsylvania

September 30, 1953

TABLE OF CONTENTS

Personnel of the Bartol Research Foundation engaged in the work described in the Third Annual Report under Contract N6ori-144.

W. F. G. Swann, Director*

William E. Danforth, Assistant Director**

Allocation of Staff Personnel:

Cosmic Rays

D. W. Kent [♯]
G. W. McClure [+]
M. A. Pomerantz [***]
D. W. Seymour [♯μ]
T. J. Tidd [ii]

Nuclear Physics

H. O. Albrecht [+]
L. Eisenbud
H. W. Fricke [#μ]
W. F. Gamp [+μ]
R. W. Gunnett, Jr. [+]
W. B. Keighton [#]
C. E. Mandeville [+]
G. W. McClure [+]
R. I. Mendenhall [+m]
F. R. Metzger [+]
W. C. Porter
B. Saraf [γ]
C. P. Swann
W. B. Todd
J. Varma [γ]
G. Watts [#μ]
W. D. Whitehead [+μ]

Investigations of Counters

G. W. McClure [+]
W. C. Porter
W. E. Ramsey [#]

Linear Accelerator

J. F. Marshall [ω]
R. A. Shatas [+]
A. E. Smith [+]

Computing:

E. A. Seaman [+μ]

Shop:

R. C. Pfeiffer, Chief Mechanician [+]
A. G. Nester, Chief Glassblower [+]
G. Faust [+]
F. S. Hockman, Jr. [+]
H. A. Lister [+]
D. A. McCauley [+]
M. A. Parker [+]
D. R. Woodruff [+μ]

* The Director maintains active participation in the projects but receives no part of his salary from the Contract.

** Dr. Danforth also maintains interest in certain parts of the work under the Contract, but receives no part of his salary from this Contract.

*** During the period of this report, Dr. Pomerantz was Visiting Professor of Physics at the Muslim University, Aligarh, U. P., India, under the Fulbright Program, and no part of his salary was charged to this contract.

+ Part time charged to Contract.

Temporary or part-time.

μ Terminated.

ω Dr. Marshall has participated in the development of the linear accelerator in connection with the use of this instrument for another project. No part of his time is charged to this Contract.

γ The work of Mr. Saraf and Mr. Varma is credited to Contract N6ori-144, but no part of their salaries is paid from the contract.

ϕ Part time cosmic-ray work. Time not charged to this contract.

π During the last quarter of the fiscal year of this report Mr. Mendenhall's activities were strictly those of an Administrative Assistant. Consequently, no part of his salary during said last quarter was charged to the contract.

I. COSMIC RADIATION

A. INDIA EXPEDITION

During the entire period covered by this report, an extensive program of investigations of the properties of the cosmic radiation in the upper atmosphere at latitudes near the geomagnetic equator has been conducted successfully. A total of 29 balloon flights were released in India, 14 at Bangalore (geomagnetic latitude 5° N) and 15 at Aligarh (geomagnetic latitude 18° N).

The experiments involved three different types of instrument which are arbitrarily designated as A, B, and C. Types A and B comprise quadruple coincidence counter trains with different geometrical arrangements. These were utilized essentially to obtain, as a function of atmospheric depth, measurements of the intensity of those cosmic-ray particles at very high altitudes having a minimum residual range defined by several different thicknesses of interposed absorber (4 cm, 7.5 cm, 18 cm of lead). Type C, which consists of a coincidence counter train containing an interposed high pressure ionization chamber, was designed to provide information regarding primary alpha-particles. The various individual experiments will be described in somewhat greater detail in separate sections

subsequently, although it is emphasized at the outset that most of the final conclusions must await the completion of detailed analyses which are at present in progress.

The cooperation of several Institutions and Organizations rendered feasible the performance of these experiments in India. The development and construction of the instruments, and the acquisition since the inception of this balloon-flight program at the Bartol Research Foundation of the considerable amount of equipment and supplies which it was necessary to ship to India, were made possible by the support of the Office of Naval Research through Contract N6ori-144. The India Expedition was sponsored by the National Geographic Society, under whose generous auspices all our previous field trips have been conducted. The home base for the operations in India was at Muslim University, Aligarh, Uttar Pradesh, where the author was privileged to occupy the post of Visiting Professor under the Fulbright Program. The rather considerable assistance which was required to carry out this work was provided by graduate students of the Physics Department, of which Professor P. S. Gill is Chairman. The participation by the University, and the great interest of the Vice Chancellor, Dr. Zakir Hussain, are gratefully acknowledged. The flights at Bangalore were conducted at the Indian Institute of Science, where facilities and assistance were kindly furnished by the Physics Department, of which Professor R. S. Krishnan is Chairman. Various arrangements were made by

the United States Educational Foundation in India of which Dr. Olive I. Reddick is Executive Secretary. Appreciation is hereby expressed to all of the above, as well as to the many individuals, too numerous to mention, from sweepers on up, who helped in one way or another.

1.) A FLIGHTS

a) Description of Apparatus.

The type A instruments have previously been described in detail[1]. Numerous measurements[2] had already been

---

1) M. A. Pomerantz, Electronics 24, 88 (1951).

2) M. A. Pomerantz and G. W. McClure, Phys. Rev. 86, 536 (1952). This article contains references to earlier publications.

---

obtained with this standard apparatus at Swarthmore, Pa. (geomagnetic latitude 52° N) and Churchill, Manitoba (geomagnetic latitude 69° N). The advantages of making observations at low latitudes with identical instruments, the reliability of which are insured by long experience with their operation, are obvious. The sole change introduced into this series of instruments was the substitution of a storage battery power-supply in place of the dry batteries utilized previously. This proved to be a tremendous advantage in view of the particular conditions which were encountered in

the field and the difficulties which would have otherwise arisen in attempting to maintain an adequate supply of dependable dry cells. A detailed description of the various pre-flight preparations and tests of each instrument will be omitted. However, it is worth mentioning that each completed instrument was carefully tested immediately prior to flight for any indication of high voltage break-down or corona discharge in a plastic vacuum chamber specially constructed for this purpose.

Information regarding atmospheric pressure, temperature within the gondola, and cosmic-ray counts were transmitted by radio, as in the past.

b) Results.

Intensity vs. Altitude curves were obtained with vertical coincidence counter trains of type A containing 4.0 cm of Pb and 7.5 cm of Pb, respectively. Data recorded in separate flights were in satisfactory agreement. The composite results, obtained by combining all of the data recorded in a specific altitude interval during both ascent and descent of the several individual instruments, are plotted in Figures 1 and 2. Measurements of the intensity in the horizontal direction were also obtained with type A instruments containing 7.5 cm of Pb.

Inasmuch as the analysis is now in progress, some of the interesting aspects will be only briefly mentioned, and

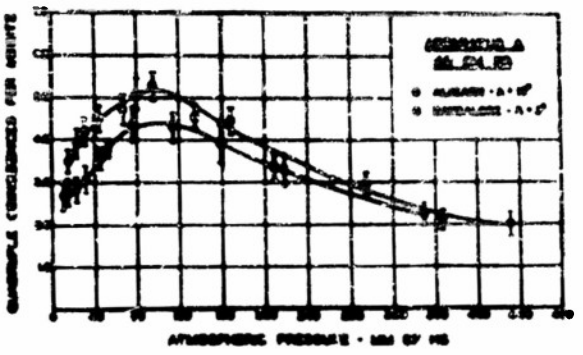

Figure 1. Combined data obtained in India with coincidence-counter train containing 4.0 cm of Pb.

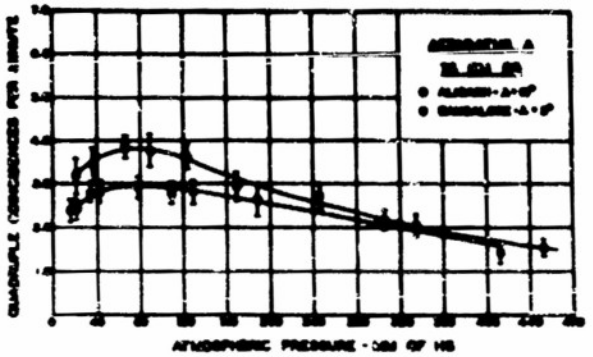

Figure 2. Combined data obtained in India with coincidence-counter train containing 7.5 cm of Pb.

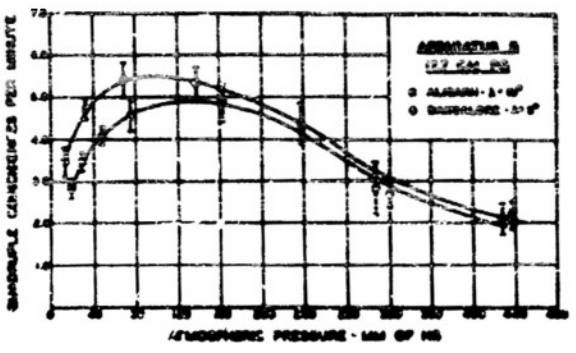

Figure 3. Combined data obtained in India with coincidence-counter train containing 17.7 cm of Pb.

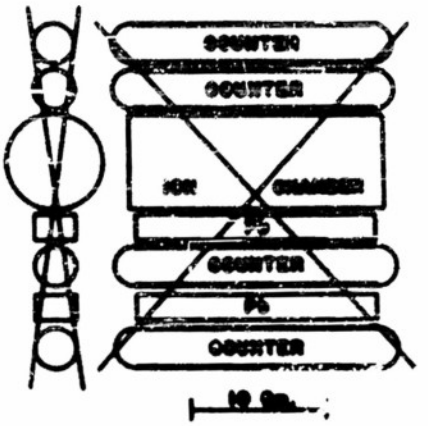

Figure 4a G. M. counter-ionization chamber coincidence train for determination of alpha-particle flux.

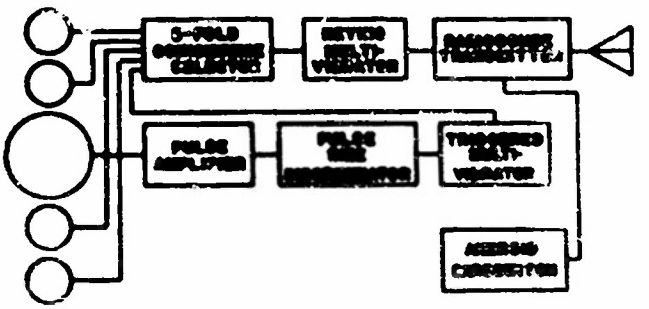

Figure 4b Block diagram showing arrangement of circuits associated with counter-ion chamber coincidence train.

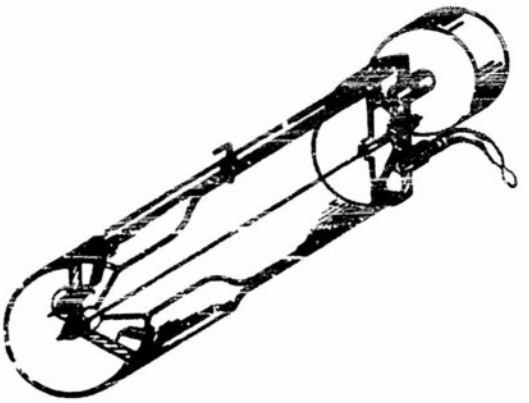

Figure 5. Diagram of high-pressure ionization chamber.

a detailed discussion of the implications will be postponed. The most striking result which is immediately apparent in Figures 1 and 2 concerns the rather pronounced latitude effect which occurs between 18° N and 3° N. Vertical coincidence measurements made by Neher and Pickering[3] in 1939-40

---

3) H. V. Neher and W. H. Pickering, Phys. Rev. 61, 407 (1942)

---

had indicated no difference between the curves at 3° N and 17° N, and this was regarded as direct evidence for a banded structure in the primary cosmic-ray spectrum as predicted by the atom-annihilation hypothesis for the origin of cosmic rays proposed by Millikan, Neher and Pickering[4]. The present

---

4) R. A. Millikan, H. V. Neher, and W. H. Pickering, Phys. Rev. 61, 397 (1942)

---

results are clearly not in accord with this conclusion, but reveal a distinct change of intensity with latitude throughout the upper portion of the atmosphere. Extrapolation of the curves in Figures 1 and 2 to the "top of the atmosphere" indicates that the primary intensity incident in the vertical direction at Aligarh is, in fact, about 43 per cent greater than the intensity at Bangalore. Independent evidence for this change with latitude has also been obtained simultaneously by the group at the Tata Institute[5]. Insofar as their

---

5) A. S. Rao, V. K. Balasubrahmanyam, G. S. Gokhale and A. W. Pereira, Phys. Rev. 91, 764 (1953).

---

measurements are comparable with ours, the results are in good general agreement.

The experiments performed by Winckler et al[6] over a similar range of latitudes, but at different longitudes, yielded a somewhat smaller latitude effect. Table I summarizes the pertinent data regarding absolute particle-intensity and latitude-ratios as determined by different observers. It is of interest to note that the measurements within the atmosphere over India differ from those in the Western Hemisphere in a sense which is opposite to that which would be expected in view of the longitude effect introduced by the eccentricity of the dipole. As a consequence of this effect, the minimum momentum required for a primary to reach the earth in a given direction at the equator is presumably higher in the Eastern Hemisphere than in the Western Hemisphere. Inasmuch as the total unidirectional intensity which reaches a given point decreases as the lowest permitted energy is raised, the absolute intensity in India might be expected to be lower than that at the same geomagnetic latitude in the Western Hemisphere. However, when a reasonable estimate is made of the intensity at the "top of the atmosphere" on the basis of the published experimental

---

6) J. R. Winckler, T. Stix, K. Dwight, and R. Sabin, Phys. Rev. 79, 656 (1950).

TABLE I Absolute Vertical Intensity Measurements Near Geomagnetic Equator

Geomagnetic Latitude	Absolute Intensity Cm^{-2} Sec^{-1} $Sterad^{-1}$	Author	Absorber	Atmospheric Depth
0°	0.027 ± 0.001	W	3 cm Pb	15 g/cm^2
0°	0.031 ± 0.001	W	0	15 g/cm^2
0°	0.028 ± 0.004	V	0	Rocket
3°	0.0227	R	10 cm Pb	Top-Extrapolated
3°	0.030 ± .002	P	4 cm Pb	10 mm Hg
3°	0.028 ± .002	P	7.5 cm Pb	20 mm Hg
3°	0.024 ± .001	P	4 cm Pb	Top-Extrapolated
3°	0.023 ± .001	P	7.5 cm Pb	Top-Extrapolated
19°	0.0364	R	10 cm Pb	Top-Extrapolated
20°	0.031 ± .001	W	3 cm Pb	15 g/cm^2
18°	0.039 ± .002	P	4 cm Pb	10 mm Hg
18°	0.036 ± .002	P	7.5 cm Pb	20 mm Hg
18°	0.035 ± .001	P	4 cm Pb	Top-Extrapolated
18°	0.033 ± .001	P	7.5 cm Pb	Top-Extrapolated

TABLE I (Continued)

Latitude Ratios	Author	Absorber	Atmospheric Depth
$I(19^\circ)/I(3^\circ) = 1.60$	R	10 cm Pb	Top-Extrapolated
$I(20^\circ)/I(0^\circ) = 1.15$	W	3 cm Pb	15 g/cm^2
$I(18^\circ)/I(3^\circ) = 1.28$	P	4 cm Pb	10 mm Hg
$I(18^\circ)/I(3^\circ) = 1.28$	P	7.5 cm Pb	20 mm Hg
$I(18^\circ)/I(3^\circ) = 1.43$	P	4 cm Pb	Top-Extrapolated
$I(19^\circ)/I(3^\circ) = 1.43$	P	7.5 cm Pb	Top-Extrapolated
$I(52^\circ)/I(3^\circ) = 7.4$	P	7.5 cm Pb	Top-Extrapolated

References

W J. R. Winckler, T. Stix, K. Dwight and R. Sabin, Phys. Rev. 79, 656 (1950)

V J. A. Van Allen and S. F. Singer, Phys. Rev. 78, 819 (1950)

R A. S. Rao, V. K. Balasubrahmanyan, G. S. Gokhale, and A. W. Pereira, Phys. Rev. 91, 764 (1953)

P Present author

curves, the apparent discrepancies are considerably reduced. The various values for the primary flux near the geomagnetic equator are then in accord at least with qualitative expectations involving the influence of the eccentricity of the dipole. However, the differences at 18° have not yet been resolved by similar considerations, and evidently represent a real effect.

The region about geomagnetic latitude 18° is characterized by a great uncertainty regarding the contribution of the penumbral region. The statement is usually made[7] that

---

7) M. S. Vallarta, Phys. Rev. 74, 1837 (1948)

---

the penumbral region is practically dark at latitudes below about 15°, so that the main cone which determines the energy limit above which all energies are allowed by the earth's magnetic fields is practically the total allowed cone. Between 15° and 35°, the allowed and forbidden regions of the penumbra are presumed to be of equal importance, but quantitative predictions are exceedingly difficult to propound. Detailed investigation has indicated that at 20° the main cone is still quite important in that only energies higher than that corresponding to it can actually arrive in a vertical direction. At latitudes higher than 35°, the limit is practically defined by the Störmer plus shadow cone, which determine the least energy which a particle must possess to be allowed by the earth's magnetic field. It

is not possible to predict the contribution of the penumbral region to the cosmic-ray intensity measured at 18°. However, it is not expected to be appreciable[8].

---

8) M. S. Vallarta, private communication.

The sole available method for directly determining the energy distribution of the primary cosmic-rays in the field-sensitive band involves the measurement of the primary intensity at various latitudes, and the assignment by geomagnetic theory of a minimum entrance energy (which, for the vertical direction, is independent of the sign of charge, but does depend upon the Z and A of the particles) on the basis of either the Störmer plus shadow cone or the main cone. It had been customary to express the relationship between particle intensity and energy as an empirical power law, simple in some instances, and rather complicated in others. Actually, the data available in the particular latitude range which has been investigated here was quite limited, and on a logarithmic plot, the various suggested laws appear to fit the previously available experimental points more or less. Our results indicate that in a simple power law representation of the form:

$$\int_{E_m}^{\infty} j(E)\, dE = k \left(1 + E_m\right)^{-\gamma} \qquad (1)$$

the minimum value of the exponent γ is 1.8 corresponding to the minimum admittance energy of 11.2 Bev for protons at 18° defined by the Störmer plus shadow cones, and the maximum value is 3.7, corresponding to the admittance energy of 12.5 Bev for protons at 18° defined by the main cone. If past practice is followed, and the contribution by the penumbra is regarded as negligible, the upper limit applies. Even if the lower value of γ were assumed to be the correct one, this is considerably higher than the average value of $\gamma = 1.1$ as determined in the region of lower energies from our measurements at 52° N and 3° N. Thus, there appears to be a departure from the assumed simple power law, and these experiments may indicate the presence of a considerable flux of particles having energies less than that defined by the main cone.

Detailed considerations of the effects of the eccentricity of the dipole may partially account for these results, but it appears that either a departure from the simple power-law spectrum or a contribution from trapped orbits (including albedo) will still be indicated.

There are various other interesting aspects of the data obtained in India. For example, it is observed (Figures 1, 2 and 3) that for all thicknesses of interposed absorber, the intensity vs. altitude curves obtained at low latitudes exhibit a maximum within the atmosphere, whereas at 52° this maximum disappears when the thickness

of lead exceeds 4 cm. As has been discussed previously[2], this is in accordance with expectation. Although there had been some controversy regarding the existence of a maximum in the intensity of the penetrating component at high latitudes[9], the experiments of Pullar and Dymond[10] have

9) M. L. Vidale, Phys. Rev. 88, 266 (1952).

10) J. D. Pullar and E. G. Dymond, Phil. Mag. 44, 565 (1953).

now completely confirmed our earlier observations and conclusions to the effect that no such maximum exists at latitudes north of 52°.

2.) B FLIGHTS

a) Description of Apparatus.

The type B instrument is similar to the type A except for the dimensions of the counter train. The pertinent geometrical data are summarized in Table II. Results obtained with this instrument at 52° N have been published previously[11].

11) M. A. Pomerantz, Phys. Rev. 83, 459 (1951).

TABLE II Summary of Geometrical Factors for Converting Counting Rates to Absolute Particle Intensities

Instrument	Effective length, ℓ cm	Effective width, w cm	Separation, L cm	$\varphi = N(0,h,t)/I(0,h,t)$		
				p = 2	p = 1	p = 0
A	19.4	0.9	11.5	1.23	1.29	1.45
B	19.4	2.3	26.6	2.33	2.50	2.52
C	18.2	3.0	24.7	4.18	4.32	4.50
φ_B/φ_A				1.90	1.94	1.74
φ_C/φ_A				3.40	3.35	3.10
φ_C/φ_B				1.80	1.73	1.78

p is defined by: $I(\theta, h, t) = I(0, h, t) \cos^p \theta$

h is atmospheric depth, and t is thickness of interposed absorber.

b) Results.

Figure 3 is a plot of the data obtained at the two stations in India. The maximum in the intensity vs. altitude curves is quite pronounced, as is the variation with latitude between 18° N and 3° N.

The mean free path of the primary radiation does not change when the minimum energy of the incident protons changes from 1.3 Bev to 13.8 Bev. The present measurements yield a value for the absorption thickness in lead of about 290 g/cm^2 at 52° N, 18° N, and 3° N.

3.) C FLIGHTS

a) Description of Apparatus.

Figure 4 is a schematic diagram of the type C apparatus. The four G. M. counters define the solid angle within which a cosmic-ray particle must travel in order to register. Interposed within the counter train is the high-pressure ionization chamber beneath which is 4 cm of lead. Thus, a particle which can actuate all of the counters must be of relativistic velocity, i.e. it produces ionization at practically its minimum rate, when it passes through the ionization chamber. Singly-charged particles (electrons, mesons, protons) which discharge all four counters produce a pulse of magnitude 1 I_{min}. Owing to the statistical fluctuations in the total number of ions produced in the chamber

by a given particle (Landau spread) and because of the variation in the path-length in the chamber owing to the finite dimensions of the counter train, there is a spread in the pulse heights associated with a particle of specified Z, but the shapes of the distributions are such that essentially no protons and all alpha particles give rise to an amount of ionization exceeding 3 I_{min}. When the apparatus is biased so that coincidences are produced only by particles which give rise to a pulse greater than 3 I_{min} in the ionization chamber, in principle it counts only fast particles of $Z \geq 2$, which are predominantly primary helium nuclei. There are various other types of event which can actuate this apparatus, and these factors must certainly be taken into account. The principal sources of spurious counts are nuclear interactions produced in the lead block by incident protons. Secondaries which travel upward into the ionization chamber can produce a pulse exceeding 3 I_{min}. Certain pertinent information obtained in the Galapagos Expedition by Dr. G. W. McClure, in collaboration with whom the present experiments were performed, will be of great benefit in the analysis of the data obtained in India.

A diagram of the ionization chamber is shown in Figure 5. The chamber is filled with pure argon at a pressure of 300 pounds per square inch. Electron collection is employed.

During the ground-run of each C-flight instrument, an integral pulse-height distribution curve characteristic of the cosmic rays near sea level was obtained in a series of runs with various bias settings. This served to check the operation of the instrument, and yielded a calibration curve for setting the bias to correspond to pulses of ionization exceeding 3 I_{min}. An additional check was provided by the pulses produced by Po-α particles emitted from the probe-source which, as described earlier, can be turned "on or off" by the application of appropriate voltages. The selected bias equivalent to 3 I_{min} corresponds to about .18 Po-alpha.

By means of a pressure-actuated switching arrangement, the total counting rate due to all particles passing through the counter train regardless of the specific ionisation was measured alternatively in the upper atmosphere during some of the flights. The intensity of particles capable of penetrating the same thickness of interposed absorber was also measured by the type A instruments containing 4.0 cm of Pb (Figure 1) and the data confirmed the particular normalisation procedure based upon geometrical considerations which was invoked to utilise the A-flight data in the interpretation of the results obtained with the C-flights.

b) Results.

The desired data were obtained at both 18° N and 5° N, but are not presented herewith pending the completion of the analysis which is required for an adequate discussion of their significance. Preliminary analysis has indicated that at the equator alpha-particles constitute at least 30% of the incident primary intensity. The method permits the determination of upper and lower limits. However, it is interesting to note that the lower limit at the equator is considerably higher than that which has been indicated by observations involving photographic emulsions[12] at higher

---

12) C. Goldfarb, H. L. Bradt, and B. Peters, Phys. Rev. Phys. Rev. 77, 751 (1950).

---

latitudes. Furthermore, the present results are not in accord with those of the only published previous attempt to derive information regarding the alpha-particles at the geomagnetic equator[13].

---

13) S. F. Singer, Phys. Rev. 80, 47 (1950).

B. PHOTOGRAPHIC PLATE EXPOSURES

A program for studying the distribution in mass of heavy primary nuclei of the Cosmic Radiation was outlined in the Second Annual Report. An expedition similar to that described in the report was made during last summer to the region of the geomagnetic pole. It was decided by the naval personnel concerned that only one flight should be attempted, and that emphasis should be placed on waiting for favorable conditions for launching and assurance of recovery. Thus, it was intended that a small number of emulsion packets, comprising the major portion of the balloon-load, might be successfully flown and recovered in the vicinity of the geomagnetic pole. Two packets, each containing thick electron-sensitive emulsions on glass backings were prepared as described in the last report and delivered to the USS Staten Island in Boston last July. In September we were informed by the director of the project that wind conditions were too unfavorable at launching opportunities available in the scheduled operations of the entire task force, and the balloon was not flown. One packet was returned to us and is being used for tests in processing techniques, since background of radiation accumulated at sea level prohibits use of the plates on subsequent flights.

A second set of plates was sent with Dr. McClure on the expedition to the geomagnetic equator described elsewhere in this report. The particular advantage of obtaining a high altitude flight at the equator is apparent from the fact that in no case will a heavy primary nucleus penetrate the earth's magnetic field if its energy is less than 10 Bev/nucleon at this latitude. A particle having an energy greater than 3.5 Bev/nucleon will have a specific energy-loss in nuclear emulsion which is essentially independent of velocity, and proportional to Z^2, where Z is the atomic number. Measurement of the linear density of δ -ray production along the trajectory of a particle traversing the emulsion will thus give a direct measure of the charge and hence the mass of the particle.

Each of the two packets sent on this expedition were flown, but in both cases the balloon failed to reach the minimum altitude required to obtain an appreciable flux of heavy primaries.

C. IONIZATION SPECTRUM OF THE PRIMARY COSMIC RADIATION AT $\lambda = 10^{\circ}$ N

Experiments described elsewhere in this report have been performed at several latitudes ($\lambda = 3^{\circ}$ N, 18° N and 52° N) with a balloon-borne instrument designed to measure the intensity of the α-particle component of the primary cosmic radiation. This instrument utilizes a G-M counter train with an interposed ionisation chamber which is biased to respond only to those particles whose specific ionisation is greater than 3 I_o. (Throughout this note I_o refers to the minimum ionisation of a singly-charged particle.) An instrument of this type counts α-particles -- whose minimum ionisation is 4 I_o -- and heavier nuclei with nearly 100 per cent efficiency and excludes protons and other singly-charged particles with the exception of: 1) a certain calculable fraction of the latter which can produce pulses $> 3\ I_o$ by large statistical fluctuations in ionisation, and 2) an unknown fraction which might produce ionization greater than 3 I_o by undergoing nuclear interactions in the telescope. The most pessimistic estimate of the contribution of effect (2) -- calculated on the basis of geometrical cross sections for proton collisions in the telescope material -- showed that protons might be responsible for a substantial fraction of the counted events, and that the instrument might therefore give an erroneously large indication of the intensity of particles with $Z \geq 2$.

In order to investigate the production of local showers, a modified instrument with a shower detector and a special recorder for obtaining a complete ionization spectrum was constructed. This instrument and the results obtained with it in a recent flight at $\lambda = 10^{\circ}$ N geomagnetic latitude are described herewith.

Apparatus

A diagram of the modified counter telescope is shown in Fig. 1. The telescope is essentially the same as those used in the earlier experiments except that the over-all length is slightly increased and a shower detector, S, composed of seven small G-M counters, is inserted directly below the ionization chamber. A cathode-ray tube oscilloscope and recording camera built into the air-borne gondola record each ionization chamber pulse associated with the quadruple coincidence $C_1C_2C_3C_4$. When less than two of the counters of tray S accompany a telescope event $C_1C_2C_3C_4$ the associated ion chamber pulse appears on a 50μ sec. time-base giving a complete display of the shape as well as the amplitude of the pulse. When two or more counters of tray S are discharged simultaneously with the main telescope discharge, the oscilloscope sweep circuit is rendered inoperative but the sweep-intensifier circuit operates in the normal way so that the ion chamber pulse appears as a vertical trace with no horizontal extension. Events of this second type are designated as shower events, and are easily identified as such on the film record by the distinctive appearance of the pulses.

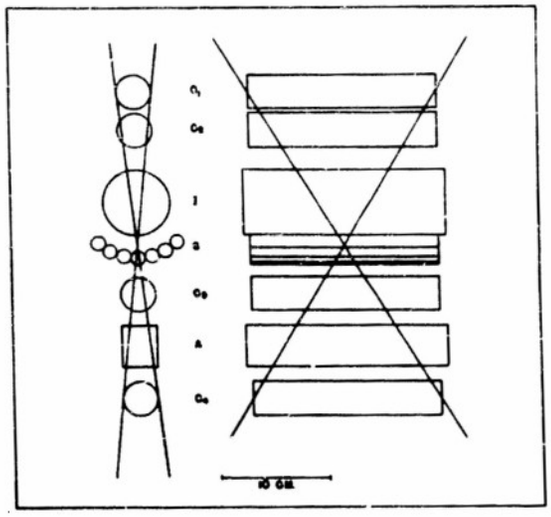

Fig. 1. Instrument for determining the specific ionization of cosmic rays. $C_1C_2C_3C_4$ - G-M counters, I-ionization chamber, S-shower counters, A-4 cm Pb absorber.

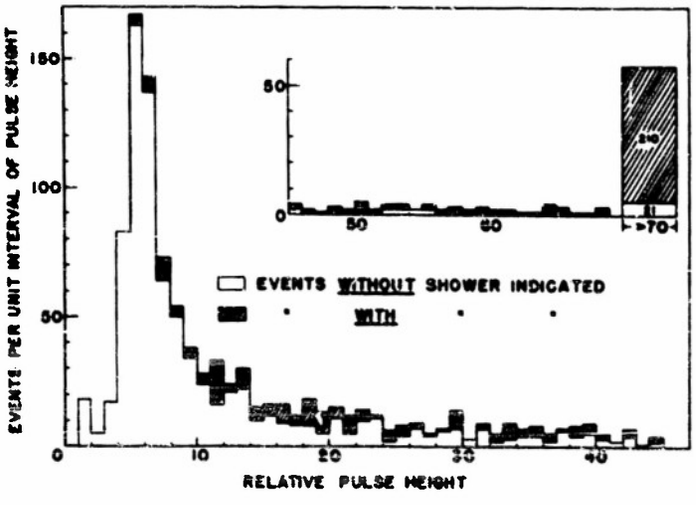

Fig. 2. Differential size distribution of ion chamber pulses accompanying quadruple coincidences ($C_1C_2C_3C_4$). Atmospheric pressure: 12.5 mm Hg. Time: 255 min., Total counts: 1294

The 4 cm Pb absorber A stops slow protons and other singly-charged particles whose specific ionizations are greater than 2 I_o and thus prevents such particles from contributing (except by large ionization fluxuation) to the realm of ionizing events $> 3\ I_o$ which is "reserved" for α-particle and heavy nucleus events.

A thermometer registering the gondola temperature and a mercury manometer which registers atmospheric pressures in the range 0 - 70 mm Hg were photographed at five-minute intervals throughout the flight. In the lower part of the atmosphere, pressure readings were obtained by means of a radiosonde baro-switch which operated a flashing light so as to mark the film record at known pressure-intervals. Another flashing light impressed time-markers upon the film record at one-minute intervals.

In flight, the instrument was housed in an air-tight aluminum sphere covered with two pliofilm bags. With this arrangement the temperature of the gondola remained above 10° C during a period of four hours at 90,000 feet.

The ionization chamber has an effective volume measuring 7 1/2" X 2 1/2" and is filled with argon at a pressure of 300 p. s. i. A more complete description of the chamber together with a pulse-height distribution obtained with sea-level mesons has been published previously[1].

---

1) G. W. McClure, Phys. Rev. 87, 680 (1952)

The differential pulse-height distribution obtained at sea level ($\lambda = 52^{\circ}$ N) agrees quite well with a calculated distribution based on the known meson spectrum and the Landau-Simon[2] theory of ionization fluctuations.

---

2) See e.g. B. Rossi, "High Energy Particles", Prentice Hall (1952)

Experimental Results

The differential pulse-height distribution obtained during a 255 min. level flight at 12.5 mm Hg ($\lambda = 10^{\circ}$ N) is shown in Fig. 2. The shaded blocks represent the distribution of shower-accompanied pulses. As determined by sea-level calibration, the peak of the histogram located at h = 6 corresponds closely to the most probable ionization I_o, of sea-level mesons. This peak can therefore be roughly construed as representing the contribution of relativistic singly-charged particles. A disappointing feature of the histogram is that the principle peak tails-off much more slowly in the pulse-height interval h = 6 to h = 18 -- i.e. in the ionization range I_o to 3 I_o -- than did the sea-level meson distribution and, furthermore, no secondary peak representative of relativistic He nuclei occurs in the neighborhood of h = 24 (4 I_o) as had been anticipated.

The fraction of the recorded events which were accompanied by a shower indication is 0.34. Because of the close

proximity of the shower tray S to the ionization chamber and also the small percentage of shower events in the neighborhood of I_o it would seem that an appreciable fraction of the shower events represent instances in which the ion chamber was traversed by more than one particle. Considering also the fact that not all shower events are detected, it becomes clear that the pulse-height distribution must be interpreted with careful allowance for possible distortion by multiple-particle ionising events.

As the path length through the material above the chamber -- including its upper wall -- constitutes only a small fraction of the geometrical mean free path for nuclear collisions (.052 for protons) one cannot explain the preponderance of shower events as resulting from local nuclear interactions above the chamber. However, if one includes the Pb absorber and counter walls below the chamber, one finds that the total nuclear collision probability is about 0.32 for protons and nearly unity for α-particles. If an allowance is made for the maximum probability of a shower indication resulting from electron knock-on production in the material above the shower tray, the "shower fraction" is reduced from 0.34 to 0.29. It seems likely that most of the remaining shower events result from local nuclear interactions in the telescope material and not to any substantial degree from external air showers, for experiments with out-of-line counter arrangements have shown that air showers can

account for only a few per cent of the counts recorded with ordinary in-line telescopes of the kind used here.

The close agreement between observed fraction of shower-events and the over-all collision probability for protons in the telescope material suggests the possible interpretation that nearly all of the particles counted at 12 mm Hg were protons and that each proton collision in the telescope gave rise to a sufficient number of secondaries to produce a shower indication. This interpretation implies that nuclear interaction in the Pb have a rather high yield of secondaries emerging in the "backward" (upward) direction which are capable of leaving the Pb block.

Although the data do not admit of a very thorough analysis of the various components of the radiation, some rather interesting conclusions may be obtained regarding the intensity of extremely relativistic singly-charged particles relative to the total. In this connection we have computed the distribution of specific ionizations (including fluctuations) of protons with an integral energy-spectrum of the form $E^{-1.5}$ with a low energy cut-off of 14 Mev (the vertical geomagnetic cut-off energy at $\lambda = 10^{0}$). When the computed distribution is plotted on the histogram so that its peak falls at roughly the same position as the maximum of the histogram (pulse-height $h = 6$) it is found that about 5 per cent of the area of the curve lies above $h = 12$. One may therefore take the

number of events below h = 12 in the histogram as the maximum number of events produced by the protons in question except for

1) A 5 per cent correction for large ionisation fluctuations.
2) A 7 per cent correction for pulses rendered larger than 2 I_o by knock-on electron production in the chamber walls.
3) A 32 per cent correction to allow for the possibility that every ray which suffered a nuclear collision in the telescope material above or below the chamber gave rise to a pulse $> 2\ I_o$.

When the above corrections -- all of which are quite conservative -- are made to the number of events $< 2\ I_o$ it is found that protons of the assumed energy spectrum can contribute at most 85 per cent of the total intensity at 12 mm Hg.

From data obtained during the ascent of the flight, counting rate vs. altitude curves have been obtained for ionizing events smaller than 2 I_o and for the total intensity. Extrapolation of these curves to zero pressure indicates that relativistic protons comprise a smaller fraction of the total intensity at the "top of the atmosphere" than at 12 mm Hg. The most conservative estimate of this fraction, gotten by making a liberal allowance for statistical uncertainties of the points upon which the extrapolations depend, indicates

that high energy protons contribute less than 75 per cent of the total primary intensity.

Any attempt to estimate the α-particle contribution to the observed pulse-height distribution is subject to rather grave uncertainties. At 12.5 mm Hg about 40 per cent of the ionizing events are larger than 3 I_o which means that not more than 40 per cent of the radiation can be attributed to α-particles. If one subtracts the maximum possible contribution from proton-induced nuclear disintegrations and other effects which might cause singly-charged particles to yield excessively large pulses, there remain about 1/4 of the events $> 3\ I_o$ (at 12 mm Hg) which must be attributed either to particles with $Z \geq 2$ or to some form of highly ionizing event not accounted for.

The present results indicate that if a good α-flux measurement is to be obtained by the ionization chamber method, it is at least necessary to locate any large absorber at a considerable distance from the chamber so as to reduce the complication introduced by local nuclear disintegrations. It is probably unwise to completely eliminate the absorber because of the possibility of interference by low-energy singly-charged particles.

II. NUCLEAR PHYSICS

A. THE LARGE VAN DE GRAAFF GENERATOR.

Following extensive tests performed on the large Bartol generator built to one-third of its final contemplated height, the complete machine was assembled during November of 1952. Initially, the machine was assembled without the accelerating tube in order to check the electrostatic behavior. Approximately 6 Mv was obtained at 125 psi pressure with tank sparks the limitation. Efforts to go to higher voltages with increased pressure were limited by failure in getting charge from the needles to the belt. Just recently efforts have been made to improve this situation but at that time we went ahead with installation of the accelerating tube.

The tube consists of three sections as described in previous reports. Two sets of baffles were placed in each tube section, thus separating the tube into six sections for suppression of return electrons.

The generator operated very satisfactorily at 5 Mv without any beam -- with the beam the conditions whereby 5 Mv could be obtained resulted in a very weak beam. It was observed that the beam was striking one or more of the baffles, thereby upsetting the voltage distribution on the

machine. From 2 to 3 Mev, however, 15 μa of beam were available after magnetic analysis. Suspecting that stray beam might be the cause of the limitation, a flat baffle with a 3/16 inch diameter hole was inserted just under the focusing electrodes of the ion source. This resulted in a beam of only about 1 μa at the lower voltages but improved the intensity at higher voltages. The hole was then opened to 1/2 inch, resulting in about 3 μa at the lower voltages and about 0.5 μa at 5 Mev. As a result of these tests it became apparent that defocusing of the beam on entering the accelerating tube might be the difficulty. Consequently, a conical baffle with a 1/2 inch hole was put in place of the flat baffle. As a result up to about 4 μa have been obtained at a voltage of 4 Mev. Charging difficulties have made it impossible to achieve higher voltages.

As it may be recalled, 50 μa of unanalyzed beam were obtained in the one-third height test section. This, however, was obtained without the baffles in the tube. When the baffles were installed the current was greatly reduced. At that time the difficulty was attributed to improper operation of the ion source. Although this was in part true, it apparently was not the complete cause.

Several attempts have been made to improve the charging situation. More recently we installed a wire mesh in place of phonograph needles with very poor results. Attempts to

wipe the charge on to the belt were unsuccessful in that the wire mesh used for this purpose broke up when in contact with the belt. Since we have a cotton belt which is quite rough, any further attempts with a mesh seem impracticable unless the belt is changed. We will next attempt use of several rows of needles. If this fails, we might try charging on both sides of the belt.

Some difficulty was encountered in proper stabilization of the generator voltage originally, but this has been recently improved greatly. Stabilization is accomplished in the standard way by taking a D. C. signal from the slits at the output focal point of the analyzing magnet. This is in turn amplified and made to control the grid of a triode controlling the corona from a set of needles facing the central electrode. Originally a relatively low voltage tube was used. It was found that varying the impedance of this tube had very little effect on the corona current. At present we are using the RCA-5890 cathode-ray tube which allows for a 30 Kv swing. For proper operation, however, a 60 Kv tube should be used.

Along with the alterations made above, experimental work has been progressing on the excitation curves for the $Li^7(p,p^1)^*Li^7$ and the $Li^7(p,n)^*Be^7$ reaction. The energy of the gamma rays from the de-excitation of $^*Li^7$ and $^*Be^7$ are 478 and 430 Kev, respectively. A NaI crystal mounted

on a photomultiplier which actuates a pulse-height analyzer is being used to observe the pulse-height distribution. Since the 430 and 478 Kev gamma rays cannot be resolved instrumentally, the shape of the 478 Kev gamma-ray distribution below the threshhold for the formation of $^{*}Be^{7}$ can be used in separating the two gamma rays above the threshhold. Preliminary curves have been taken but no results can be reported at this time.

In addition to this work, the $Li^{7}(p,n)$ reaction is being used as a variable energy neutron source for the study of the excitation curve for the formation of the metastable states in $Hg^{(199)m}$ and $Ba^{(137)m}$. Preliminary studies indicate that the metastable state for $Hg^{(199)m}$ is formed through a higher level while that for $Ba^{(137)m}$ is not.

B. RADIOACTIVITY.

During the past year we were concerned with the study of angular correlations of even--even nuclei and with the development of methods for the investigation of resonance fluorescence of gamma rays.

I. Angular Correlation Measurements.

The even--even nuclei are especially well-suited for angular correlation measurements: all ground states have spin 0+ and 98 per cent of the nuclei have spin 2+ in the first excited state. The only unknown parameters affecting the angular correlation are, therefore, the J-value of the second excited state and the multipole order of the first transition. The angular correlations expected for various values of J_2 differ greatly and can easily be identified experimentally. Due to the spin value 0 in the ground state the second transition is always a pure multipole which means that one never has to consider the mixture--mixture correlations which make the interpretation of angular correlation experiments in odd A nuclei so ambiguous.

The following isotopes were studied:

$Mn^{52} \longrightarrow Cr^{52}$; $Mn^{56} \longrightarrow Fe^{56}$; $As^{76} \longrightarrow Se^{76}$

$Sb^{124} \longrightarrow Te^{124}$.

a) Mn^{52} -- Cr^{52}

Mn^{52} decays into Cr^{52} in a triple cascade. The order of emission of the gamma-rays is known from inelastic proton scattering experiments and from a recent study of the decay $V^{52} \longrightarrow Cr^{52}$.

All three angular correlations have been measured. The analysis in terms of a unique spin assignment to the three excited states of Cr^{52} is under way; it is complicated by the possibility of mixtures in the first two gamma-rays of the triple cascade.

b) Mn^{56} -- Fe^{56}

The decay scheme of Mn^{56} is given in Figure 1. Using pulse-height selection for both detectors it was possible to separate the contributions of the different cascades.

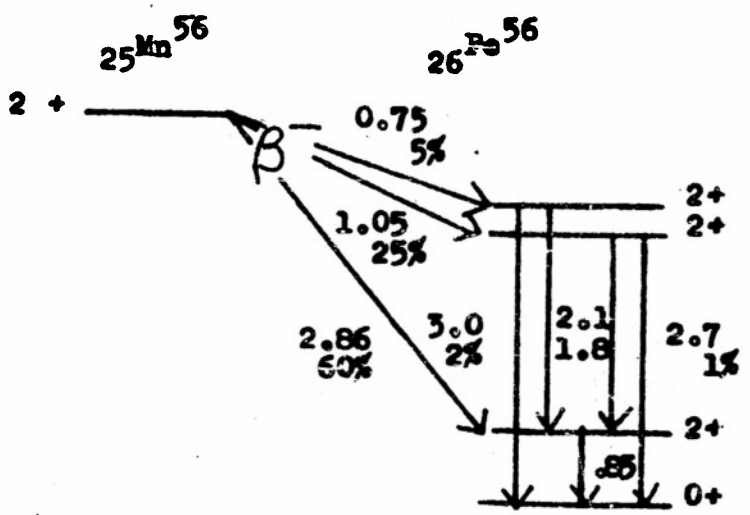

Fig. 1. Disintegration Scheme of Mn^{56} (ref. 4 & 5). The Spins and Parities are the Result of this paper.

The analysis of the correlations leads to the assignment of spin 2+ to all the three excited levels of Fe^{56} involved in the decay of Mn^{56}. The 2 -- 2 transitions are mixtures of 2 per cent (1.8 Mev transition) and 8 per cent (2.1 Mev transition) E2 with 98 and 92 per cent M1, respectively. Based on these 2+ spin values and on considerations concerning the decay of Co^{56} one can assign spin 2, even parity to the ground state of Mn^{56}, (Phys. Rev. 92, No. 4, 904-906, 1953).

c) As^{76} -- Se^{76}

Coincidence studies of the gamma rays emitted by As^{76} indicate that the decay scheme of As^{76} is more complicated than had been reported so far. We observed, for instance, coincidences indicating the presence of a 1.2 -- 1.2 Mev cascade.

The angular correlation of the main 0.55 -- 0.65 Mev cascade was investigated using pulse-height selection. The observed correlation, which, in spite of the pulse-height selection, still contains small contributions from other cascades, has the form $W(\theta) = 1 - 0.95 \cos^2 \theta + 0.99 \cos^4 \theta$. This unambiguously characterizes the spins of the levels involved as 2 - 2 - 0 in agreement with the conclusion reached by Kraushaar and Goldhaber on the basis of the "bulk" correlation. Although the determination of the exact E2/M1

mixing ratio is difficult due to the superposition of other cascades, the large values of the coefficients indicate that E2 accounts for at least 85 per cent of the transition.

c) Sb^{124} -- Te^{124}

The decay scheme of Sb^{124} is so complicated as to allow only the measurement of the two most energetic cascades: 2.1 -- 0.6 Mev and 1.7 -- 0.6 Mev. The observed correlations fit a 3-2-0 assignment with less than 0.1 per cent admixture of quadrupole radiation. In view of the large admixtures usually found between E2 and M1 (see Se^{76}, Fe^{56}) it was concluded that the 3-2 transition in Te^{124} had to be E1 with possibly some M2 admixture. This was later confirmed by conversion measurements at Princeton. The existence of a small admixture of M2 to the E1 radiation indicates that the E1 transition is probably slowed down by a factor of 100 while the M2 transition follows Weisskopf's lifetime estimate closely (Phys. Rev. 90, 1953).

A similar transition with $\sim 10^{-2}$ per cent M2 admixture was found in Sr^{88} by Steffen and by Varma, Saraf and Todd.

The angular correlation measurements, in addition to giving us the J-value sequences in several even-even nuclei, thus yielded information concerning the relative lifetimes of E1/M2, and M1/E2 transitions. Direct measurements of the lifetime of some of these transitions would be very

useful. They would tell us whether the mixture is due to the slowing down of the dipole component or whether it is due to the speeding up of the quadrupole transitions.

II. Resonance Fluorescence Studies.

The Resonance Fluorescence studies were started with the hope of developing a method for the measurement of lifetimes shorter than 10^{-13} seconds. However, it turned out that there are very few transitions -- at least in radioactive decays -- which are as fast as 10^{-13} seconds. One of the reasons is the absence of E1 transitions going to the ground state, which deprives one of the fastest transitions. Furthermore, it became evident that the M1 transitions are slower than predicted on the basis of Weisskopf's lifetime estimate. This circumstance for transitions forced us to improve the method and make it adaptable to transitions in the region 10^{-12} to 10^{-13} seconds, into which probably most of the observed E2 transitions and M1 transitions fall. Experiments with Au^{198} and Hg^{203} [illegible] this method has resulted in that the resonance fluorescence method can be extended to lifetimes which represent the limit of electromagnetic transitions. The basic idea of the resonance fluorescence method is illustrated in Figure 2 for the case of $P(^2D^{\circ}$

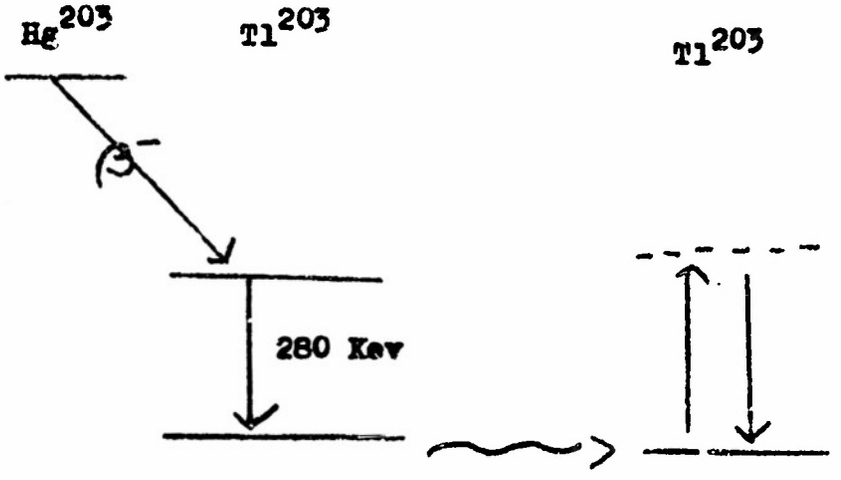

Figure 2.

The 280 Kev gamma-ray transition going to the ground state of Tl^{203} is used to irradiate the stable isotope Tl^{203}. It is expected that some of the Tl^{203} gamma-rays will be absorbed by the Tl^{203} nuclei and then re-emitted in random directions. If one observes at a large angle with respect to the exciting beam, the resonance-scattered radiation can be easily separated from the Compton-scattered radiation by energy discrimination. The only effect competing with resonance fluorescence which cannot be eliminated using energy discrimination is elastic (Rayleigh + Thomson) scattering of gamma-rays. A first step consisted in the observation of elastic scattering of the Ba^{137} (663 Kev) gamma-rays from materials with different Z.

Using the arrangement shown in Figure 3, in connection with a single channel pulse-height analyser, it was possible to observe elastic scattering for Z-values as low as 30, the elastic scattering from lead being several times larger than the cosmic-ray background.

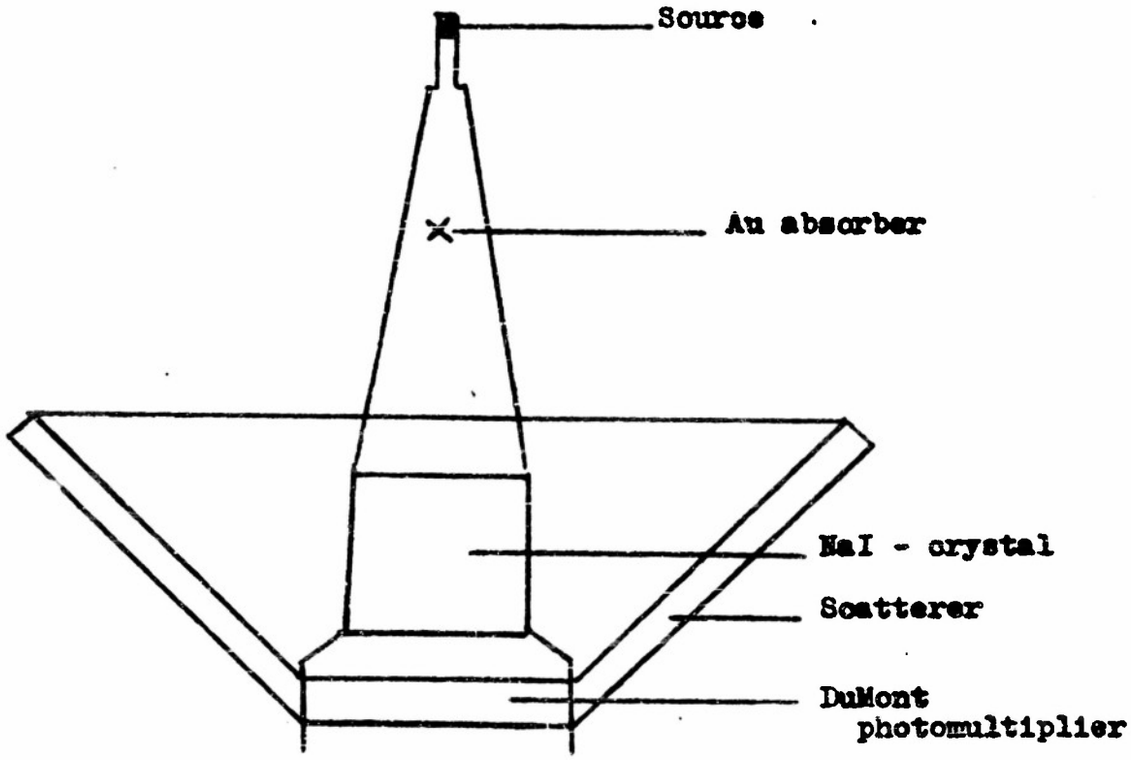

Figure 3.

A measurement of the elastic-scattering cross section for 280 Kev at an average angle of 110 degrees indicated that the theoretical prediction for the cross section is correct to within a factor of two.

Although the cross section for resonance fluorescence is of the order of 10^{-21} cm^2 at exact resonance, the observation of the resonance fluorescence is difficult because one never is in exact resonance due to the recoil in the emission as well as in the absorption process. The main endeavor is therefore directed at finding a way to compensate for the energy loss due to the gamma recoil. The methods which have been successful so far all use motion in the direction of emission with the idea of imparting to the gamma-ray some extra energy via the Doppler-effect.

We have tried to use the recoil motion due to the radiation preceding the gamma-ray transition as a means of compensation for the energy losses in the emission and absorption processes. For this method to be successful, the lifetime of the gamma-ray transition has to be shorter than the time between collisions of the recoiling nuclei with the surrounding matter. In solids this time is of the order of 10^{-13} seconds and therefore strongly limits the range of applicability of the method. From the absence of any observable resonance scattering of Mo^{97} γ-rays (from Nb^{97}) we were able to set an upper limit of 10^{-12} seconds for the lifetime of the 0.665 Mev excited state in Mo^{97} (Phys. Rev. 91, 1953). This indicates that this M1 transition has a lifetime at least 10 times longer than predicted by Weisskopf's lifetime formula.

Although a factor of 10 is a small deviation, it seems to indicate that the trend of low energy M1 transition to be $\sim$ 100 times slower than predicted is continued at higher energies.

The limitation imposed on the measurements by the short collision times in solids can be eliminated by using vapors. In our most recent experiments which are still under way, we used Hg^{203} in vapor form and have been able to extend the range of applicability to 10^{-9} seconds.

Preliminary lifetime estimates for the 209 Kev state in Hg^{199} and for the 280 Kev state in Tl^{203} are 3.10^{-10} and 5.10^{-10} seconds, respectively.

III. Search for Anamolous Positively-Charged Particles from P^{32}.

Introduction

When a β^- emitter is placed in a magnetic cloud chamber, there appear among the tracks which start or end at the source a certain small number which are curved in a sense opposite to that of the majority of the emerging electron tracks. These tracks have generally been reported to comprise between 10^{-2} and 10^{-4} of the total number of tracks observed and have been attributed to one or more of the following phenomena*.

---

* Ref. 1 contains a complete bibliography of earlier work on the subject.

---

1) electrons scattered from the walls back into the source. (or electrons returning to the source after describing a complete circle partially out of view).

2) electrons emerging from the source and multiply scattered in the gas so as to assume a reverse curvature.

3) positrons created in the source by the action of decay electrons, bremsstrahlung or nuclear γ-radiation.

4) positively-charged particles distinct from the positron.

In nearly every investigation so far reported the anamolous tracks have been far too numerous (always at least 10^{-4} per decay-electron) to be attributed to 3) and, in one case at least, fairly strong evidence suggests that neither 1) nor 2) are capable of accounting for the observations.

A few of the many investigations of this phenomenon have attributed the observed tracks to 3) in spite of violent conflict with theory and without an exhaustive investigation of the possibility of completely accounting for their results by the less interesting alternatives 1) or 2).

The most recent and careful investigation of the question has been carried out by Groetzinger and Ribe[1] who

---

1) G. Groetzinger and F. Ribe, Phys. Rev. 87, 1003, 1952.

---

used a P^{32} source (no nuclear γ-rays) in a magnetic cloud chamber with several different source geometries. A particularly interesting feature of this work is the careful analysis and elimination of effect 2) as a substantial contributor to the observed "positive" tracks. These authors also present fairly strong evidence that the tracks are not all 1), and suggest that some unknown positively-charged particle is responsible. (Possibility 3) was excluded as

contrary to an independent experimental upper limit of 1.3×10^{-5} positrons per P^{32} decay electron[2]).

---

2) K. T. Bainbridge (account of Harwell Conference) Nature, 160, 492 (1947).

In attempting to explain why the cloud-chamber positive-particle yields from P^{32} (about 10^{-4} "positrives" per β^- decay) were greater by a factor of ten than the upper limit observed with a β-ray spectrometer[2], Groetzinger and Kahn[3] hypothesized that the tracks might

---

3) G. Groetzinger and D. Kahn, Phys. Rev. 80, 108 (1950).

---

be caused by an unstable elementary particle having a half-life so short that it could escape detection in instruments having a long path between source and detector. Evidence consistent with this hypothesis has been obtained with small sized β-ray spectrometers by Groetzinger and Kahn[3] and also by Yuasa[4]. The former investigators utilized an unevacuated

---

4) T. Yuasa, Compt. Rend. 234, 619 (1952).

180° spectrometer with 4 cm path-length and the latter an evacuated 180° instrument with a 7 cm path-length.

This communication describes an attempt to verify these last-mentioned results with a small spectrometer designed with

particular care to eliminate some of the background effects which could give rise to an erroneous indication of positively-charged particles emitted from the source.

Apparatus

Two cross-sectional views of the spectrometer are shown in Fig. 1. Around the circumference of an annular channel machined in the brass cylinder are spaced a series of five G-M counters so arranged that particles which start at the source S and pass completely around the channel traverse the sensitive volume of each counter. The channel has a central radius of curvature of 17/32" and a rectangular cross section measuring 1/16 by 5/8 inches. Between each adjacent pair of counters is machined a rectangular cavity intersecting the channel and forming a sort of slit system to reduce glancing-angle scattering from the walls. The open space formed by the channel and counters is sealed at one end by a permanent plug and at the other by a Pb block with an "O" ring gasket. The P^{32} source** was evaporated

---

** P^{32} chemical form: PO_4 in weak HCl solution. Procured from AEC, Isotope Division, Oak Ridge, Tenn.

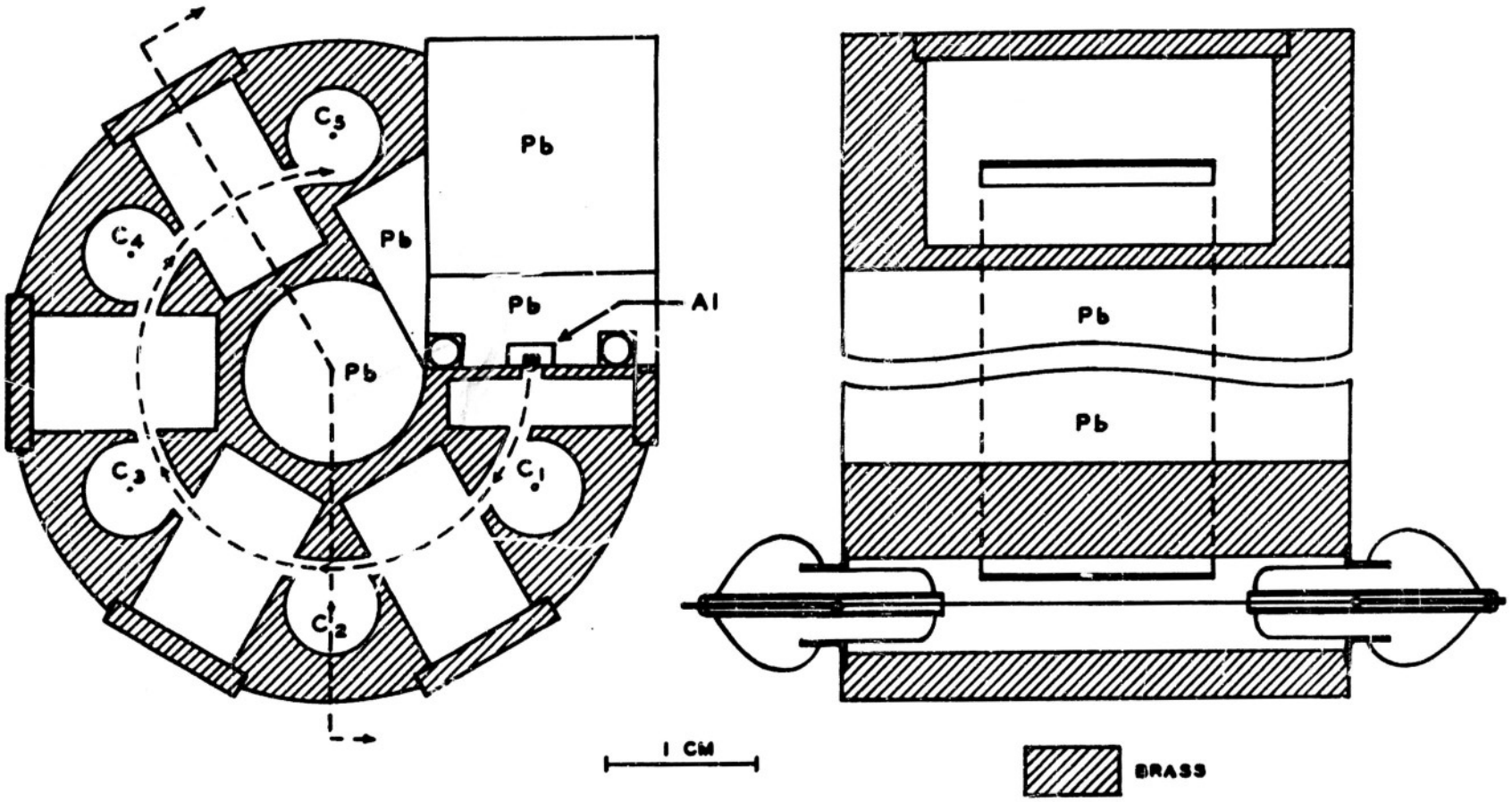

SPECTROMETER

Figure 1.

Cross sectional diagram of spectrometer showing G-M counters C, source S, and lead absorber Pb. Cross-hatched material is brass.

into a small 1/32" thick Al boat which nested into the Pb block exposing the bare source directly to the channel.

The entire instrument was filled with a self-quenching G-M counter gas mixture (90% Argon, 10% Butane) at a total pressure of 5 cm Hg. In traversing the 6 cm path-length around the channel, a particle encounters no windows of solid material and is required to penetrate only 0.13 mg/cm^2 of gas.

The lead blocks behind the source and in the center of the spectrometer cylinder shield the counters from the source bremsstrahlung so as to minimize both the probability of accidental coincidences and the production in C_5 of photo electrons which might traverse the instrument in the backward direction and give a spurious positive-particle indication. The instrument was mounted in a magnetic field variable from 0 to 2000 gauss supplied by an electromagnet with 2.5" diameter pole faces spaced 2.5" apart. The field was essentially uniform over the volume of the spectrometer.

Procedure

The detection of five-fold coincidences between all of the circumferential G-M counters was originally conceived as a method of obtaining good suppression of cosmic-ray background and at the same time of insuring that only particles which really traversed the channel would be counted. While the former objective was satisfactorily met

by this arrangement, there existed a weak tendency for adjacent counters to discharge one-another by photo-electric interaction. Thus, for example, an electron which traversed counters C_1, C_2, C_3 and not C_4, C_5 could give rise to a five-fold coincidence with probability of about 10^{-4}. Furthermore, when sources of sufficient strength to allow performance of the experiments in a reasonable time were used, counters C_1 and C_2 counted at such high rates that their operation was considered unreliable.

After several unsuccessful attempts to reduce the interactions between adjacent counters it was decided to perform the experiment with two-fold coincidences between counters C_3 and C_5 and to use an anti-coincidence tray of G-M counters placed directly above the instrument as a means rejecting cosmic-ray counts. This tray had a solid sensitive area measuring 4" by 8" and was centered 3 inches above the central axis of the spectrometer. In this location the tray overlapped considerably the solid angle defined by counters C_3 and C_5.

Experimental Results

The results of principle interest are shown in Fig. 2. Anticoincidence rates measured with the field oriented to favor the detection of β^- particles from the source are indicated by the (-) curve, and rates with corresponding fields of the opposite polarity are indicated by the (+) curve. The

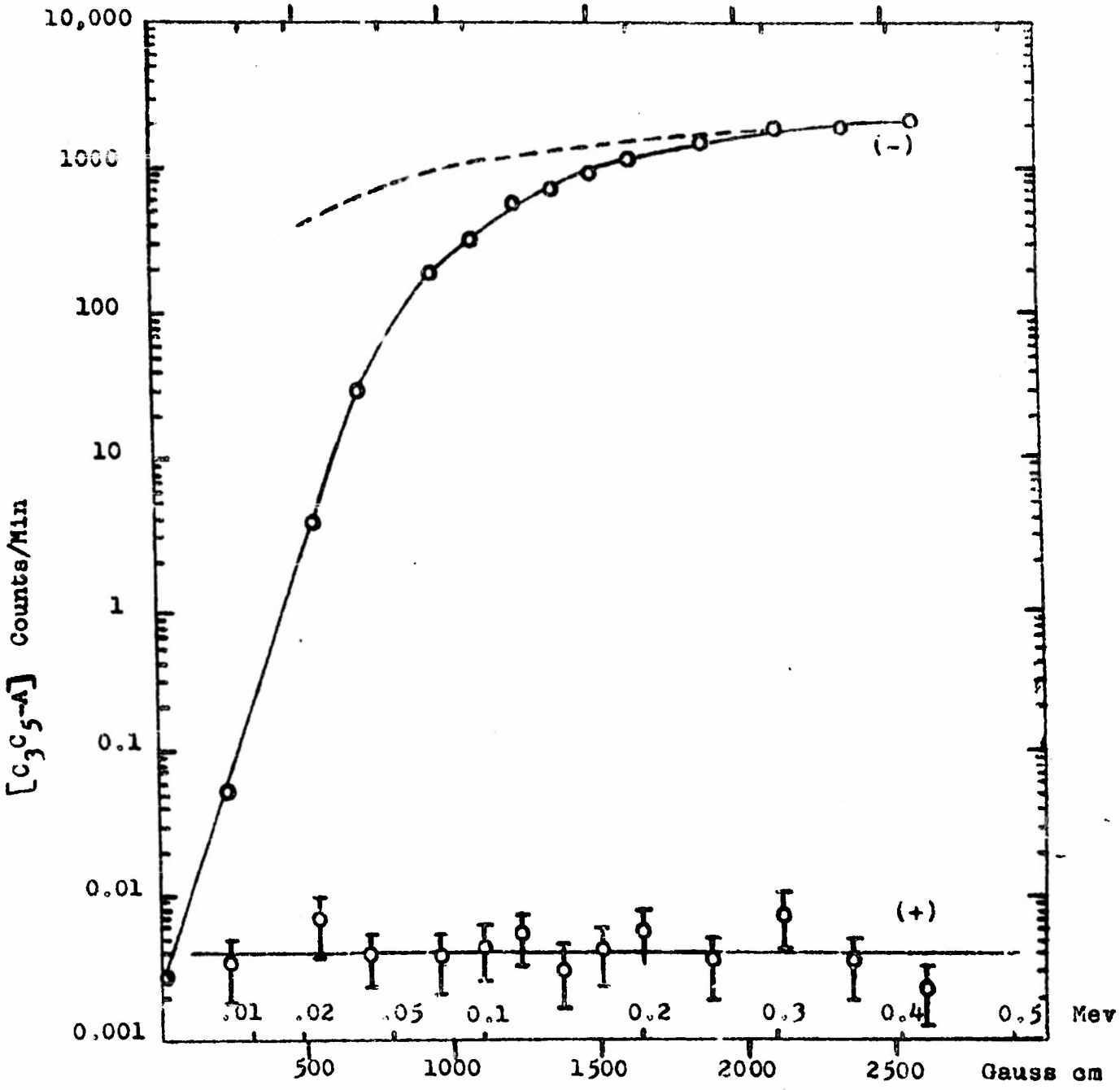

Fig. 2 Measured anticoincidence rates with P^{32} source. The (-) curve was obtained with the magnetic field polarity favoring the passage through the spectrometer of negatively-charged particles, and the (+) curve with the opposite field polarity. The dashed curve is the P^{32} β-spectrum as determined by Agnew.

data were obtained over a period of approximately 10 days and were corrected for decay of the P^{32} source during the period. The cosmic-ray background anticoincidence rate, measured with the source removed, was approximately 5×10^{-4} min^{-1} or about one-tenth of the average rate represented by the (+) points. Within the statistical uncertainties the (+) rates are independent of field strength.

Subsidiary experiments were performed to seek a correlation between the recorded (+) rates and the rate at which counter 5 was discharged by P^{32} bremsstrahlung. It was discovered that an extra P^{32} source placed between the two Pb blocks behind the regular source increased the anti-coincidence rate in about the same proportion as the bremsstrahlung rate of counter five at several different (+) field-settings above 400 gauss. This indicated that many of the observed (+) counts (at least 50%) were caused by bremsstrahlung-produced secondary electrons which were released in counter 5 and traversed the channel in the backward direction to counter 3. Even without corrections for this effect the (+) to (-) ratios in the interval $H\rho$ = 700 to 2700 gauss cm. are considerably smaller than expected from the cloud chamber results and the prior small-spectrometer data when the latter are taken to indicate a real positive-particle effect. For this reason it did not seem worthwhile to attempt a precise evaluation of the residual spurious phenomena.

Because of the low pressure of the gas mixture and the short path-length of the β-rays through the G-M counters, particles which traversed the channel were not counted with 100 per cent efficiency. The efficiency of counter C_3 has been determined by taking the ratio of the 3-fold coincidence rate ($C_3C_4C_5$) to the 2-fold rate (C_4C_5) at several different (-) field settings. The results of these measurements are given in Table I.

The variation of the counting efficiency over the $H\rho$ range investigated together with the scattering introduced by the gas and the finite thickness of the source render the (-) curve in Fig. 2 only a crude approximation to the true β^- spectrum of P^{32}. A rough estimate of the multiple scattering loss as a function of $H\rho$ has been made by calculating the probability that a ray leaving the source with the proper direction and momentum to allow traversal of the center of the channel in vacuum will, in the presence of the gas, be scattered so as to miss the entrance slit of counter C_5. The results of this calculation, based upon empirical scattering data for Argon[5] and an estimate of

---

5) G. Groetzinger, M. Berger and F. Ribe, Phys. Rev. 77, 584 (1950)

---

the Butane scattering is shown in Table II.

TABLE I

Efficiency of Counter C_3 vs $H\rho$

$H\rho$	820	1090	1370	1630	1870	2120	2350	2580
Efficiency of C_3	0.72	0.65	0.57	0.56	0.49	0.45	0.45	0.41

TABLE II

Calculated Fraction of β-rays Removed from the Channel by Multiple-Scattering vs $H\rho$

$H\rho$	750	1000	1500	2000	2500	3000
Fraction Removed	.92	.75	.65	.52	.43	.37

The measured β^- spectrum corrected for the efficiency variation of counters C_3 and C_5 (the efficiency of C_5 is assumed identical to that of C_3 because of the similar geometries of the two counters), for the multiple-scattering loss as approximated above, and for the variation of the $H\rho$ acceptance-interval as a function of $H\rho$ yields the dashed curve shown in Fig. 3. Comparison with the true spectrum of P^{32} as measured by Agnew[6] indicates fairly good

---

6) H. Agnew, Phys. Rev. 77, 655 (1950)

---

agreement above $H\rho$ = 1200, but considerable departure at low momenta where the scattering calculation is least accurate and where the form of the spectrum is most sensitive to the thickness of the source and the nature of the source-backing.

Discussion

Since electrons and positrons of the same momentum are scattered similarly (if anything, positrons are somewhat less strongly scattered), the curves in Fig. 2 give directly at each $H\rho$ value an upper limit to the ratio of positrons to electrons emitted from the source. This ratio varies from 1.6×10^{-4} at $H\rho$ = 700 gauss cm to 2×10^{-6} at $H\rho$ = 2700 gauss cm.

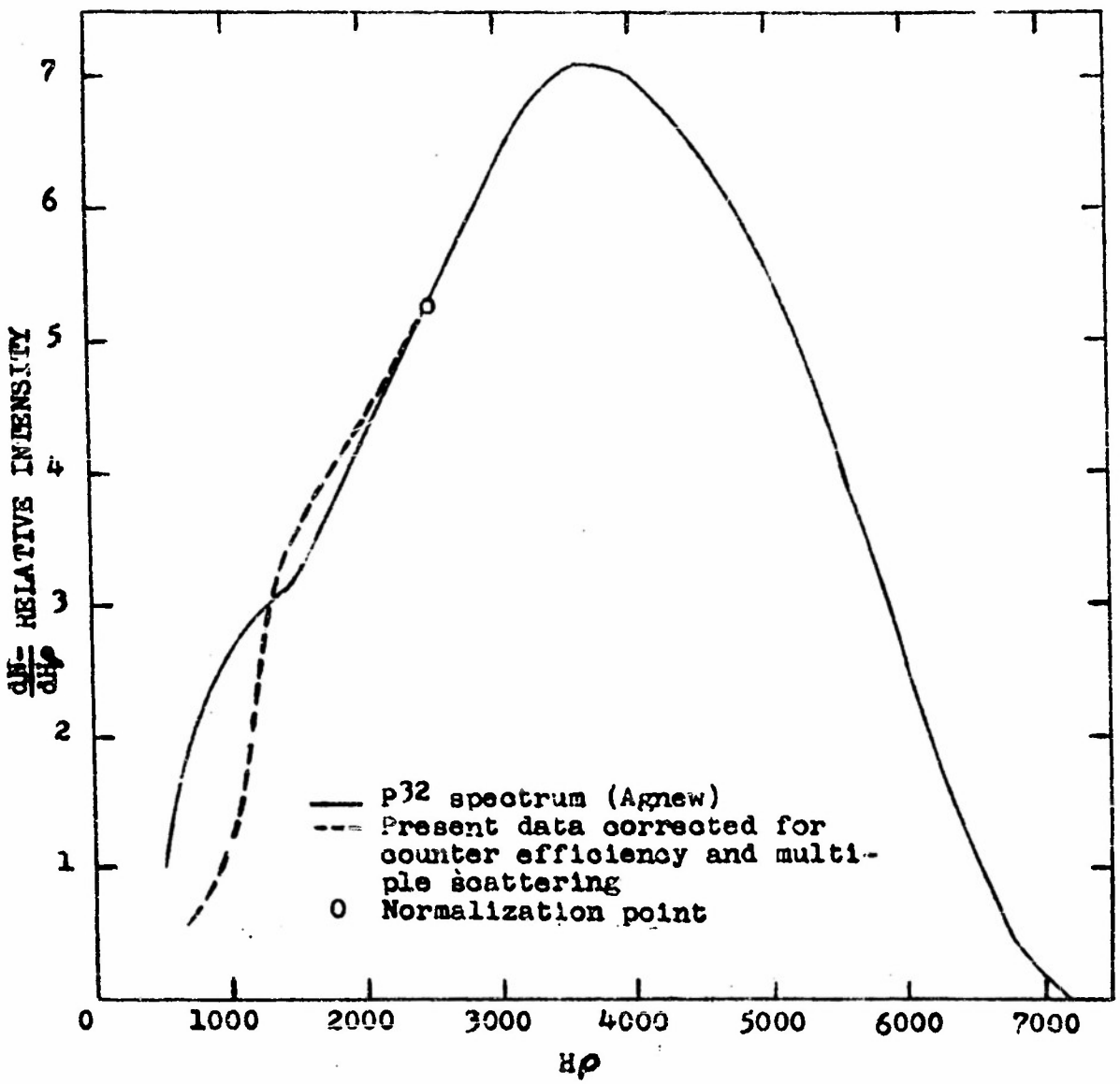

Fig. 3 P^{32} spectrum as measured by Agnew (solid curve), and the present data corrected for multiple scattering in the gas within the spectrometer and for the G-M counter inefficiency (dashed curve).

At $H\rho = 1600$ the (+) to (-) ratio is 3×10^{-6} while the corresponding value measured by Groetzinger and Kahn[3] with a small (unevacuated) spectrometer is 8×10^{-4}. For particles with $H\rho > 700$ gauss cm the cloud-chamber data of Groetzinger and Ribe[1] indicate an over-all positive-particle to negative-particle ratio of $\sim 2 \times 10^{-4}$. If one breaks the latter data down into momentum-intervals and assumes that the cloud-chamber electron spectrum is the same as that measured with a β-ray spectrograph, it is found that the positive-to-negative ratios in each of the $H\rho$ intervals 700 - 1400, 1400 - 2100 and 2100 to 2800 gauss cm exceeds the corresponding value measured with the present instrument by at least a factor of 50. (Most of the "positive" tracks observed in the cloud chambers investigation are included in the $H\rho$ intervals selected for comparison.) The small-spectrograph measurements of Yuasa[4] yield positive-to-negative ratios which are in agreement with the cloud-chamber data of the same author and also in rough agreement with the Groetzinger and Ribe results.

If one chooses to adapt the point of view that the larger upper limits given by other investigators for the positive-particle yield from P^{32} reflect the presence of a real positively-charged particle and not just a spurious effect, one must at the same time endow the particle with properties which might cause it to escape detection in the present instrument. One may envision, for example, a particle that is much more strongly scattered or has a much lower specific

ionisation than an electron of the same momentum. Although the existing data on multiple-scattering of the cloud-chamber "positives"[7] is of somewhat limited statistical accuracy,

---

7) G. Groetzinger and F. Ribe, Phys. Rev. 79, 904 (1950)

---

the tracks do not seem to be sufficiently more strongly scattered than electrons to seriously suppress their detection in the present instrument.

The question of a lower specific-ionisation may be approached as follows:

Using a theoretical expression for the variation of G-M counter-efficiency[8] with the specific ionization of a tra-

---

8) see e.g. G. McClure, Phys. Rev. 90, 796 (1953)

---

traversing ray, one finds that a specific ionisation less than 1/4 that of an electron of the same $H\rho$ must be attributed to the particle in question in order that its detection-efficiency be suppressed the required amount in the present instrument. Although there is no specific mention of the ionization of the cloud-chamber "positives" relative to electrons, a ratio of 1 to 4 could hardly have escaped notice, for electron tracks themselves are quite thin and are difficult to photograph clearly.

The fact that the positive particle yields from P^{32}, as observed here, is at least 50 times smaller than the anamolous-track yield determined by cloud-chamber observations, can hardly be explained on any other grounds than that the majority of the cloud-chamber tracks in question are really electrons returning to the source.

IV. The Disintegration of Mo^{99}

Introduction

Earlier coincidence studies[1] showed the disintegration scheme of Mo^{99} to be rather complex. Subsequent measurements[2-6] have led to the conclusion that Mo^{99} decays with the emission of two, or possibly three, groups of beta-rays, and gamma-rays having energies of 1.8, 40, 140, 142, 181, 367, 741, and 780 Kev. A careful study[5,6] of the disintegration of the 6-hour isomer of Tc^{99} has revealed that it decays with cascade emission of the 1.8 Kev and 140 Kev quanta, and that the 142 Kev gamma-ray is the associated cross-over transition. The

1) C. E. Mandeville and M. V. Scherb, Phys. Rev. 73, 848 (1948)

2) H. Medicus, D. Maeder and S. Schneider, Helv. Phys. Acta 22, 603 (1949)

3) J. M. Cork, H. B. Keller and A. E. Stoddard, Phys. Rev. 76, 986 (1949)

4) M. E. Bunker and R. Canada, Phys. Rev. 80, 961 (1950)

5) H. Medicus, D. Maeder and H. Schneider, Helv. Phys. Acta 24, 72 (1951); Phys. Rev. 81, 652 (1951)

6) J. W. Mihelich, M. Goldhaber and E. Wilsop, Phys. Rev. 82, 972 (1951)

disintegration scheme of Mo^{99}, as advanced by Medicus et al[5], is based upon coincidence measurements between spectrometrically selected beta-rays and gamma-rays detected in an anthracene scintillation counter. However, the problem of the precise location in the scheme of the 181 and 367 Kev gamma-rays has remained unresolved. Accordingly, with the utilization of two single channel pulse-height analyzers in coincidence, the gamma-ray spectrum and the various cascade relationships have been re-investigated.

The Measurements

For the purposes of the present investigations, a source of Mo^{99} was obtained when a quantity of MoO_3 was irradiated by slow neutrons in the Oak Ridge pile. Because no gamma-rays other than those already reported were observed, extensive chemical purification was deemed unnecessary. On occasion, however, Tc^{99m} was separated from its parent element by the method of Coryell and Sugarman[7].

---

7) Charles D. Coryell and Nathan Sugarman "Radiochemical Studies: The Fission Products". (National Nuclear Series, McGraw-Hill Book Company.

In Figure 1 is shown the pulse-height distribution generated by the gamma-rays of Mo^{99} in a crystal of thallium-activated sodium iodide which is three centimeters thick. In

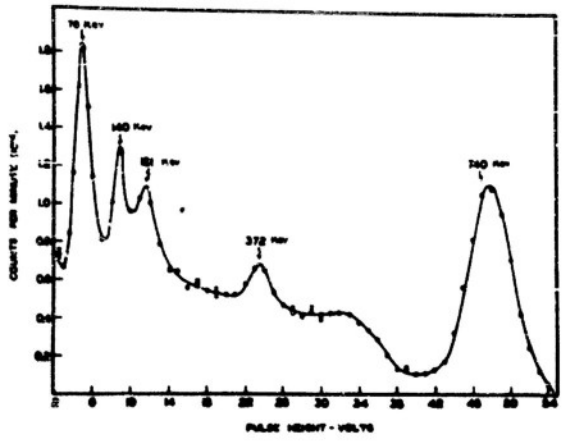

Fig. 1. Pulse-height distribution from NaI-Tl irradiated by gamma-rays emitted in the disintegration of Mo ^{99} in equilibrium with Tc ^{99m}. The radiations have been filtered by lead (2g/cm ^{2}) to reduce the intensity of the 140 Kev radiation.

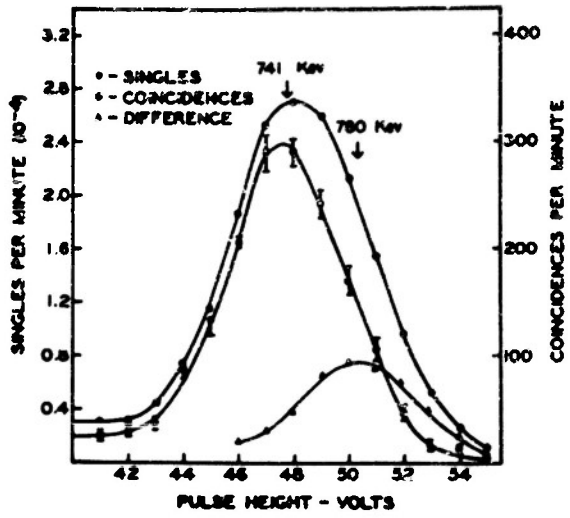

Fig. 2. Coincidence study of the 741 Kev - 140 Kev cascade. The data show that the 780 Kev line is non-coincident with any 140 Kev radiation.

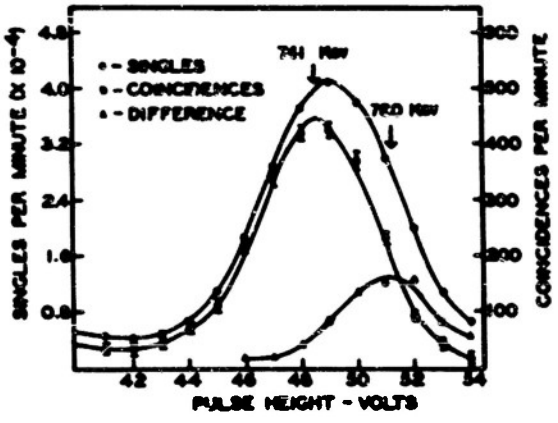

Fig. 3. Coincidence study of the 741 Kev - 181 Kev cascade. The data show that the 780 Kev line is non-coincident with any 181 Kev radiation.

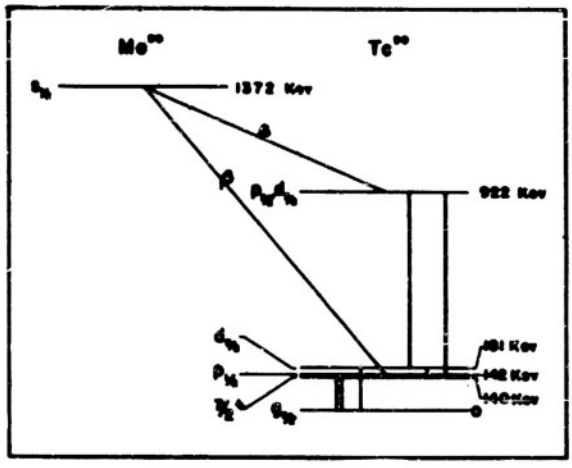

Fig. 4. Term scheme for Mo ^{99} and Tc ^{99m}.

Fig. 5. Gamma-ray spectrum in the region of lower energies of Mo ^{99} and Tc ^{99m} (Tc ^{99m} partially removed by chemical separation). The spectrum of "singles" is to be compared with the spectrum of soft gamma-rays in coincidence with the 741 Kev radiation.

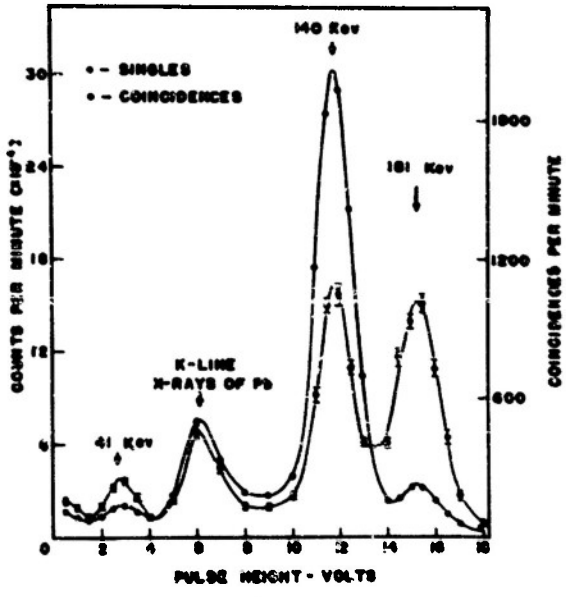

the case of the particular curve of Figure 1, the radiation incident upon the detecting crystal had been filtered by a lead absorber of thickness about 2 g/cm^2 to reduce in intensity the 140-142 Kev radiation relative to the harder gamma-rays. The radiation at 78 Kev arises from the emission from the absorber of the K-line of lead, following photoelectric absorption of the intense 140 Kev gamma-ray. To observe carefully the region of lower energies and to detect the 41 Kev radiation, without lead absorber and without interference from the K-line, an additional curve, not illustrated in this paper, was obtained. In this case, to reduce the intensity of the 140 Kev line, approximately two-thirds of the 6-hour Tc activity was removed from the molybdenum by chemical separation. Unless the intensity of the 140 Kev line line is reduced somewhat, a source of Mo^{99} strong enough to give a clear picture of the spectral region below 140 Kev will at the same time give rise to a piling up of 140 Kev pulses at the linear amplifier, distorting the spectral region above 140 Kev. From the pulse-height spectrogram of Figure 1, it is clear that only those gamma-rays which have been previously reported are present in the sample of Mo^{99} under study. These gamma-rays were observed many times during twelve half-periods of decay and were found to decay with the same half-period.

To study the disintegration scheme of Mo^{99}, gamma-gamma coincidence rates were measured between the two members of all possible pairs of gamma-rays.

To ascertain the relation between the 140 Kev radiation and the harder gamma-rays, the data of the curves of Figure 2 were collected. The single counting rate in the vicinity of 760 Kev is plotted along with a coincidence rate which was obtained with two pulse-height analyzers in coincidence by setting one analyzer at the photo-peak of the 140 Kev radiation and moving the window of the second through the region of 760 Kev. On comparing the half-widths and locations in the energy of the two peaks, it is seen that the 140 Kev radiation is coincident only with the 741 Kev line. The difference curve, also shown in Figure 2, is peaked at 780 Kev, showing that the 780 Kev radiation is non-coincident with the 140 Kev line. A similar curve is shown in Figure 3 in which coincidences have been recorded between the 741 Kev gamma-ray and the 181 Kev line. A third set of curves, not shown as a figure, was obtained relative to coincidences between the 41 Kev gamma-ray and the hard radiations. Again it was found that coincidences were present only between the 741 Kev radiation and the softer quantum. To avoid difficulties growing from the presence of the intense 140 Kev radiation associated with the decay of the 6-hr. metastable level, a partial separation of Tc from Mo was performed before obtaining the data of the curves of Figures 2 and 3. The soft gamma-ray at 41 Kev was also found to be coincident with the 140 Kev quantum. In performing coincidence measurements between the gamma-rays of energies 140 and 41 Kev.

care was taken that the back-scattered quanta from one crystal did not enter the other crystal. A proper choice of absorbers placed between the two crystals eliminated any back-scattering effects.

No coincidences were detected between the 372 Kev gamma-ray and any other gamma-rays in the spectrum. A search was also carried out to find two 372 Kev quanta in coincidence, but none were found. The resolving time of the coincidence circuit was 10^{-7} sec. Absence of coincidences may, therefore, be interpreted as evidence that the 372 Kev transition terminates at a metastable level of lifetime long compared with 10^{-7} second or that the 372 Kev line arises from the presence of a radioactive impurity.

The foregoing coincidence data are consistent with the interpretation that the 780 Kev gamma-ray terminates at the 6-hr. metastable level in Tc^{99}, 142 Kev above the ground state and that the 741 Kev gamma-ray leads to a level 181 Kev above the ground state of Tc^{99}. The level at 181 Kev decays with the emission of the 181 Kev quantum or with cascade emission of the gamma-rays of energy 41 and 140 Kev. The cascade relation among the various gamma-rays is depicted in the disintegration scheme of Figure 4. To determine the per cent of the total beta-ray emission which leads to the level at 922 Kev in Tc^{99}, beta-gamma coincidences were measured. The beta-ray counter was an anthracene crystal and photo-tube biased to count pulses generated by beta-rays

of energy greater than 50 Kev. It should also be mentioned that the harder beta-spectrum was found to be non-coincident with gamma-rays, in agreement with earlier findings[1, 5]. From the gamma-ray counter, all pulses corresponding to a gamma-ray energy greater than 400 Kev were accepted. From a carefully caloulated solid angle and the counting-efficiency of the gamma-ray counter, the 0.5 Mev beta-rays were found to constitute 14.5 per cent of the total beta emission. This result is in close agreement with the data obtained by Medicus, et al[5].

The level at 181 Kev can de-exoite by way of either of two modes of gamma-ray emission: by the emission of a single gamma-ray of energy 181 Kev or the 41 and 140 Kev quanta in cascade. To determine the probability of de-excitation of the 180 Kev level by either mode, coincidences were measured between the 741 Kev gamma-ray and the entire low energy spectrum. The pulse-height distribution of single counts in the region of low energy is plotted along with the coincidences between the low energy gamma-rays and those of energy 741 Kev as shown in Figure 5. In actuality, all pulse heights corresponding to energies greater than 400 Kev were accepted in the high energy gamma-ray counter. The low energy gamma-ray counter was shielded from recoil quanta by a lead absorber of thickness 3 g/cm^2. The aluminum-magnesium oxide jacket in which the crystal of the low energy gamma-ray counter was encased, was estimated to reduce the intensity

of the 41 Kev gamma-ray by 30 per cent. If the conversion coefficients of the 140 Kev and 181 Kev radiations are neglected, it is evident from a consideration of the areas under the peaks of the coincidence curve that the number of disintegrations proceeding by way of the 181 Kev branch is about equal to the number in which de-excitation occurs by way of the 41 Kev-140 Kev transitions. If the conversion coefficient ($\alpha = N(e^-)/N(\nu)$) of the 140 Kev gamma-ray is taken to be 10 per cent[5], the branching ratio of the 41 Kev-140 Kev and 181 Kev transitions is 1.2/1. A one-to-one ratio should exist for the areas under the 41 Kev and 140 Kev peaks of the coincidence curve. The actual area of the 41 Kev peak recorded in Figure 5 is considerably smaller, indicating a relatively large conversion coefficient for the 41 Kev line. From the areas and the conversion coefficient of the 140 Kev radiation, the total conversion coefficient for the 41 Kev radiation is calculated to be $\sim$5. From the determined efficiency for detection of 181 Kev radiation, the solid angle of its detector, and the data of Figure 5, the ratio of intensities of the 741 and 780 Kev gamma-rays was calculated to be 2.6.

Discussion of Results

The ground state of Tc^{99} has the orbital $g_{9/2}$. The two levels immediately above the ground state at 140 Kev

and 142 Kev are characterized[5,8] by 7/2+ and $p_{1/2}$. The two

8) M. Goldhaber and R. D. Hill, Rev. Mod. Phys. 24, 179 (1952)

beta spectra have values of log ft such that both of them may be considered to fall in the category of either first-forbidden spectra ($\Delta I = 0, \pm 1$; yes!) or ℓ-forbidden spectra ($\Delta I = \pm 1$, no! $\Delta \ell = \pm 2$). The ground state of Mo^{99} ($N = 57$, $Z = 42$) may have any one of several orbitals[9, 10];

9) Mayer, Mozskowski and Nordheim, Rev. Mod. Phys. 23, 315 (1951)

10) M. G. Mayer, Phys. Rev. 78, 16 (1950)

$g_{7/2}$, $d_{5/2}$, $d_{3/2}$, or $s_{1/2}$. It has been previously shown that the harder beta-spectrum of Mo^{99} is non-coincident with gamma-rays[1] and terminates[5] at the level of orbital $p_{1/2}$. Were the ground state of Mo^{99} a $d_{5/2}$ configuration, an allowed beta transition, $d_{5/2} \rightarrow 7/2+$ would be present rather than the forbidden transition $d_{5/2} \rightarrow p_{1/2}$. Similarly, if the ground state of Mo^{99} be assumed to be a $g_{7/2}$ level, transitions to 7/2+ or $g_{9/2}$ would be dominant. None of the above mentioned allowed transitions are observed; therefore, $d_{5/2}$ and $g_{7/2}$ are rejected as possible orbital designations for the ground state of Mo^{99}. The orbital assignment of $d_{5/2}$ can also be eliminated. It is, however, first necessary to establish the characteristics of the 181 Kev level

in Tc^{99}. The conversion coefficient of the 41 Kev gamma-ray identifies it as magnetic dipole radiation ($\Delta I = 0, \pm 1$; no!). Since this transition terminates at 7/2+, possible orbital values for the 181 Kev level are $d_{5/2}$, 7/2+, and 9/2+. Assignment of 7/2+ or 9/2+ to the 181 Kev level is ruled out by the absence of a gamma-ray transition from the 922 Kev level to either the ground state or the level at 140 Kev leaving the orbital of the 181 Kev level to be $d_{5/2}$. If the ground state of Mo^{99} were of orbital $d_{3/2}$, an allowed beta transition terminating at the 181 Kev level would be present. This spectrum is not observed.

The remaining possible orbital assignment for the ground state of Mo^{99} is $s_{1/2}$. If the softer beta spectrum were given a first-forbidden classification, the level at 922 Kev in Tc^{99} would have orbitals of $p_{1/2}$ or $p_{3/2}$. If the spectrum is interpreted as ℓ-forbidden, the assignment of the 922 Kev level would be $d_{3/2}$. The measurements of the present investigation show that the 741 Kev and 780 Kev gamma-ray transitions to levels of orbitals $d_{5/2}$ and $p_{1/2}$ have the same order of magnitude of probability of occurrence. If the 922 Kev level is described as $p_{3/2}$, the multipolarities of the 741 and 780 Kev gamma-rays are respectively E1 and M1. If instead of $p_{3/2}$, the level assignment is taken as $d_{3/2}$, the multipole properties of the two hard gamma-rays are interchanged. Since the measurements of the present investigation have shown the 741 Kev gamma-ray to be more intense

than the 780 Kev line, an orbital assignment of $p_{3/2}$ for the 922 Kev level is favored.

This fact exoludes the possibility that the 922 Kev level have the orbital $p_{1/2}$, because were it so, the 741 and 780 Kev gamma-rays would be classified respectively as M2 and M1 which transitions are known to have greatly differing lifetimes.

C. PHOSPHORESCENCE STUDIES

The Storage of Energy in Some Activated Alkali Halide Phosphors

Introduction

The alkali halides are universally known as efficient phosphors for use in scintillation counting. A particular example is, of course, NaI-Tl. There are other properties of these materials which are useful though indirectly related to the fluorescent emission. Two such characteristics are:

(1) Phosphorescent afterglow, emission of light from the excited phosphor after cessation of irradiation.

(2) Energy storage in the irradiated phosphor.

The phosphorescence of item (1) above results from the escape of electrons from shallow traps. The kinetic energy of escape is supplied by the temperature of the surroundings in which the phosphor finds itself. Thus, the phosphorescent emission at liquid nitrogen temperature is far less than that encountered at room temperature (25°). If the trap depths are sufficiently great, thermal agitation at room temperature may be insufficient to dislodge the trapped electrons which will remain "stored" in excited states in the solid. They

will escape, however, if the phosphor is heated (thermostimulation) or irradiated by near ultraviolet, visible, or red light (photostimulation).

The primary excitant may take any one of several forms: X-rays, beta rays, gamma rays, alpha particles, or ultraviolet light. Irradiation by the more energetic excitants removes the electrons from the filled band, placing them in the conduction band of the phosphor. These electrons may be subsequently trapped in imperfections, forming, for example, F-centers, F'-centers, etc. The ultraviolet light, however, is not energetic enough to bring about this condition through absorption of a single photon. It may, however, excite to metastable states bound electrons in the heavy activator ion.

Whether metastable state or imperfection trap, the potential barrier for escape may be so great that thermal liberation at room temperature is very rare. The idea immediately presents itself that the alkali halides which exhibit storage could serve as dosimeters for nuclear radiation. After receipt of an initial burst of nuclear radiation, the irradiated phosphor can be interrogated days, weeks, or months afterwards to ascertain the previously received dosage.

Various aspects of the crystal dosimeter problem have been discussed in several previous publications by other authors. The use of alkali halides as the dosimetric material has already been considered in some detail. In particular,

Kallmann et al[1] have reported on many characteristics of the

1) M. Furst and H. Kallmann, Phys. Rev. 82, 964 (1951) ibid. 83, 674 (1951), Kallmann, Furst and Sidran, Nucleonics 10, No. 9, 15 (1952), Bittman, Furst and Kallmann, Phys. Rev. 87, 83 (1952).

silver-activated alkali halides, and the measurement of dosages by them has also been similarly described by Friedman and Glover[2]. The silver-activated alkali halides

2) H. Friedman and C. P. Glover, Nucleonics, 10, No. 6, 24 (1952).

have been reported to have particularly good storage properties, though storage is not limited to them alone.

Many of the alkali halide phosphors are double-banded; that is, emission is to be found in both ultraviolet and visible bands. Under certain circumstances, the two bands can be studied separately in photomultiplier tubes with the aid of properly chosen filters. However, a more convenient method of separating the two bands is to use a photosensitive Geiger counter for ultraviolet detection and a photomultiplier tube such as the RCA-5819 for measurement of the visible emission. The RCA-1P28 is also of considerable value, because it responds to both visible and ultraviolet. When enclosed in a cylinder of soft glass, the 1P28 will, of course, respond to the visible radiation alone. The Geiger counter is of particular value in measurement of the photostimulated release of

the "stored" ultraviolet, because it does not respond to the stimulating radiation. Measurement of the photostimulated emission can proceed simultaneously with stimulation. This advantageous feature of the photosensitive Geiger counter has been previously emphasized[2, 3, 4].

---

3) C. E. Mandeville and H. O. Albrecht, Phys. Rev. 91, 566 (1953).

4) Mikao Kato, Sci. Papers, Inst. Phys. and Chem. Res. (Tokyo) 41, 113 (1944),
ibid. 41, 135 (1944),
ibid. 42, 35 (1944),
ibid. 42, 95 (1944).

It should be remarked that the present investigation as well as those described in references 1, 2 and 3 are concerned with fluorescence, phosphorescence, and energy storage as related to irradiation by nuclear particles. Similar and closely-related phenomena are to be associated with irradiation by ultraviolet. Silver and thallium-activated alkali halide phosphors were intensively studied by Kato[4] and more recently by Etzel, Schulman, Ginther and Claffy[5].

---

5) Etzel, Schulman, Ginther and Claffy, Phys. Rev. 85, 1063 (1952).

Many references to earlier papers in which ultraviolet was employed as the primary exitant can be found in the accounts

of these latter investigations. In particular, it should be said that Kato used a photosensitive Geiger counter throughout the course of his work and pointed out specifically in the fourth paper of his series the advantages of the spectral response of the Geiger counter in observing the photo-stimulated emission of ultraviolet while the stimulating near ultraviolet light is on.

All of the measurements described below, whether relating to spontaneous phosphorescence or long-period energy storage, were carried out at room temperature (25° C).

The Thallium-Activated Alkali Halides

A logical starting point for this discussion is the behavior of the thallium-activated alkali halides, because they have already received so much attention[6, 7, 8]. In Particular,

---

6) W. Buenger and W. Flechsig, Z. Physik 69, 637 (1932).

7) P. Pringsheim, Revs. Modern Phys. 14, 132 (1942).

8) Johnson and Williams, J. Chem. Phys. 21, 125 (1953). This paper contains many references to earlier work of Williams and associates.

---

the phosphorescence of KCl-Tl at room temperature is considered to be dominated by a phosphorescent emission related to a trap depth of 0.67 ev and to excited states of Tl^+ in close proximity to other Tl ions, probably Tl^+ ions adjacent in the crystal

lattice[9]. Since the excited electron never leaves the thallous

9) F. Seitz, J. Chem. Phys. 6, 150 (1938).

ion of which it is a part, the decay is exponential in character, persisting above background for several hundred minutes. This type of behavior is exceptional to the usual in that exponential decay laws are commonly associated with half-periods of a few microseconds or less and seldom with a decay-time of hours. The results of ultraviolet irradiation of KCl-Tl and NaCl-Tl (thallium concentration 0.1 per cent by weight in either specimen) are shown in Figure 1(a)*. The decay law is

* Most of the phosphors employed to obtain the data of this paper were polycrystalline masses produced by fusion in a platinum crucible and subsequent rapid cooling on a glass plate. The characteristics of these phosphors were found to be much the same as those of single crystals. This has also been the experience of others (see reference 8).

entirely different in the two cases. The curves for NaCl-Tl could be considered a combination of exponentials and power laws. The curves for KCl-Tl are more nearly exponential on the log I-log t plot than are similar curves of many other phosphors studied at this laboratory. However, the curve shape is not that of a single pure exponential plot. [By way of explanation it should be said that to obtain the curves of Figure 1(a), the irradiated phosphorescing material

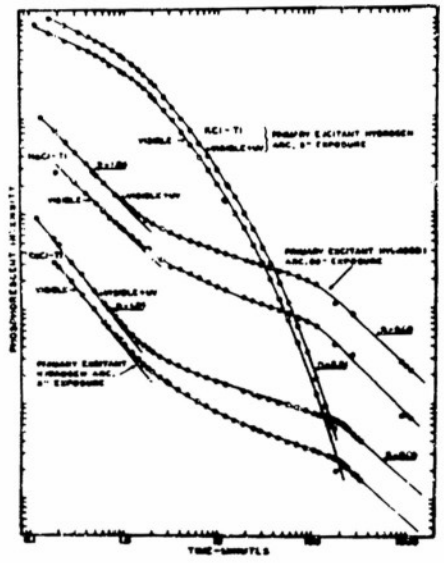

Fig. 1. (a) Decay of NaCl+0.1 per cent TlCl and KCl+0.1 per cent TlCl after excitation by uv. Excitation and decay at room temperature (25 C). The decay of the visible band is detected in an RCA-1P28 phototube with soft glass filter and that of the ultraviolet band and the visible together in a 1P28 without filter.

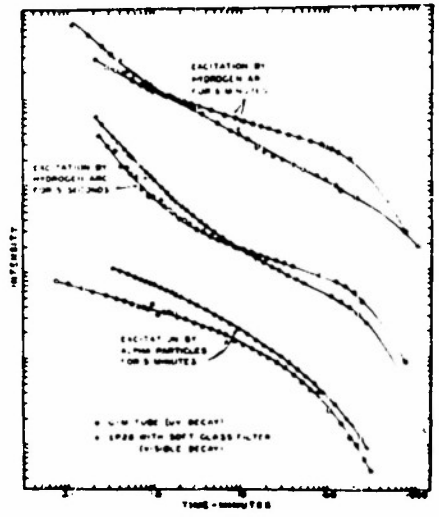

Fig. 1. (b) Excitation of NaCl+0.1 per cent TlCl (percentage TlCl concentration given by weight) by ultraviolet light and by alpha particles. In this case, the ultraviolet alone was detected in a photomultiplier 6-dt tube, and the visible alone in a filtered RCA-1P28. The differing modes of decay of the two bands is to be noted.

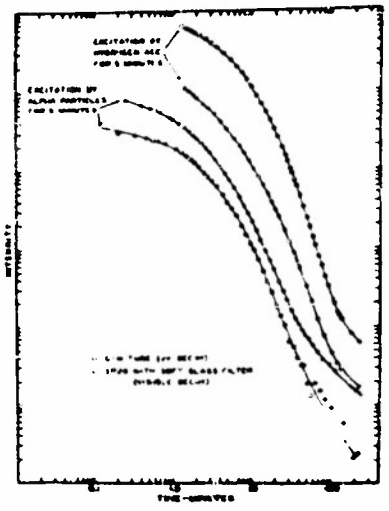

Fig. 1. (b) Decay of KCl+0.1 per cent TlCl after excitation by alpha particles and ultraviolet light. The decay of visible and ultraviolet emission has been studied separately by a proper choice of detectors.

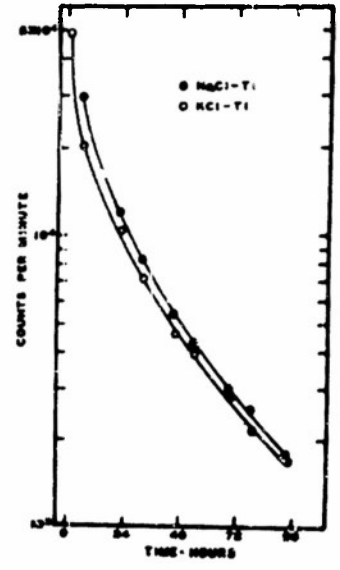

Fig. 2. Photostimulated emission of ultraviolet light from NaCl-Tl and KCl-Tl following excitation by a dosage of 20r of X-rays of maximum energy 25 Kev. The emission is observed simultaneously with photostimulation during periods of 6 seconds spaced at intervals of several hours.

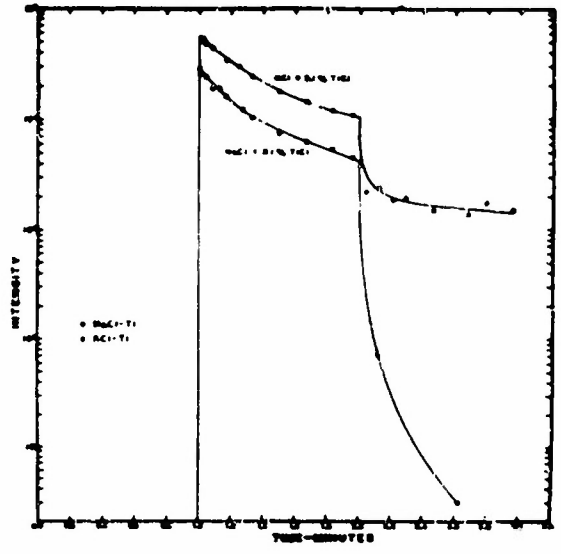

Fig. 3. Photostimulated emission of ultraviolet from KCl-Tl and NaCl-Tl (TlCl concentration 0.1 per cent by weight). The phosphors were given a dosage of 20r of X-rays and stored for 24 hrs., after which time they were photostimulated for a period of one minute. KCl-Tl exhibits a photostimulation afterglow of considerable intensity.

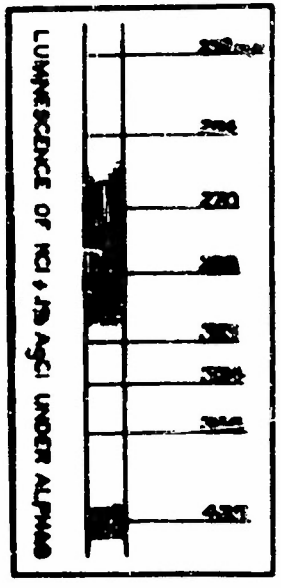

Fig. 4. Luminescent emission of KCl+Ag irradiated by alpha particles.

was placed between two 1P28 photo-tubes, one covered by a cylinder of soft glass. In this way the decay of the visible band alone could be measured in one tube and that of the visible and ultraviolet together in the other.] For the KCl-Tl phosphor, the decay law appears to be essentially the same in both spectral regions. The time of irradiation by ultraviolet from a hydrogen arc is given on the Figure for each set of two decay curves. The slopes of decay on the log I-log t plot are indicated at various points. For example, at $t \sim 100$ min, the decay of KCl-Tl has assumed a slope of $n = 2.21$. It is to be particularly noted that on the time-interval 2 min $< t <$ 200 min, the slope on the log I-log t plot of the decay curve of the visible band of NaCl-Tl is greater than is the same quantity associated with the decay of the ultraviolet band; that is, the slope is "steeper". This effect is studied further in Figure 1(b) where additional curves concerning NaCl-Tl are presented. To obtain these curves, the 1P28 tube detecting uv and visible light together was replaced by a G-M tube responding only to the ultraviolet. The relative "flatness" of the pure ultraviolet decay on the above mentioned time-interval is thus enhanced**.

** In an earlier publication (see reference 11) the writers described experiments which were designed to show that the ultraviolet band of NaCl-Ag follows a law of decay which differs from that of the visible band. The published measurements were performed with the use of a

photosensitive G-M tube as the ultraviolet detector and a photomultiplier as the detector of visible light. In the course of the measurements (reference 11), the question arose whether the differing decay laws were real or were purely instrumental in nature. It was thought that perhaps the photosensitivity of the G-M tube could vary with counting rate. To test this point, after the paper of reference 11 was submitted for publication, the G-M tube was replaced by an RCA-1P28 phototube. The decaying NaCl-Ag was placed between the two RCA-1P28's, one filtered by a soft glass filter, the other unfiltered. The decay curve of ultraviolet and visible together was found to be "steeper" than the curve of visible light alone. When the soft glass jacket was transferred from one phototube to the other, the differing decay laws were again encountered, attesting the reproducibility and general validity of the phototube measurement and confirming the earlier measurement with the photosensitive G-M tube.

In the case of all of the ultraviolet excited curves concerning NaCl-Tl in Figures 1(a) and 1(b), a rapid decay is in evidence at times below one minute. This mode of decay does not appear, however, in the case of the alpha-particle excited curve of Figure 1(b). From the various curves of Figures 1(a) and 1(b) it is apparent that the intensity of the short-period decay relative to the remainder of the decay curve is reduced as the excitation-time is increased.

In Figure 1(c), the alpha-particle excited phosphorescence of KCl-Tl is compared with the ultraviolet-excited

phosphorescence. From the very similar appearance of the two sets of curves, it can be concluded that the phosphorescence can be very probably attributed to the same mechanism. Moreover, the visible and ultraviolet decay laws appear to be very nearly the same. Again, it should be pointed out that the ultraviolet measurements of Curve 1(c) were obtained with a photosensitive G-M tube, whereas using the RCA-1P28, ultraviolet and visible bands were detected simultaneously in the unfiltered curves of Figure 1(a)***.

*** The two curves of each set of curves of Figures 1(a), 1(b) and 1(c) were always recorded simultaneously by placing the phosphorescing material between the two detectors. For example, when the detectors were RCA-1P28 with soft glass filter and photosensitive G-M tube, the visible band was recorded in the 1P28 and the ultraviolet band was recorded simultaneously with it in the G-M tube.

A new crystalline melt was used in obtaining the data of each of the separate Figures of Figure 1. For example, to obtain the measurements of Figure 1(b), a specimen of NaCl-Tl was twice excited by ultraviolet and finally by alpha particles. The irradiated material was, of course, completely de-excited by photostimulation between the successively obtained sets of curves.

Irradiated samples of KCl-Tl and NaCl-Tl were examined at a time many hours after initial excitation to ascertain

the extent of energy storage of "light storage" in the crystalline material. In this instance samples of KCl-Tl and NaCl-Tl were irradiated for about one hour with X-rays to receive a total dosage of ∼20r. The excited samples were then placed in a dark cavity at a distance of 7 cm from a one-watt tungsten lamp. The photostimulated emission of ultraviolet was recorded in a Geiger counter during a period of 6 seconds while the stimulating light was on. This observation of photostimulated ultraviolet, emitted in six-second bursts, was repeated at intervals of several hours over a time of about 96 hours to obtain the curves of Figure 2. From the curves it is clear that after three days a counting rate of several thousand counts per minute is obtainable from either phosphor with the use of the relatively weak source of stimulating light. Measurements have shown that the number of stored electrons are appreciably reduced by the six-second period of photostimulation so that the curves of Figure 2 may be taken as only an approximate indication of the rate of decay of the stored light in KCl-Tl and NaCl-Tl.

In another experiment, samples of KCl + 0.1 per cent TlCl and NaCl + 0.1 per cent TlCl (percentages by weight) were irradiated for one hour by X-rays of maximum energy 25 Kev to receive a total dosage of ∼20r. The irradiated materials were then stored in darkness for twenty-four hours. At the end of this time the samples were removed from storage,

placed in a dark cavity, and irradiated with light of wavelength greater than 3600 Å from the tungsten lamp. The photostimulated emission of ultraviolet was recorded in a photosensitive Geiger counter as shown in Figure 3. The ultraviolet emission of NaCl-Tl is seen to rise sharply, remain high while the stimulating light is on and drop to essentially nothing when the stimulating light is extinguished at the end of one minute. In contrast with this behavior, KCl-Tl exhibits after one minute of photostimulation, a very considerable post-stimulation afterglow. The situation is just the reverse of that encountered in the case of the Ag-activated alkali halides[3]; then, the post-stimulation afterglow is associated with NaCl-Ag, and the ultraviolet emission of KCl-Ag drops sharply with cessation of irradiation by the stimulating light[3].

The Silver-Activated Alkali Halides

Copious light emission and good storage properties are to be found among the Ag-activated alkali halides. When KCl-Ag is irradiated by ultraviolet or by nuclear particles the spectrum of luminescence is composed of two bands centered respectively at ~2800 Å and ~4350 Å. An emission spectrum resulting from alphas on KCl-Ag is shown in Figure 4 as obtained with the use of a small Hilger quarts spectrograph.

A polycrystalline melt of KCl-Ag (AgCl content 0.1 per cent by weight), dimensions 1 cm x 1 cm x 0.5 cm,

weighing one gram, was irradiated in darkness by 25 mc of polonium alpha particles for thirty minutes. Immediately after cessation of bombardment by alphas, the sample of KCl-Ag was irradiated by filtered light ($\lambda > 3600$ Å) from the tungsten lamp having a total power dissipation of only one watt. The lamp was located seven centimeters from the KCl-Ag which was maintained at a constant temperature of 25° C by water-cooling. The decay of KCl-Ag under continuous photostimulation is shown in Curve A of Figure 5. The detector was a photosensitive Geiger counter. In the early stages of the photostimulated decay, a considerable dead-time loss was encountered because of the high initial counting rate. The actual counting rate is roughly indicated by the broken line. From Curve A, it is clear that the crystal was exhausted of stored energy in about one thousand minutes of photostimulation by the one-watt tungsten lamp. After complete de-excitation, the same crystal was again irradiated by polonium alpha particles, and the normal unstimulated phosphorescence was measured as a function of the time, as shown in Figure 5, Curve B. It was estimated that 1.36×10^6 counts lay under Curve A and that 3.6×10^4 counts are under Curve B, only 2.6 per cent of Curve A. When the crystal of Curve B was exhausted by photostimulation commencing at 1500 minutes, an additional 3×10^5 counts were observed. According to Curve A, $\sim 10^6$ counts should have been recorded.

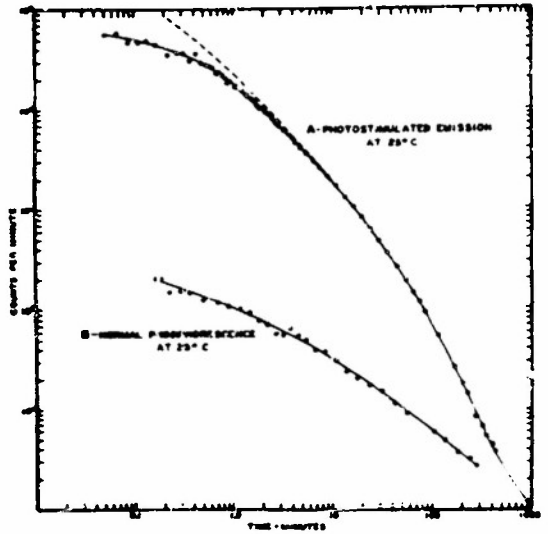

Fig. 5. Phosphorescence of KCl-Ag excited by alpha particles. Curve A, decay of the ultraviolet band under constant photostimulation; curve B, spontaneous phosphorescence at room temperature.

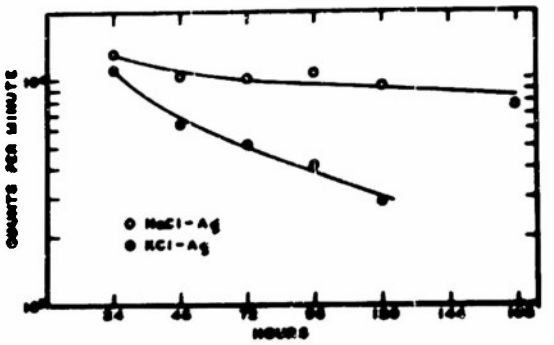

Fig. 6. Photostimulated emission of ultraviolet. Each phosphor had received a dosage of three roentgens at time zero.

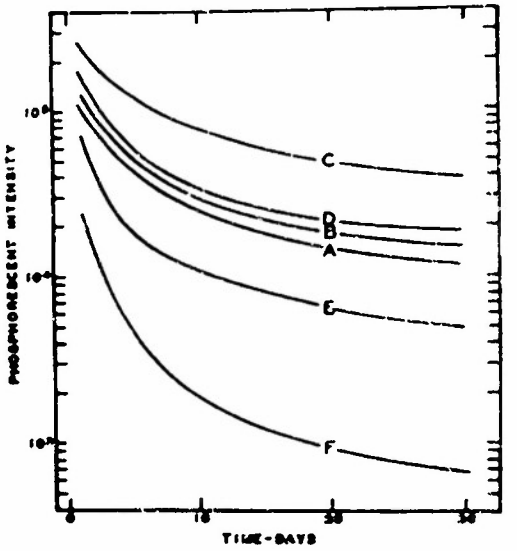

Fig. 7. Photostimulated emission of ultraviolet band of NaCl-Ag. Samples of identical volume were each given a dosage of 28r of X-rays. The emission was observed during a period of six seconds of photostimulation at intervals of twenty-four hours. The curves are lettered in order of decreasing silver concentration. See Figure 8 for percentages of AgCl by weight.

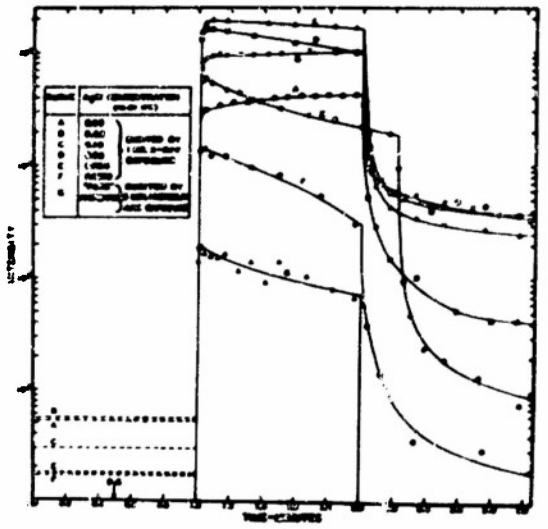

Fig. 8. Semi-logarithmic plot of photostimulated emission of ultraviolet band of (NaCl-Ag. The materials were irradiated by 28r of X-rays and stored for twenty-four hours in darkness, at the end of which time they were photostimulated for one minute by a 1 watt tungsten lamp at a distance of seven centimeters from the phosphor. The counting rate during the one minute of photostimulation and one minute thereafter is recorded. The highest counting rate is obtained for a silver chloride concentration of 0.10 per cent by weight.

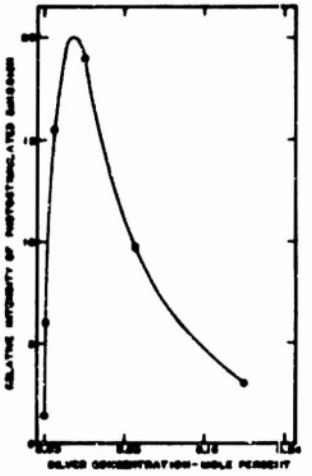

Fig. 9. Intensity of the photostimulated emission of the ultraviolet band of NaCl-Ag as a function of the concentration of AgCl in mole per cent.

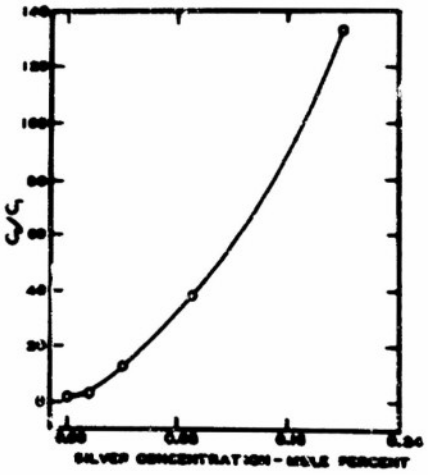

Fig. 10. Ratio of post-stimulation phosphorescence to co-stimulation phosphorescence. These data are taken from Figure 8. C_2/C_1 is specifically defined in the text.

The result indicates that $\sim 7 \times 10^5$ counts or 70 per cent of the stored energy was lost through thermal processes in about 1500 minutes. In the course of the 30-minute bombardment by alphas, which preceded both Curve A and Curve B of Figure 4, 2.06×10^6 counts were recorded in the G-M tube in the form of short-lived fluorescence and unstimulated phosphorescence. The excitation, photostimulation, and counting were carried out with adequate exclusion of extraneous light.

A comparison of the storage properties of KCl + 0.1 per cent AgCl and NaCl + 0.1 per cent AgCl is shown in Figure 6. The respective polycrystalline masses (equivalent in weight) of either phosphor had received a dosage of 3r during an excitation time of 10 minutes. The "stored light" was subsequently released, in six-second bursts by photostimulation at intervals of twenty-four hours. The observation of photostimulated ultraviolet was made during the six-second stimulation period. The counting rate thus obtained and plotted in Figure 6 may be taken as a rough measure of the amount of stored energy remaining in the crystal after an elapse of time specified by the axis of abscissas of the curves. From these two curves, it is clear that better storage properties are exhibited by NaCl-Ag than by KCl-Ag. There is, however, the post-stimulation afterglow[3] of NaCl-Ag which from the viewpoint of practical application could present a problem. This matter will be discussed later.

To ascertain what silver concentration leads to the best "light storage", polycrystalline melts of NaCl-Ag were prepared in which the silver concentration varied from 0.5 per cent AgCl by weight to 8×10^{-4} per cent AgCl by weight. Identical quantities of each phosphor were irradiated for one hour to receive $\sim$20r of X-rays****.

**** The volume of the irradiated phosphors was usually 1 cm x 1 cm x 0.5 cm.

They were stored in darkness and photostimulated by the one-watt tungsten lamp for 6 seconds daily. The counting rate observed during the six-second stimulation period is plotted in Figure 7. The measurements were continued over a period of thirty days. From the curves of Figure 7, it is clear that a silver concentration corresponding to addition of about 0.1 per cent AgCl by weight yields the maximum light emission during photostimulation. Here again, it should be made clear that as in the case of Figure 2, the curves of Figure 7 do not represent the actual decay of the stored energy in NaCl-Ag. The amount of stored energy is perturbed by the measurements themselves. Each six-second burst of photostimulated light drawn from the phosphor reduces in not negligible amounts the total of remaining stored energy. One sample of NaCl + 0.1 per cent AgCl showed, after 5 six-second periods of photostimulation, about 15 per cent less

activity than an identical specimen, which had not been previously photostimulated at all. The appreciable reduction of the stored light by the brief periods of photostimulation could be, of course, eliminated by using a weaker tungsten bulb.

A second batch of polycrystalline samples of NaCl-Ag of differing silver concentration were similarly tested as shown in Figure 8. In this case, the crystals were again irradiated to receive ~20r and stored in darkness. Twenty-four hours after excitation, each phosphor was photostimulated for about one minute. The ultraviolet emission was recorded during the one minute of photostimulation as well as afterwards to measure the post-stimulation afterglow. Here again, the initial rise in counting rate upon onset of photostimulation is greatest when the added AgCl is 0.1 per cent by weight. The various values of the initial counting rate (t = 1 minute, time zero is taken as one minute before the photostimulating light is turned on) are plotted in Figure 9. The maximum of ultraviolet emission between AgCl concentrations of 0.02 and 0.10 per cent by weight is clearly evident. In Figure 9, the AgCl concentration is given in mole per cent. Another quantity obtainable from Figure 8 is also plotted. This is C_2/C_1 where C_2 is the counting rate at t = 2 minutes arising from the post-stimulation afterglow and C_1 is the co-stimulation emission of ultraviolet at the instant of initial

photostimulation at t $\sim$1 minute. The quantity C_2/C_1 is seen to increase with silver content. These data are shown in Figure 10.

Discussion of Results

From the standpoint of practical dosimetry, the data of the foregoing discussion should be of some value. It has been emphasized that the entire investigation including excitation and all measurements has been carried out at room temperature (25° C), the situation which is met in practice. Many phosphors store energy at liquid nitrogen temperatures, their filled traps emptying during the approach to room temperature. These materials would obviously have no practical value.

The curves of Figure 7 show that certainly the storage is effective enough for accurate measurements. For example, the curve corresponding to an AgCl concentration of 0.10 per cent by weight, curve C, indicates a counting rate of forty thousand counts per minute obtainable during photostimulation at the end of thirty days. Using a sufficiently weak stimulating light, counting rates of certainly several thousand counts per minute might be obtained without appreciably altering the amount of stored energy. Thus, in the event of an error in making a first reading of the dosage, the phosphor could be "re-read". If successive readings are separated by only short-time intervals, it is

obvious that the post-stimulation afterglow such as that exhibited by NaCl-Ag[3] and by KCl-Tl (see Figure 3), could yield misleading results. It has been previously shown[1], that NaCl-Ag can be re-used after having received a dosage of millions of roentgens. Thus, after having received a sizeable initial dose, the phosphor dosimeter can be de-excited and made ready for receipt of another dose of nuclear radiation. It is easy to visualise the collection of small light-tight capsules containing activated alkali halide dosimeters which had been previously located in an area subjected to atomic attack. These containers could be opened and read under standard conditions of photostimulation and detection to ascertain the previously received dosage. Knowing the time of the disaster, curves similar to those of Figure 7 could be used to calculate the initial dose. It is evident that considerable work of a developmental nature must be carried out to standardize a phosphor dosimeter of the type described above. It would probably be necessary to develop single crystals of uniform response as well as a detection "kit", the components of which (counter, etc.) could be manufactured reproducibly in quantity.

Turning to the more technical aspects of the data, it might be said that it would be difficult to ascribe the bands of emission of the silver-activated alkali halides to definite excited states of the silver ion without detailed calculations. The ground state[10] of Ag^+ is $^1S_0$.

10) R. F. Bacher and Samuel Goudsmit, Atomic Energy States, (McGraw-Hill Book Co., Inc., New York) p. 38 (1932).

The first group of excited states are D states which are sufficiently separated in energy from the ground state to account for the emission bands. However, direct transitions between S and D states are forbidden by parity considerations, if spectroscopic selection rules are to be followed. In an earlier paper[11], an attempt was made to explain the behavior

11) C. E. Mandeville and H. O. Albrecht, Phys. Rev. 90, 25 (1953).

of the phosphorescence of NaCl-Ag only by the presence of imperfection traps. This discussion cannot be regarded as a full interpretation, because the formation of metastable excited Ag^+ was not considered. The excited states of Tl^+ giving rise to the emission bands of KCl-Tl have been accurately identified[8].

It should perhaps also be remarked that the curve of Figure 9 is very similar in general shape to the curves for luminescent efficiency versus activator concentration which have been calculated for various other phosphors[12].

12) See for example Johnson and Williams, J. Chem. Phys. 18, 1477 (1950).

The specific case of NaCl-Ag has not yet been treated with a quantitative theoretical approach.

D. CONCERNING COUNTERS.

Observation of the Positive Ion Flux at the Cathode of a G-M Counter.

Introduction

In discussing features of G-M counter-behavior related to the motion of the positive-ion sheath, many investigators have represented the ion sheath in cylindrical counters as a lamina of charge which remains infinitely thin during the entire process of formation and radial expansion toward the cathode. Recently Wilkinson[1] has shown theoretically that

---

1) D. H. Wilkinson, Rev. Sci. Instr. 23, 463 (1952).

---

owing to mutual repulsion between ions, the sheath can puff itself up while in transit to the cathode until it may occupy as much as half the volume of the counter before the first ions are collected. While the thin-sheath approximation is entirely adequate for calculating dead-times, a more precise description of the sheath must be utilised in any attempt to correlate the time-distributions of delayed spurious-counts with the arrival of positive ions at the cathode.

In preparation for a detailed study of the origin of spurious counts, we have devised a technique (independently suggested by Wilkinson) for observing the rate of impingement

of positive ions upon the cathode of a G-M counter as a function of time after a discharge. The main purpose of this paper is to describe this technique and to compare the measured cathode ion-fluxes in typical counters with Wilkinson's theory.

Apparatus

The experimental arrangement is diagramed schematically in the upper portion of Figure 1. A copper-wall counter of 0.738 in. internal diameter and having a Tungsten wire 0.003 in. diameter was used in all of the experiments. In the cylinder wall, a 3/16 in. hole was drilled and wire screening of mesh 325* was soldered over this hole. To receive positive ions

---

* Supplied by W. S. Tyler Company

---

passing through the grid, a centimeter square collecting-plate curved to conform to the cathode cylinder was placed .080 in. outside the grid. The probe was connected directly to the first grid of a local preamplifier and shunted to ground with a resistance of such value as to yield an input RC time-constant of 10 μsec. As the current-impulses to the probe lasted approximately 100 μsec., the chosen input time-constant yielded an amplifier input-voltage closely comparable in shape to the ion-flux impulse arriving at the counter cathode. The amplifier output pulses were viewed on a

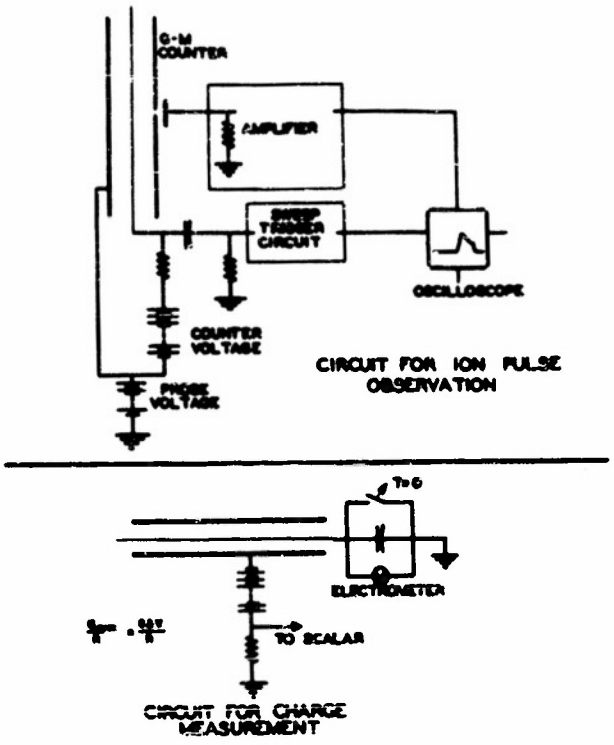

Fig. 1. Schematic diagrams of circuits used for observing the positive ion flow (above) and total charge developed in the discharge (below).

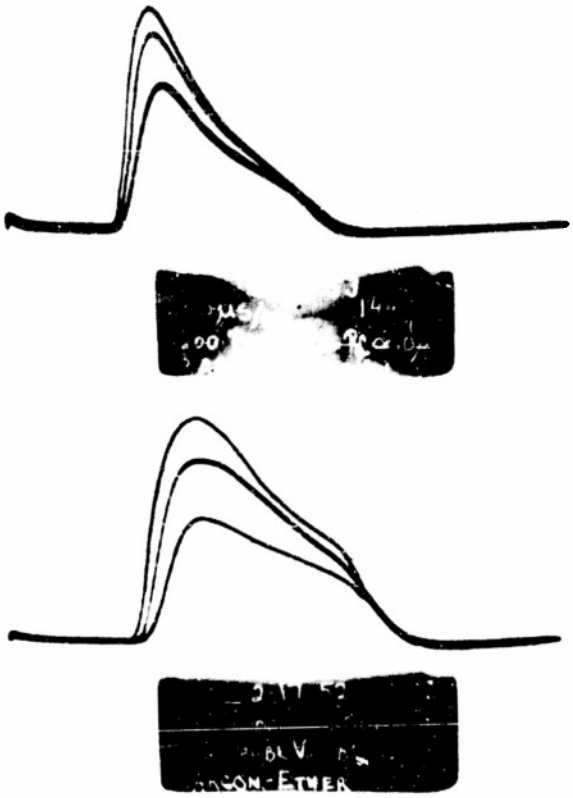

Fig. 2. Typical positive ion flux pulses displayed on a horizontal oscilloscope time base. Above--Argon-alcohol mixture Below--Argon-ether mixture. Dependence of pulse shape upon probe-voltage is indicated.

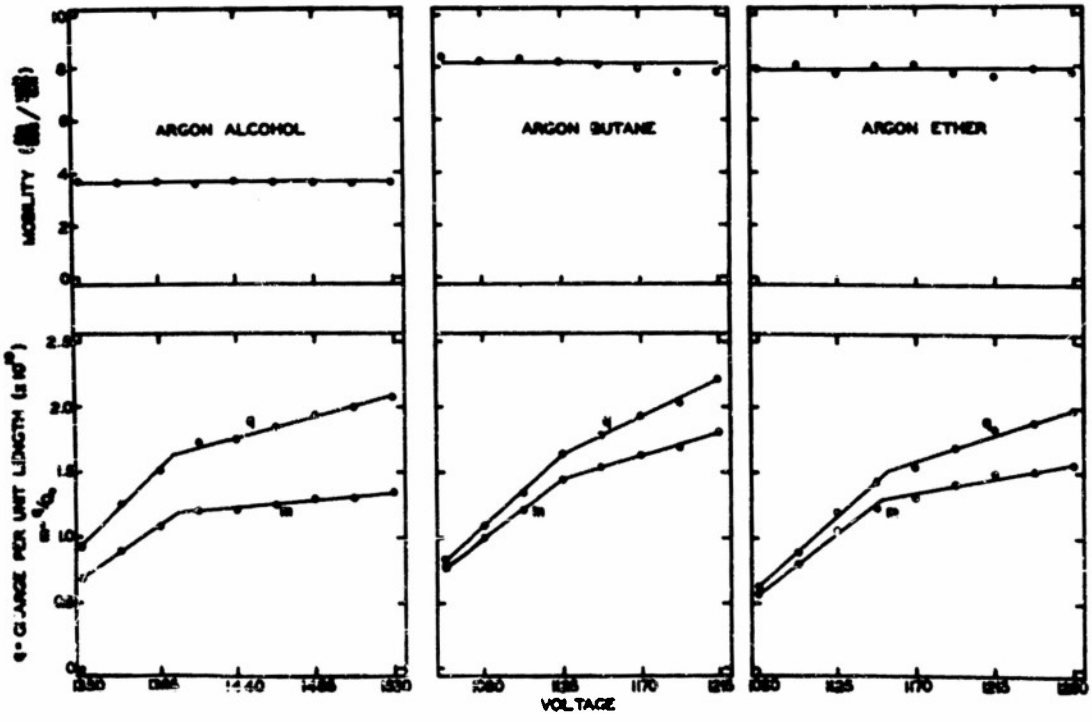

Fig. 3. Lower curves -- variation of q and m with counter operating potential for several gas mixtures. Upper curves -- calculated ion mobilities in corresponding mixtures.

Tektronix oscilloscope with its horizontal sweep triggered by the current impulses through a 500 Ω resistance connected in series with the counter wire. This method of triggering initiated the sweep within 10^{-6} sec. after the start of each discharge.

For the purpose of measuring the average charge per pulse, (a quantity required for computation of the ion sheath motion from the theory) a simplified version of a method used by Stever[2] was employed. In the lower section

---

2) H. G. Stever, Phys. Rev. 61, 38 (1942).

---

of Figure 1 is shown a diagram of the circuit used for the charge-measurement. The components are a 0.5 μfd. mica condenser, a Central Scientific Company electrometer, a scaler, and a shorting switch. The potential was applied to the counter with the switch across the condenser closed. At some arbitrary time called t = 0, the shorting-switch was opened simultaneously with a switch that turned the scaler on. When the voltage across the condenser reached 1.0 volts, the scaler was turned off and the number of counts n on the scaler recorded. The relation $\frac{C\Delta V}{n}$ therefore gives the average positive-ion space charge per pulse in coulombs.

The following three gas mixtures were used in the course of the investigation.

A. 80 mm Argon, 20 mm ethyl alcohol
B. 103 mm Argon, 17 mm butane
C. 59 mm Argon, 9 mm ethyl ether

The counter was filled on a glass vacuum system evacuated by means of a fore pump to approximately 10^{-3} mm Hg before admission of mixture B. In the case of mixtures A and C, however, satisfactory counter performance could not be attained without prior evacuation of the system to 10^{-6} mm Hg.

Experimental Results

Oscillograms of the ion-flux pulses obtained with mixture A and C are shown in Figure 2. These photographs are each triple exposures obtained by applying potentials of 300, 600, and 900 volts between the cathode and collection probe while maintaining fixed cathode-to-anode potentials of 1440 and 1170 volts with mixtures A and C respectively. The successive increases in pulse height associated with 300 volt increases in the probe potential indicate that the ion-flux is partially interoepted by the grid in this range of collection-potentials. Owing to the occurrence of sparking between the grid and probe, it was not possible to utilize collection-potentials greater than 900 volts. While this

limitation introduced some shape-distortion in the recorded pulses, the starting and ending-time of the pulses were little affected by probe potential charges.

With the collection-potential applied between the cathode and the ion probe reduced to zero, no probe-pulses were visible on the oscilloscope time-base. This was a sufficient indication that the positive-ions directed toward the grid induced practically no charge upon the collecting probe until they passed through the grid.

The pulses shown in Figure 4 (traced from photographs) indicate the effect of counter-voltage variation upon the ion-pulse obtained with mixture C. Sets of curves similar to those shown in Figure 4 were obtained also with the argon-alcohol and the argon-butane mixtures. The use of these curves together with Wilkinson's theory permits one to estimate the mobilities of positive ions in the various mixtures, as will be described below.

In the lower section of Figure 3 are plotted measured values of the positive-ion space-charge q, created per unit length of the wire per discharge as a function of counter-operating potential V. Curves are shown for each of the gas mixtures investigated. The ratio $m = q/Q_o$, where Q_o is the calculated charge per unit-length on the central wire in the quiescent condition, is also plotted as a function of V for each gas. The quantities m and Q_o are used in calculating ion-mobilities and in computing the theoretical ion-flux at the counter cathode as a function of time.

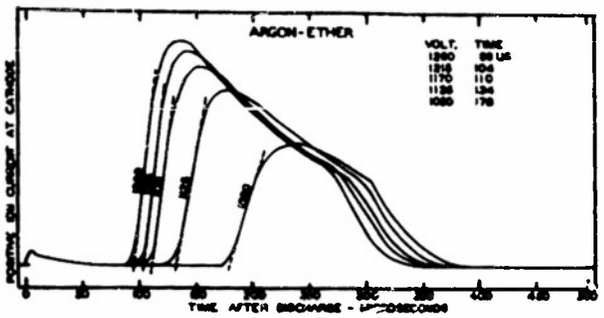

Fig. 4. Positive ion flux at various operating potentials. Argon–ether mixture.

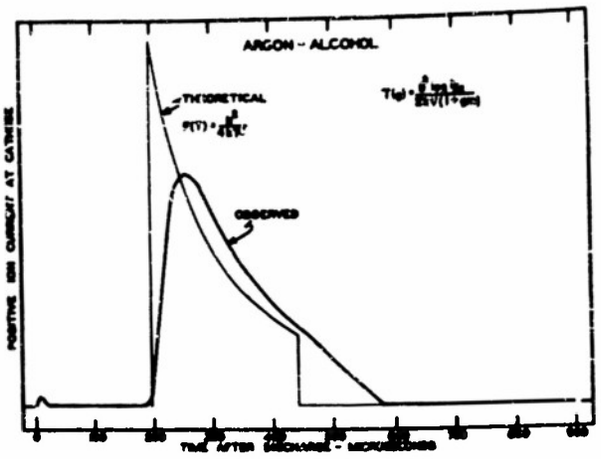

Fig. 5. Comparison of observed and theoretical ion flux.

Fig. 6. Double exposure showing normal ion pulse and superimposed double pulse resulting from two discharges in rapid succession.

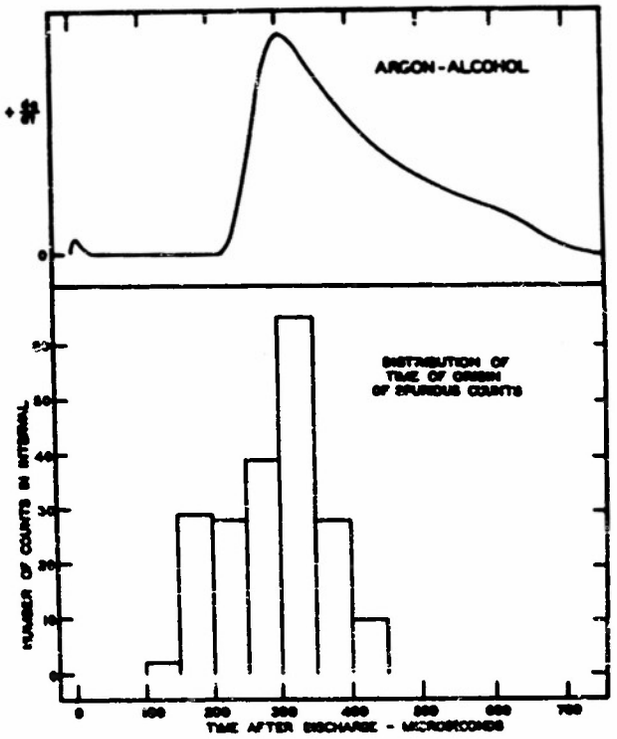

Fig. 7. Statistical distribution of delayed spurious counts (histogram) and positive ion flux (upper curve) each measured under the same counter operating conditions.

Theory

Consider a cylindrical G-M counter with wire radius a, cathode radius b and an applied potential V. The external circuit resistance will be assumed sufficiently small that the wire-to-cathode potential remains essentially constant during the discharge. We concern ourselves with the behavior of the ion sheath subsequent to the instant when gas amplification ceases, assuming that from this time onward the sheath consists of ions of one kind, all having the same mobility. We neglect diffusion, which has a relatively slight effect on the spacial development of the ion sheath, and consider each ion to move with a radial velocity v proportional to the field strength X. Letting Q_o devote the charge per unit length on the wire in the absence of space-charge, q the charge per unit length in the ion sheath (a constant along the axial dimension) and f(r,t) the fraction of the space-charge lying between the wire and radius r at time t, we have for the general specification of the field:

$$X(r,t) = \frac{2}{r}\left\{ Q_o + qf - q\int_a^b \frac{df}{dr}\,\frac{\log b/r}{\log b/a}\,dr \right\} \qquad (1)$$

$$Q_o = V / 2 \log b/a$$

Applying the condition of charge-continuity one obtains the equation

$$\frac{1}{K}\frac{\partial}{\partial t}\left(\frac{\partial f}{\partial r}\right) = X\frac{\partial^2 f}{\partial r^2} - \frac{1}{r}\frac{\partial f}{\partial r} + \frac{\partial f}{\partial r}\frac{\partial X}{\partial r} \qquad (2)$$

where K is the ion mobility.

Substitution of X from Equation 1 into Equation 2 yields a rather complex integrodifferential equation for $f(r, t)$ whose general solution is a matter of extreme difficulty. By neglecting the integral term in Equation 1, one obtains a much simpler equation, whose solution has been shown by Wilkinson to predict ion transit times differing in practical cases by only a few per cent from those given by the more precise equation. (The integral term in Equation 1 represents the charge induced on the wire by the ion sheath.)

The solution to the simplified problem yields the following result for the cathode ion-flux F as a function of time T after the discharge.

$$F(T) = \frac{b^2}{4Kt^2} \; ; \quad T_1 \leq t \leq T_o \qquad (3)$$

$$F(T) = 0 \begin{cases} t < T_1 \\ t > T_o \end{cases}$$

T_1 and T_o represent the collection times of the outermost and innermost ions, respectively, and are given by

$$T_1 = b^2 \ln {}^{b}/_{a} \Big/ \left[2 KV (1 + m) \right] \qquad (4)$$

$$m = {}^{q}/_{Q_o}$$

$$T_o = b^2 \ln {}^{b}/_{a} \Big/ 2KV \qquad (5)$$

It will be noted that the above relations contain no parameters descriptive of the sheath configuration at time t = 0. This comes about because of the neglect of terms which are vanishingly small in the practical case where all ionization occurs within a very short distance from the central wire. Assuming that the initial ionization occurs within a few wire-diameters away from the central axis of a counter of typical construction one can show that F (T) is practically unaffected by the choice of the initial distribution of ions and reduces essentially to the form given above. (Experiments with beaded-wire counters have clearly shown that in self-quenching mixtures, the ionization is confined to a region of the order of that assumed here.)

Comparison of Observed and Calculated Ion Fluxes

By inspection of Equations 3 and 4 it is evident that the specification of T_1 (the transit time of the outer ions) together with the quantities a, b, V and m completely determines the shape of the ion-flux F (T), the end-point T_o, and the ion mobility K. In Figure 5 we have plotted an observed pulse (mixture A; V = 1485 V, M = 1.3) together with the theoretical flux F (T) fitted by matching T_1 with the leading edge of the observed pulse. (The amplitude of the theoretical pulse is chosen arbitrarily.)

While there are several definite points of similarity between the observed and calculated pulse shapes, there is a considerable difference between the two shapes near the leading and trailing edges. The nature and magnitude of the discrepancy is quite similar for the various gas mixtures and can be explained partially by considering the effects of diffusion, amplifier distortion and grid-to-probe transit time.

According to the kinetic theory of gases the following general relationship exists between the coefficient of diffusion D and the mobility K of singly-charged heavy ions.

$$D = .0235\ K \qquad (6)$$

where D is expressed in cgs units and K is in cm/sec. Neglecting the effect of inhomogeneous field upon the diffusion, the ions contained at time T = 0 in an elementary lamina of the sheath will, upon reaching the cathode, be disbursed into a nearly gaussian radial distribution with an rms thickness $\sqrt{2\ DT}$ (where T is the average transit-time of the ions of the lamina under consideration). Upon integrating the spreading of the individual lamina over the entire sheath, one finds that the trailing edge of the sheath -- which is sharply defined in the absence of diffusion -- becomes smeared out over a distance of approximately $-\Delta r = 3.3\sqrt{2\ D\ T_c}$. Then the tail of the ion-flux pulse

should be smeared out over a time-interval

$$\Delta T = KX_o \Delta r = 3.3\, KE_o \sqrt{2\, DT_o} \qquad (7)$$

where K is the ion mobility and X_o is the electric field at the cathode when the ion sheath is completely collected. Using the K-value arrived at in the fitting shown in Figure 5 the evaluation of the Equations 6 and 7 yields ΔT = 28 μsec. for the tail of the theoretical pulse. The ΔT value of the observed pulse-tail (the time-interval between the break at 470 usec. and the end of the pulse-tail at 580 μsec) is approximately 4 times greater than the ΔT expected to arise from diffusion. In estimating the diffusion spread by the above over-simplified procedure we have used approximations which tend to exaggerate the distortion of the pulse-tail. This may be understood by noting that ions which diffuse behind the inner boundary of the sheath find themselves in a field of higher intensity than those nearer the boundary. Consequently, there is a tendency for the lagging ions to "catch up" with the sheath and to reduce the over-all diffusion spread to a value less than that calculated above.

An analysis of the distortion introduced by the finite grid-to-probe transit-time and the imperfect differentiation of the amplifier input circuit shows that a ΔT of approximately 30 μsec., in addition to that introduced by diffusion, should be imposed upon the rise and fall time-intervals of the theoretical pulse plotted in Figure 5.

The arguments presented here, although admittedly rough, seem to exclude the possibility that a precise treatment of diffusion and instrumental effects would completely explain the discrepancies between the observed pulse in Figure 5 and the theoretical shape. There exists, however, the possibility that additional broadening might be introduced by the mixed character of the ions immediately after the discharge, and/or by the formation of ions belonging to two or more distinct mobility groups (by the attachment of impurity molecules to ions of the quenching vapors).

Spurious Counts

The photograph shown in Figure 6 is a double-exposure showing a normal ion-pulse of the type discussed above, together with a pulse with a double-peaked structure. The double pulse represents an event in which the counter was discharged twice in rapid succession. The first discharge triggered the sweep and before the ions generated in this discharge were completely collected, a second discharge occurred. According to expectation, the ion sheath of the second discharge so increased the electric field in the outer regions of the counter that the collection of the remainder of the first sheath was greatly accelerated. This is indicated by the less-than-normal width of the first pulse. Also worthy of note is the fact that the second sheath contains fewer ions than a normal sheath. This is a

result of the fact that the later discharge occurred at a time when the field at the central wire was reduced by the presence of uncollected space-charge from the prior discharge.

The study of a large number of events of the double-peaked variety photographed on a continuously moving film yielded the statistical distribution of spurious counts shown in Figure 7. The histogram in the lower portion of the figure represents the relative probability that a spurious count occurred in each 50 μsec. interval of a time-base triggered by a non-spurious pulse. The time of spurious count initiation was determined by the location of a small inductive pip on the time-base. The upper portion of Figure 7 is a normal ion-pulse obtained under the same operating conditions as the histogram and is plotted on the same time-scale. In obtaining the spurious count data the counter was operated at a rate such that the chance of a random count occurring in the first 1000 μsec. of any trace was negligible.

The distribution of spurious counts displays several points of interest. In the first place, it is evident that a number of such counts occurred before the first ions from the preceding discharge had reached the cathode (i.e. sooner than 250 μsec. after the sweep was triggered). This clearly indicates that not all spurious counts are related to the neutralization of positive ions at the cathode, and would seem to be a result either of the Auger effect, or of the

emission from excited gas atoms of photons sufficiently energetic to eject photo-electrons from the counter walls. The occurrence of spurious counts in the interval from 0 to 100 μsec. is prohibited by the 100 μsec. dead-time of the counter.

A second point of interest is that the histogram has a maximum at a time coincident with the peak of the cathode ion-flux (~300 μsec.). This indicates that a part of the spurious counts are associated with ion-impact upon the cathode. It is, however, of considerable importance to note that the histogram cuts off sharply at 450 μsec. whereas the ion-flux of a normal discharge proceeds with gradual abatement until about 700 μsec. This observation is very difficult to explain on any basis other than that the sheath contains ions of at least two distinct mobilities. The outer edge of the sheath seems to contain ions of a type which has a relatively strong tendency to produce spurious counts upon impact whereas the tail of the sheath is comprised of another class of ions exhibiting a much smaller tendency to release electrons from the cathode. If the sheath is indeed not homogeneous in ionic composition, as this indicates, there is very good reason for expecting the observed ion-flux to depart more from the calculated shape than the prior considerations imply.

Positive Ion-Mobilities

The above discussion indicates that one should not expect to obtain precise values of ion-mobilities with data of the present kind. However, one may get some rough estimates by inserting in Equation 4 measured-values of V, a, b, m and setting T_1 equal to the time-axis intersect of a straight line drawn along the leading edge of the ion-pulse (see extrapolations plotted in Figure 4). In the upper part of Figure 3 are plotted values of the mobility computed in this manner for gas mixtures A, B, and C at various operating voltages. The K-values remain constant against voltage variations of the order of 20 per cent. It is a well-known fact that the mobilities of ions in a given mixture of pure gases can be drastically altered by adding impurities in concentration no greater than a few parts per million, and can also depend upon the age of the ions. As no drastic precautions were taken to avoid impurity-contamination in this work, there is a considerable likelihood that impurity concentrations of a magnitude sufficient to interfere with the mobility of the quenching gas-ions were present. For this and other reasons the mobility-values given here must be regarded as rather crude approximations.

Conclusions

The experimental results directly confirm Wilkinson's prediction that the ion-sheath in a G-M counter is drastically thickened during its transit to the cathode. Within the uncertainties associated with factors neglected in the theory (e.g. diffusion and inhomogeneous ionic composition) the observed ion-flux pulses are in accord with the predictions of the theory.

The ion-probe method utilized in the present work is a sensitive means of determining what proportion spurious counts in a given type of counter are associated with positive ion-impact at the cathode and under certain conditions the method can indicate the presence of two or more groups of positive ions possessing different mobilities.

III. LINEAR ACCELERATOR.

By virtue of improvements which have been introduced during the past year, the linear accelerator is now a very satisfactory tool for studies of the interactions with matter of electrons having energies up to 1.5 Mev. During this period the beam-current has been increased approximately a hundred-fold, and the overall stability of the machine has been improved to such an extent that it can now be maintained in almost constant operation with a minimum of attention.

The linear accelerator is now being utilized primarily for investigating secondary electron emission from thin targets. Various aspects of this phenomenon have been considered from the theoretical and experimental points of view with the support of Contract Nonr 198(00) with the Office of Naval Research and Contract DA-36-034-ORD-1216RD with the Office of Ordnance Research. Although certain phases, for example, the production of delta rays by high energy electron bombardment of metals, are of immediate interest in the broad field of nuclear physics, the support previously provided by Contract N6ori-144 is not required at the present time. The detailed description of this work as a portion of this Annual Report has therefore been discontinued in view of the fact that periodic reports are submitted under the aforesaid contracts.

PUBLICATIONS

All of the work described in this Annual Report (appearing between dates of October 1, 1952 and September 30, 1953) will be published in suitable form in various scientific journals--primarily THE PHYSICAL REVIEW, NUCLEONICS, JOURNAL OF CHEMICAL PHYSICS, or the JOURNAL OF THE FRANKLIN INSTITUTE.

Recently published works carried out under this Contract are:

"Gamma-Rays from Sn^{125}", by C. E. Mandeville, E. Shapiro, R. I. Mendenhall, E. R. Zucker, and G. L. Conklin, Phys. Rev., Vol. 88, No. 3, 554-555, November 1, 1952.

"Radiations from Zr^{97} and Nb^{97}", by C. E. Mandeville, E. Shapiro, R. I. Mendenhall, E. R. Zucker and G. L. Conklin, Jour. of the Franklin Institute, Vol. 254, No. 5, November, 1952.

"Gamma-Radiations from Zr^{95} and Nb^{95}", by C. E. Mandeville, E. Shapiro, R. I. Mendenhall, E. R. Zucker, and G. L. Conklin, Phys. Rev., Vol. 89, No. 3, 559-561, February 1, 1953.

"Extending the Efficient Range of G-M Counters", by W. C. Porter, Nucleonics, Vol. 11, No. 3, 32-35, March, 1953.

"The Alpha-Particle Induced Phosphorescence of Silver-Activated Sodium Chloride", by C. E. Mandeville and H. O. Albrecht, Phys. Rev., Vol. 90, No. 1, 25-28, April 1, 1953.

"Spin and Parity of the 2.3-Mev Excited State of Te^{124}", by Franz R. Metzger, Phys. Rev., Vol. 90, No. 2, 328-329, April 15, 1953.

"The Phosphorescence of Thoria", by C. E. Mandeville and H. O. Albrecht, Phys. Rev., Vol. 90, No. 5, 992-993, June 1, 1953.

"Specific Primary Ionization of H_2, He, Ne, and A by High Energy Electrons", by G. W. McClure, Phys. Rev., Vol. 90, No. 5, 796-803, June 1, 1953.

PUBLICATIONS (Continued)

"The Storage of Energy in Silver Activated Potassium Chloride", by C. E. Mandeville and H. O. Albrecht, Phys. Rev., Vol. 91, No. 3, 566-567, August 1, 1953.

"The "Chemical Knife"; Preservation of Ozone for Thirty-Six Days", by H. O. Albrecht, Jour. of Chemical Physics, Vol. 21, No. 8, 1421-1422, August, 1953.

"Lower Limit for the Lifetime of the 665-Kev Excited State of Mo^{97m}", by F. R. Metzger and W. B. Todd, Phys. Rev., Vol. 91, No. 5, 1286-1287, September 1, 1953.

"Radiations from Arsenic^{77} and Germanium^{71m}, by B. L. Saraf, J. Varma and C. E. Mandeville, Phys. Rev., Vol. 91, No. 5, 1216-1218, September 1, 1953.

ON H. ALFVÉN'S THEORY OF THE EFFECT OF MAGNETIC STORMS ON COSMIC RAY INTENSITY

by W. F. G. Swann

Director, Bartol Research Foundation of The Franklin Institute, Swarthmore, Penna.

Introduction

H. Alfvén[1] has proposed an ingenious theory to explain the effect of magnetic storms on cosmic ray intensity. It is founded upon the assumption that a mass of highly conducting gas originating in a region where there is a large magnetic field emerges as a stream, carrying the magnetic field with it as a result of its high conductivity. The case is considered in which the magnetization is perpendicular to the velocity of the stream, in which case the motion of the matter, in its own magnetic field brings about a condition in which a stationary observer sees a change displacement in a direction perpendicular to the velocity and to the magnetic field.[2] Alfvén's theory, as presented, is confined to the case where the stream of gas moves in a non-conducting medium, and our discussion will be limited, in the first instance, to this case. The argument of Alfvén is to the effect that the field along the axis of y is $-vH/C$, and the potential change of a cosmic ray

1) H. Alfvén, Phys. Rev., 75, 1732 (1949).

2) In all that follows, we shall denote by S the so-called laboratory system with respect to which the motion is observed. S' shall denote a system moving with the gas. The velocity, v, shall be parallel to the axis of x. The magnetic field, H, shall be along the axis of z which shall be perpendicular to the plane of the paper, so that the axis of y shall be in the plane of the paper and perpendicular to the velocity.

in crossing the beam is vhH/C, where h is the width of the beam and C is the velocity of light. It is thus concluded that if T is the kinetic energy, the change in kinetic energy in crossing the beam is δT, where

$$\delta T = vhHe/C \qquad (1)$$

where e is the charge on the particle.

The change of kinetic energy leads to an expression for the change of cosmic ray intensity, in a manner which does not concern us here,[3] since our problem involves the change in kinetic energy, and in particular the relation (1).

3) Incidentally, there appears to be an error in Alfven's calculation of the relation between change of intensity and change of energy. This matter is discussed in the present writer's paper "Cosmic Rays", Journ. Frank. Inst. 251, 120-155 (1951). See in particular pages 146-147.

Discussion of the Theory

Relativistic Considerations:

In connection with the derivation and implications of equation (1), one must observe that we are here dealing with a problem in which the magnetic field moves with the matter. It will be convenient to concentrate our attention upon a finite slab, as represented in Fig. 1.

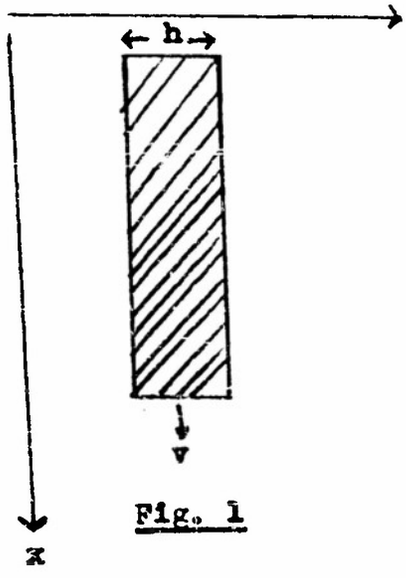

Fig. 1

Now we must observe that in the system S' which moves with the slab, there is no electric field, but only a magnetic field.

As a consequence, the cosmic ray particle never gains any energy in terms of measurements made in S'. If W is the energy of the particle[4]

---

4) It is to be observed that $T = W - m_0 c^2$

---

and M the momentum, we have that M_x, M_y, M_z, iW/C constitutes a 4-vector. Thus[5] WU_x, WU_y, WU_z, iW/C constitutes a 4-vector where U is the velocity

---

5) The essentials of the derivation immediately following are given in my paper cited under footnote 3). See page 134.

---

of the cosmic ray particle in S. Thus if dashed letters refer to the system S', and if $\beta = (1 - v^2/c^2)^{-1/2}$,

$$W = \beta\left(W' + \frac{vU'_x W'}{c^2}\right) \tag{2}$$

If, in the system S', the particle experiences a change in U'_x, from U'_{x1} to U'_{x2}, then since W' does not change in S', we shall have a change in W, given by $W_2 - W_1$, where

$$W_2 - W_1 = \frac{\beta W'(U'_{x2} - U'_{x1})v}{c^2} \tag{3}$$

Now the greatest possible value of $U'_{x2} - U'_{x1}$ is $\pm 2C$. Thus, if $|W_2 - W_1|$ is the absolute value of the change of W, we have

$$|W_2 - W_1| < \frac{2\beta W' v}{C} \tag{4}$$

From (2)

$$W_1 = \beta W'\left(1 + \frac{vU'_{x1}}{c^2}\right)$$

so that

$$|W_2 - W_1| < \frac{2W_1 v}{C\left(1 + \frac{vU'_{x1}}{c^2}\right)}$$

Now the smallest possible value of $(1 + vU'_{x1}/C^2)$ is $(1 - v^2/C^2) = \beta^{-2}$. Hence

$$|W_2 - W_1| < \frac{2\beta^2 W_1 v}{C}$$

$$|T_2 - T_1| < \frac{2\beta^2 v}{C}(T_1 + m_0 C^2) \qquad (5)$$

and unless v is comparable with C

$$|T_2 - T_1| < \frac{2v}{C}(T_1 + m_0 C^2) \qquad (6)$$

Alfvén's Numerical Conclusions:

Now Alfvén[1] considers a cosmic ray of energy 3×10^{10} e.v., and demands, through his formula (1) a ten percent change, with $h = 5\times10^{12}$, $v = 2\times10^{8}$ cms/sec. He finds $H = 3\times10^{-4}$.

With the above value of v, the quantity β is practically unity, and our formula (b) gives

$$\frac{T_2 - T_1}{T_1} < \left(\frac{4}{300}\right)\left(1 + \frac{10^9}{3\times10^{10}}\right)$$

$$< 1.37\times10^{-2}$$

Thus, Alfvén, from the aforesaid data, calculates a 10 percent change in T, and we have shown that the maximum possible change is 1.37 percent. Moreover, in calculating the value we have not had occasion to utilize any quantity but v. What is the origin of the discrepancy in this matter?

Origin of the Discrepancy:

It will be shown that the aforesaid discrepancy lies chiefly in the fact that Alfvén's magnetic field $H = 3\times10^{-4}$ would never allow a cosmic ray particle to pass through the slab. The easiest way to see this is from consideration of radius of curvature. Let us consider

matters in S'. If ρ is the radius of curvature of our cosmic ray in the field H', we have, if m is the relativistic mass,

$$\frac{m U'^2}{\rho} = \frac{H'e U'}{C}$$

$$\rho = \frac{m U' C}{H'e} = \frac{m C^2}{H'e}\left(\frac{U'}{C}\right) = \frac{W'}{H'e}\left(\frac{U'}{C}\right) \qquad (7)$$

$$\rho < W'/H'e$$

For[6] $W' = 3x10^{10}$ e.v. and $H = 3x10^{-4}$

$$\rho < \frac{3x10^{10}}{300x3x10^{-4}} = \frac{10^{12}}{3}$$

---

6) We need not concern ourselves with the difference between W' and W in the calculation.

Thus the radius of curvature is fifteen times less than the thickness ($5x10^{12}$ cms) assumed for the slab. A particle entering the slab in S' could not possibly travel a distance greater than 2ρ parallel to the axis of y before returning and emerging from the slab. Thus, no particle can penetrate right through the slab under the conditions cited. No second or third "try" in the event of the particle's seeking re-entry can be any more successful. Thus, the example cited by Alfvén represents a situation impossible of realization.

It is of interest to trace the above story by another path starting with Alfvén's expression (1), viz.

$$\delta T = \frac{vhHe}{C}$$

which we must assume to certainly fail if $h > 2\rho$. Since

$$H_z = \beta(H_2' - \frac{v}{c} E_y') = \beta H_z' \qquad (8)$$

$$\delta T = \frac{\beta vhH'e}{C}$$

Now we can substitute for H_e' in terms of ρ by using (7). Thus

$$\delta T = \frac{\beta W' U' v h}{\rho C^2}$$

δT increases with increase of h, and its maximum value is reached when $h = 2\rho$, thus

$$\delta T < \frac{2\beta v}{c}\left(\frac{U'}{C}\right)W' < \frac{2v\beta}{c} W' \qquad (9)$$

which is the same as the result (4) obtained directly from the relativity transformation.

<u>Correction between relativistic formula and Alfvén's formula when the latter is applicable.</u>

On the other hand, we can show that if the conditions of smallness of change of energy is satisfied, then Alfvén's result follows from the relativity transformation. Thus if θ_1' is the angle made by the cosmic ray with the plane of the slab at entrance in S' and θ_2' is the angle made at emergence, when emergence occurs, we have, referring to (3)

$$U_{x2}' - U_{x1}' = U' \cos \theta_2' - U' \cos \theta_1'$$

Now, if ds' is an element of path in the slab

$$dy = \sin \theta' \, ds' = \rho \sin \theta' \, d\theta'$$

where ρ is the radius of curvature, which, in this case, is constant. Thus

$$-h = \rho(\cos \theta_2' - \cos \theta_1') = \frac{\rho}{U'}(U_{x2}' - U_{x1}') \qquad (10)$$

Now

$$\frac{m U'^2}{\rho} = \frac{H' e U'^2}{C} \qquad (11)$$

Hence, from (10) and (11)

$$U_{x2}' - U_{x1}' = \frac{H' e h}{mC} = \frac{H_e' h C}{W'}$$

so that (3), which is derived from relativity, yields

$$W_2 - W_1 = \frac{\beta H' e h v}{C}$$

or, since, from (8), $H_z = \beta H'$

$$|T_2 - T_1| = |W_2 - W_1| = \frac{H e h v}{C} \qquad (12)$$

which is Alfvén's result limited however, as aforesaid, to an upper limit defined by (5), a limit which amounts to a fraction 2v/C of the energy itself, and which is in general much less than 10 percent. No assumption of large magnetic field or large value of h can enable $(W_2 - W_1)$ to assume a value larger than that determined by (5).

It is of some interest to inquire how the relativity transformation symbolized by its results in (5) seems to "know" of the impossibility of penetrating the slab under the conditions stated. The fact is that the transformation from the pure magnetic field in S' to the combined electric and magnetic fields E and H in S is one obeying relativity. Also the force equation of electrodynamics which tells us that there is no gain of energy of the particle in S' while there may be a loss or gain in S is also an equation obeying relativity; and if these equations had permitted the passage of the particle through the slab under conditions in which (12) had given a greater value of $W_2 - W_1$ than was permitted by (5), an algebraical inconsistency would have been involved.

Case of a Continuous Beam.

In Alfvén's paper, he assumes a continuous stream of gas emerging from the sun. If such a gas spreads on its journey, the value of v will vary. This appears at first sight to introduce a complication. However, the complication is obviously trivial as regards its practical effects. Thus, consider any portion of the beam through which the path of a cosmic ray particle is contemplated. If

S' applies to this portion of the beam, and if v is its velocity, the motion in S' will be determined by the magnetic field in S' and by an electric field which comes essentially from the change displacement in other parts of the beam which do not move with the velocity v.[7] The

---

7) There is, of course, no charge displacement in S'.

---

field produced in S' by these displacements amounting as it does to the field produced by the charges on a "condenser" when evaluated outside of the region between the plates of the condenser will be negligible for our purposes. A formal, exact, analysis of all that is here involved would result in a lengthy presentation whose end point would, in the nature of things, involve but a small correction on the conclusions which would be drawn by ignoring it.

CASE WHERE THE SLAB MOVES IN A CONDUCTING MEDIUM

Limiting case of infinite conductivity. The fact that we have supposed the slab to carry its internal magnetic field with it demands, for logical consistency, that the external medium, if infinitely conducting, shall resist change of magnetic field within itself to the extent that the magnetic field H remains zero everywhere outside of the slab as viewed in the system S. If the conductivity of the region external to the slab is ohmic as viewed in S, then even though in the limit it tends to infinity, no space charge will arise in S, and consequently[8] by the relativity transformation, there will

---

8) Some care is necessary in drawing this conclusion, as is evidenced by the fact that a system which viewed from S appears as a uniformly magnetized sphere, appears in the other system as having in addition equal and opposite charge densities displaced along a line perpendicular to the magnetic induction in the sphere and to the velocity, v. It will, in fact, be recalled that if U is the vector potential, and ϕ the scalar potential, U, $i\phi$ constitute a 4-vector, so that the zero value of ϕ in one system does not guarantee $\phi' = 0$ for the other system. The apparent paradox in relation to the invariance of total charge becomes resolved as follows:

The densities ρ and ρ' for a given sign of electricity, let us say negative, are related in the two systems by

$$\rho' = \beta \rho \left(1 - \frac{u_{x1}\, v}{c^2}\right)$$

where u_{x1} is the velocity in the system x.

Suppose now we superpose a positive density $\rho+$ in S, such that $\rho_+ + \rho_- = 0$. We shall have

$$\rho_+' = \beta\rho_+ \left(1 - \frac{u_{x2}\, v}{c^2}\right)$$

Then

$$\rho_-' + \rho_+' = \beta\left[\rho_-\left(1 - \frac{u_{x1}\, v}{c^2}\right) + \rho_+ \left(1 - \frac{u_{x2}\, v}{c^2}\right)\right]$$

$$= \beta\left[\rho_+ + \rho_- - \frac{v}{c^2}\left(\rho_+ u_{x2} + \rho_- u_{x1}\right)\right]$$

Hence, if, and only if $(\rho_+ u_{x2} + \rho_- u_{x1}) = 0$, can we conclude that $\rho_+' + \rho_-' = 0$ follows from $(\rho_+ + \rho_-) = 0$. In our present problem, since $H = 0$ in S, curl $H = 0$ and the total current density $(\rho_+ u_{x2} + \rho_- u_{x1})$ is zero, and the desired result follows.

---

be no space density in S'. The only charge of any kind will be on the surface of the slab. From symmetry the only possible surface charge will be a density[9] σ' at $y = h/2$ and $-\sigma'$ at $y = -h/2$.

---

9) σ' will be sensibly constant except near the edges of the slab.

The field component E_{yo}' in S' just outside the slab at its mid-point will be a small negative fraction $-\xi$ of the field inside the slab which is $-4\pi\sigma'$. Thus $E_{yo}' = 4\pi\xi\sigma'$.

If λ_1 is the conductivity within the slab, the y component of the current density at $x = h/2$ will be $-4\pi\sigma'\lambda_1$. The corresponding component outside will be[10] $(E_{yo}' + \frac{v}{c} H_{zo}')\lambda_2$. Thus

---

10) Observe that $v_x = -v$

---

we must have

$$-4\pi\sigma'\lambda_1 = (4\pi\sigma'\xi + \frac{v}{c} H_{zo}')\lambda_2. \qquad (12)$$

Now since H is zero at all points outside the slab as measured in S, we have for a point outside the slab

$$0 = H_z = \beta(H_z' - \frac{v}{c} E_y') \tag{13}$$

Thus

$$\frac{v}{c} H_{z0}' = \frac{v^2}{c^2} E_y' = \frac{v^2}{c^2} (4\pi \epsilon \sigma')$$

Thus from (12)

$$-4\pi \sigma' \lambda_1 = 4\pi \epsilon \sigma' (1 - \frac{v^2}{c^2}) \lambda_2 \tag{14}$$

However, this is a relation between λ_1 and λ_2 which depends upon ϵ and v only, and these quantities have nothing to do with the conductivity of the media.[11] The only possibility is represented by $\sigma' = 0$, which permits (14) to hold with any assignment of the ratio λ_1/λ_2.

---

11) We again remark that such a relation as (12) has sense as λ_1 and λ_2 both tend to infinity.

If $\sigma' = 0$, we have, of course $E_x' = E_y' = E_z' = 0$ at all points outside the slab. As a consequence, in the same region $H_z' = 0$ on account of (13), and $H_y' = 0$ because

$$0 = H_y = \beta(H_y' + \frac{v}{c} E_z')$$

Moreover $H_x' = H_x = 0$.

The fact that the state of no electric or magnetic field outside of the slab in either S or S' constitutes a solution of the problem is obvious by direct inspection, since it calls for no currents outside the slab in S' resulting from the motion of that slab. Inside the slab itself there is nothing but a magnetic field, and the whole problem reverts completely to the problem we have already considered when we attributed zero conductivity to the medium outside of the slab.

The conclusions are exactly the same.

How is the condition of zero external field realized in S'?

It is of interest to inquire how it can come about that the "magnetized" slab can exist in the external medium which itself shows no magnetic field in either S or S'. The fact is that, in the simple case, the magnetic field in the slab demands a current sheet circulating around its boundary in planes perpendicular to the axis of z. This sheet in itself would call for a return magnetic flux outside the slab, a flux which was small in amount at any point but widely spread out so that its total integrated value was equal to the total flux through the slab. Now the phenomenon which provides for the cancellation of the magnetic field outside the slab is another current sheet flowing in the reverse sense outside the first one and again in planes perpendicular to the axes of z. If these two current sheets have different cross-sectional areas,[12] they can cancel as regards production of magnetic field outside the intermost, but give a resultant uniform field inside the smaller. In the limit, when the currents are infinitely large, their cross-sections can afford to differ by only infinitesimal amounts, and this condition represents the limiting one applicable for infinite conduction in the medium external to the slab.

12) We refer here to the cross-section of the whole "solenoid structure" which constitutes such a sheet. This cross-sectional area is, of course, sensibly equal to that of the slab.

In case this above picture presents any difficulty, we may cite the particular simple example of a uniformly charged rotating

sphere. We shall not trace the details of calculation for this case, which are elementary, and generally known. Such a sphere gives, at points outside a magnetic potential Ω, where

$$\Omega = \frac{M \cos \theta}{r^2}$$

Here $M = \sigma \omega a^4$, where σ is the surface density in e.m.u., ω is the angular velocity and a is the radius.

The field inside is uniform and is given by H, where

$$H = \frac{2M}{a^3}$$

It will thus be seen that if we have two spheres of radii a_1, and a_2 with σ's adjusted so that $M_1 = -M_2$ these spheres will cancel as regards magnetic field outside of the larger, while inside the smaller they will have a resultant magnetic field given by

$$H_1 - H_2 = 2M \left(\frac{1}{a_1^3} - \frac{1}{a_2^3}\right)$$

$a_1 - a_2$ is small $(= \delta a)$ we may write

$$H_1 - H_2 = \frac{-6M \delta a}{a^4}$$

Case where conductivities λ_1 and λ_2 are finite.[13]

---

13) The effect of finite conductivity has been discussed in the writer's paper "Cosmic Rays", Journ. Franklin Inst. 251, 120-155 (1951). The conclusions drawn at the bottom of p. 134 and the top of p. 135 require correction in the light of the development in the present paper.

The complete problem here involved can become one of considerable complexity. The currents arising from the motion will affect the magnetic field, moreover the charge distributions arising on the slab to provide for continuity of current flow across the slab boundaries will bring about a-components of the current density at any rate in

regions remote from the central regions and [8] will destroy even the conclusion that the volume charge density shall be zero in S if it is zero in S' and vice-versa.

We shall not attempt an exhaustive solution of the problem, but shall content ourselves with a kind of model founded upon the considerations represented in equation (13), but without the restriction that the magnetic field shall be zero in S for points external to the slab.

We have in S a slab with face A at potential V/2 and face B at potential -V/2 respectively, A and B being at $x = h/2$ and $x = -h/2$ respectively. Outside the slab, the current density is determined entirely by the field arising from this potential difference. Inside the slab we have a force per unit charge given by $E_y - vH_z$. The line integral of the external field from A to B is V. The line integral of the internal total force per unit charge from B to A is $-V - vHh/C$.

Suppose R_e is the ordinary external resistance which would be measured between the two surfaces of the slab, if the slab itself were of zero conductivity, and R_i the resistance which would be measured if the conductivity of the external medium were zero. Then we have

$$I = \frac{V}{R_e} = \frac{-V - vHh/C}{R_i} \tag{15}$$

Hence,

$$V\left(\frac{1}{R_e} + \frac{1}{R_i}\right) = \frac{-vHh}{C R_i}$$

$$V = -\left(\frac{R_e}{R_i + R_e}\right) \frac{vHh}{C}$$

The field E inside the slab is

$$E = \left(\frac{R_e}{R_i + R_e}\right) \frac{vE}{C} \tag{16}$$

This has its largest value $E = vH/C$ when $R_e = \infty$ which represents the case first discussed in this paper and the result given by Alfven. We have already studied the other extreme where $R_e = 0$ and where there is no magnetic field external to the slab as observed in S. In this case the result $E = vH/C$ also evolves. We can form a quasi-quantative picture of the intermediate as follows:

It is easy to see that the induced currents external to the slab tend to reduce the field which would have been present in their absence. They reduce the field not only in the lateral region, but in the interior of the slab. Thus the field H in (16) is really too large, and it represents the field actually in the slab, (16) should be multiplied by a factor greater than unity. While we have not traced everything in detail, it is reasonably obvious that the net effect will result in a value of E which is never greater than the value vH/C where H is the actual field in the slab. This result being attained exactly in the two unity cases where $R_e = \infty$ and where $R_e = 0$ respectively

Reprinted from THE PHYSICAL REVIEW, Vol. 91, No. 5, 1216–1218, September 1, 1953
Printed in U. S. A.

Radiations from Arsenic 77 and Germanium 71*†

B. L. SARAF,‡ J. VARMA,§ AND C. E. MANDEVILLE
Bartol Research Foundation of the Franklin Institute, Swarthmore, Pennsylvania
(Received May 21, 1953)

The radionuclide As^{77} has been shown by scintillation spectrometry to emit gamma rays of energies 32, 87, 160, 247, 270, and 520 kev. It is estimated that these quanta are associated with beta-ray branches totaling about 2.5 percent of the total beta radiation. The continuous gamma-ray spectrum accompanying orbital electron capture in Ge^{71} has been shown to have an end point at 225±12 kev. Log ft is calculated to be 4.4($\Delta I=0, 1$; no), consistent with an assignment of spin ½ to the ground state of Ge^{71} in accord with the theory of the shell model.

Some data relative to gamma rays from Os^{190} and Ge^{77} are included.

INTRODUCTION

WITH the advent of scintillation counting, sensitivities of detection have become available for nuclear investigations which make possible the detection of gamma rays of intensity several orders of magnitude less than that previously observable by the earlier methods. Accordingly, it has been decided to reexamine "pure" beta-ray emitters in search of faint gamma radiation. The results of some researches in this direction are presented in connection with the decay of the 40-hr As^{77} along with some measurements relating to the continuous gamma-ray spectrum of the 11-day Ge^{71}.

ARSENIC 77

The beta rays of As^{77} have been shown to have a maximum energy of 0.700±0.007 Mev.[1] Very early measurements[2,3] gave evidence of no detectable gamma radiation. The residual nucleus is Se^{77}, which is also produced[4] by orbital electron capture in Br^{77}. Gamma rays having quantum energies of 160, 237, 284, 298, 520, 641, and 813 kev have been observed[4] to follow K capture in Br^{77}, indicating energy levels in Se^{77} as shown in Fig. 1.

For the purposes of the present investigation, As^{77} was grown from its 12-hr parent, Ge^{77}, when GeO_2 was irradiated by slow neutrons in the Oak Ridge pile. The energy spectrum of the gamma rays of As^{77} as determined from the pulse height distribution resulting from gamma rays on NaI(Tl) is shown in Fig. 2. This distribution was observed on twelve occasions over a time of four half-periods, and the ordinates of the spectrum were found to decay at all points with a half-period of 40 hr, that of As^{77}. Measurements were not commenced until sufficient time had elapsed to make negligible the 12-hr Ge^{77}. Moreover, the measurements on As^{77} were always preceded by a chemical separation of arsenic from germanium. The energies, with an estimated accuracy of five percent, are 87, 160, 247, and 520 kev, with approximate relative intensities of 3, 1, 20, and 6, respectively.

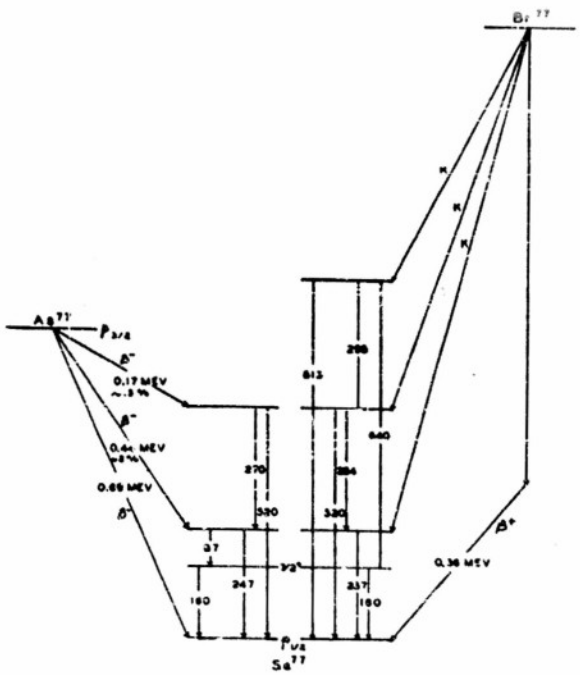

FIG. 1. Disintegration scheme for As^{77} and Br^{77}.

* Assisted by the joint program of the U. S. Office of Naval Research and the U. S. Atomic Energy Commission.

† A preliminary account of these results was presented at the Conference on Nuclear Spectroscopy and the Shell Model of the Nucleus, Indiana University, May 14–16, 1953, and also in Bull. Am. Phys. Soc. 28, No. 4, 12 (1953).

‡ On leave of absence from Agra College, Agra, India.

§ Permanent address, Morena (M.B.), India.

[1] R. Canada and A. C. G. Mitchell, Phys. Rev. 81, 485 (1951).

[2] U. S. Atomic Energy Commission Catalog and Price List No. 3, March 1, 1947, September 1, 1947, and No. 3, July, 1949, describe the number of gamma rays emitted by As^{77} as "none." This description may be based upon the measurements of E. P. Steinberg and D. W. Engelkemir, *Radiochemical Studies: The Fission Products* (McGraw-Hill Book Company, New York, 1950), Paper No. 54, National Nuclear Energy Series, Plutonium Project Record, Vol. 9, Div. IV, who mention no detectable gamma rays from As^{77}.

[3] Mandeville, Woo, Scherb, Keighton, and Shapiro, Phys. Rev. 75, 1528 (1949), stated in the introduction of their paper that As^{77} emits no gamma rays. This remark was a citation of the comments of reference 2. There are no published data in the paper by Mandeville *et al.* relating to the gamma rays of As^{77}. However, an unpublished beta-ray absorption curve was obtained by Mandeville *et al.* to find the absorption limit, and no gamma-rays were detected in a Geiger counter beyond the beta-ray end point. The present writers could detect several hundred counts per minute, gamma rays from As^{77}, in a Geiger counter shielded from the beta rays in the presence of a relatively intense pile-produced source.

[4] R. Canada and A. C. G. Mitchell, Phys. Rev. 83, 955 (1951).

Gamma-gamma coincidences were measured in two scintillation counters in coincidence. The coincidence rate was noted for various settings of integral pulse-height discriminators in either channel. From the data, it was found that the coincidence rate decreased as the discriminator setting in one channel was increased, until when the discrimination level was greater than the height of pulses in the photoelectric peak of a 270-kev gamma ray, all genuine gamma-gamma coincidences ceased. With both integral pulse-height discriminators set to pass pulses only of height corresponding to 247 kev or more, a considerable number of genuine gamma-gamma coincidences remained, suggesting that the intense 247-kev line is complex. To locate accurately the photoelectric peak of the radiation in cascade with the 247-kev gamma ray, the pulses from either phototube were passed through single channel differential pulse-height discriminators, one set at the photopeak of the 247-kev line. As the base line of the coincident

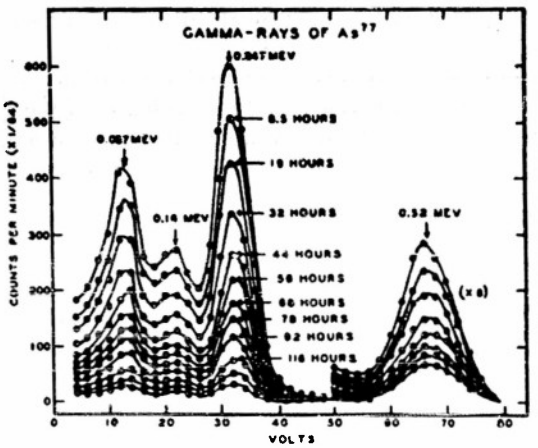

FIG. 2. Pulse-height distribution of gamma rays from As^{77} on NaI-Tl.

differential pulse-height discriminator was raised above 247 kev, the gamma-gamma coincidence rate was found to have a maximum at 270 kev, giving the location in energy of the photopeak of the gamma ray in cascade with the 247-kev line. From the single counting rates in either channel and the gamma-gamma coincidence rate, the intensity of the 270-kev gamma ray relative to that of the 247-kev line was estimated to be two percent. In subsequent measurements, a gamma ray at 32 kev, not shown in Fig. 2, was detected. The gamma ray at 520 kev was found to be noncoincident with the other quantum radiations. The cascade relation between the various gamma rays as indicated by the coincidence experiments is shown in Fig. 1.

The absolute intensity of the beta rays of As^{77} was measured in a thin-walled Geiger counter (window thickness 3 mg/cm^2), and the intensities of the gamma rays were estimated from the areas under the photoelectric peaks and the calculated efficiency of the sodium iodide crystal. From the energies and relative

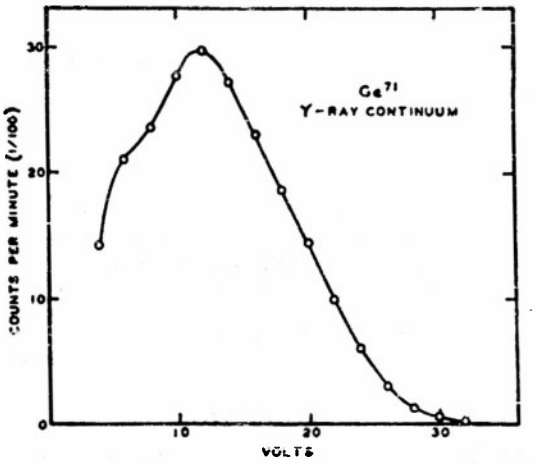

FIG. 3. Pulse-height distribution arising from the gamma-ray continuum of $Ge^{71}+\epsilon^- \rightarrow Ga^{71}+\nu+\gamma$.

intensities of the gamma rays, the values of log ft for the associated beta-ray spectra were calculated in the order of ascending energy to be 6.6, 7.2, and 5.7, the latter value referring to the beta spectrum leading to the ground state of Se^{77}. Thus, the ground-state transition is allowed, and the remaining two spectra are first forbidden. Beta-gamma coincidences were measurable between the inner spectrum at 0.44 Mev and the 247-kev gamma ray.

As previously indicated, the gamma-ray energy measurements and coincidence data have been combined with those of Canada and Mitchell[4] to give the decay scheme of Fig. 1. As^{75} is known to have a spin of $\frac{3}{2}$. Since As^{77} differs from As^{75} by two neutrons, its ground state orbital is assumed to be $p_{\frac{1}{2}}$ in agreement with the prediction of the nuclear shell model. The spin of Se^{77} has been shown[5] to be $\frac{1}{2}$. Therefore, the beta spectrum at 0.700±0.007 Mev (noncoincident with gamma rays, log $ft=5.7$) is properly characterized by[6] $p_{\frac{1}{2}} \rightarrow p_{\frac{1}{2}}$ ($\Delta I=1$, no). The 160-kev metastable state has been classified[7] as being the initial state of an $E3$ transition with spin $7/2^+$. The values of log ft for the two inner beta spectra correspond to ($\Delta I=0, 1$; yes,) ruling out the possibility that either of them terminate at a level in Se^{77} of spin 9/2. Assignment of spins to the remaining excited levels of Se^{77} shown in Fig. 1 is made difficult, because of the great number of configuration levels which can result from $(g_{9/2})^3$.

GERMANIUM 71

The radiations of Ge^{71} have been shown to include no charged particles or monoenergic nuclear gamma rays.[8,9,3] This activity decays solely by orbital electron

[4] S. P. Davis and F. A. Jenkins, Phys. Rev. 83, 1269 (1941).
[5] Mayer, Moszkowski and Nordheim, Revs. Modern Phys. 23, 315 (1951).
[6] M. Goldhaber and A. W. Sunyar, Phys. Rev. 83, 906 (1951).
[7] Seren, Friedlander, and Turkel, Phys. Rev. 72, 888 (1947).
[8] McCown, Woodward, and Pool, Phys. Rev. 74, 1311 (1948).

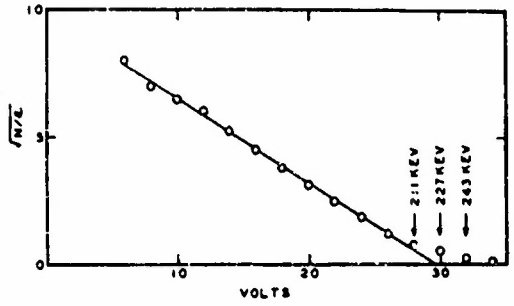

FIG. 4. Fermi plot of the gamma ray spectrum of Ge^{71}.

capture. It has been shown theoretically[10] that a small fraction of K-capture disintegrations are accompanied by emission of a continuum of quanta and corresponding continuum of neutrinos rather than the usual monoenergic neutrino. Examples of this mode of decay have been found[11,12] in Fe^{55} and in argon 37.[13] Since Ge^{71} decays only by K capture and always to the ground state of Ga^{71}, it was thought to offer an excellent opportunity for the detection of its related gamma-ray continuum. Accordingly, Ge^{71} produced by slow neutron capture in the Oak Ridge pile was studied.

The pulse-height distribution of the continuous gamma-ray spectrum of Ge^{71} is shown in Fig. 3. The Fermi plot of the data of Fig. 3, given in Fig. 4, yields an end point of 225 ± 12 kev. Because of the low specific gamma-ray activity of the source of Ge^{71}, it was necessary to employ a relatively thick, broad, source of irradiated GeO_2. Consequently, the points of Fig. 3 were not corrected for absorption, instrumental resolution, or detection efficiency as a function of gamma-ray energy. The energy of disintegration of Ge^{71} to Ga^{71} by K capture is, of course, equal to the end point of the continuum.

The spin of the ground state of Ga^{71} has been measured[14] and found to be $\frac{3}{2}$. The spin of Ge^{71} is predicted by the shell model[15] to be $p_{\frac{1}{2}}$. From the end point of Fig. 4, log ft is 4.4, and the transition is allowed ($\Delta I=0$, ±1; no), consistent with the shell model prediction. These interpretations and data are summarized in the decay scheme of Fig. 5.

If the ground-state spin of Ge^{71} is taken to be $p_{\frac{1}{2}}$, the shell model theory indicates that an isomeric level should be present in Ge^{71} of spin $g_{9/2}$, giving rise to an

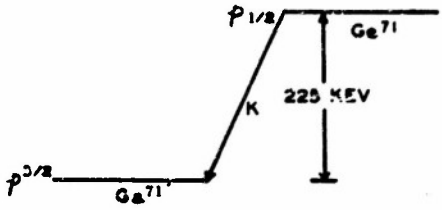

FIG. 5. Decay of Ge^{71}.

$M4$ transition. This gamma ray has apparently not yet been observed.

OSMIUM 193 AND GERMANIUM 77

The gamma rays of Os^{193} ($T=32$ hr) have been studied by Swan and Hill,[16] who find a gamma ray at 72.4 kev. Indications of gamma rays at 215, 323, and 460 kev were reported by them,[16] but they were not definitely assigned to Os^{193}. Very recently,[17] Cork *et al.* have re-examined the gamma rays of Os^{193} and found in a magnetic spectrograph nine lines, ranging in energy from 73 kev to 557.8 kev. Three of these reported gamma rays have also been observed in a scintillation spectrometer by the writers. The measured quantum energies were in the interval 200 kev$<E_\gamma<$600 kev at 280, 460, and 560 kev, differing little in energy from the values reported by Cork *et al.*[17]

The gamma rays of Os^{193} were also measured periodically over a time of about 80 hours by the method of coincidence absorption. The hard gamma ray previously reported at 1.58 Mev[18] was again found to be present, but its intensity decayed with a half-period of $\sim$20 hr, suggesting it to be the 1.43-Mev quantum of Ir^{194}.

In the course of studying the gamma rays of As^{77}, the gamma spectrum of the parent element, Ge^{77}, was also noted. The results were essentially the same as those of Smith,[19] except that two high-energy quanta at 2.3 and 2.7 Mev, respectively, unobserved by Smith, were present and decayed in intensity with the 12-hr half-period of Ge^{77}.

ACKNOWLEDGMENT

The writers are indebted to Dr. Walter B. Keighton of Swarthmore College for having carried out the several separations of germanium from arsenic required in the course of these measurements. They also wish to acknowledge the kind interest of Dr. W. F. G. Swann, Director of The Bartol Research Foundation.

[10] P. Morrison and L. I. Schiff, Phys. Rev. 58, 24 (1940); J. M. Jauch, Oak Ridge National Laboratory Report 1102 (1951).
[11] Bradt, Gugelot, Huber, Medicus, Preiswerk, Scherrer, and Steffen, Helv. Phys. Acta 19, 222 (1946); D. Maeder and P. Preiswerk, Phys. Rev. 84, 595 (1951).
[12] Bell, Janch, and Cassidy, Science 115, 12 (1952).
[13] C. E. Anderson, Phys. Rev. 87, 662 (1952).
[14] J. S. Campbell, Nature 131, 204 (1933).
[15] M. G. Mayer, Phys. Rev. 78, 16 (1950).
[16] J. B. Swan and R. D. Hill, Phys. Rev. 88, 831 (1952).
[17] Cork, LeBlanc, Nester, Martin, and Brice, Phys. Rev. 90, 444 (1953).
[18] Mandeville, Scherb, and Keighton, Phys. Rev. 74, 888 (1948).
[19] Alan B. Smith, Phys. Rev. 86, 98 (1952).

Reprinted from THE PHYSICAL REVIEW, Vol. 91, No. 5, 1286–1287, September 1, 1953
Printed in U. S. A.

Lower Limit for the Lifetime of the 665-kev Excited State of Mo^{97}†

F. R. METZGER AND W. B. TODD
Bartol Research Foundation, of the Franklin Institute, Swarthmore, Pennsylvania
(Received July 15, 1953)

ACCORDING to Goldhaber and Hill[1] the 665-kev gamma ray emitted in the decay of Nb^{97} is probably a magnetic dipole transition between states with orbitals $g_{7/2}$ and $d_{5/2}$. As the Nb^{97} decay involves a rather energetic beta ray which can compensate for the gamma-ray recoil, Nb^{97} seemed to be a favorable case for a lifetime measurement using resonance scattering.[2]

A measurement of the nuclear resonance scattering of a gamma ray is a determination of the width of the initial nuclear level involved in the transition. The resonance scattering technique is especially well suited for lifetimes of the order of 10^{-13} second and shorter (widths $\geq 6\times10^{-8}$ ev). This is just the region into which, according to Weisskopf's lifetime formula,[3] the magnetic dipole transitions of $\approx mc^2$ energy should fall. The only $M1$ transition in this energy range whose lifetime is known is the 478-kev transition in Li^7. From an observation of the Doppler broadening due to the motion of the Li^{7*} nucleus in the $B(n,\alpha)$ reaction, Elliott and Bell[4] deduced a lifetime of 7×10^{-14} second, which is even somewhat shorter than expected from Weisskopf's formula. On the other hand, the lifetimes of several low-energy $M1$ transitions have been measured by Graham and Bell[5] using delayed coincidence techniques. Most of these lifetimes were found to be ~100 times longer than predicted from Weisskopf's formula. If the 665-kev Mo^{97} gamma ray belonged to this "slow" group, resonance scattering would not be observable with our present means; if, however, the 665-kev gamma ray followed Weisskopf's formula, a large nuclear resonance scattering effect could be expected.

Ten milligrams of ZrO_2 enriched[6] in Zr^{96} were bombarded in the Brookhaven pile and yielded a 0.3-millicurie source of Zr^{97} and its daughter Nb^{97}. The gamma rays from this source were scattered alternately from Mo and Zr scatterers. The scattered radiation was observed with a scintillation spectrometer which accepted only pulses corresponding to the 665-kev photoelectron line. As the difference in atomic number between Zr and Mo is small, Rayleigh scattering from the two scatterers was almost the same. The small difference in Rayleigh scattering was determined in a separate experiment using the 663-kev gamma ray from Cs^{137}.

After correcting for the difference in Rayleigh scattering the counting rates for the Nb^{97} source with the Mo and Zr scatterers were identical, the experimental uncertainty being two percent.

If one assumes the contribution of the resonance scattering from the Mo scatterer to be two percent of the counting rate (i.e., equal to the uncertainty), and if one takes into account that only a small percentage of the gamma rays is emitted while the nucleus still has the momentum imparted to it by the beta ray, one arrives at an upper limit for the width of the 665-kev excited state of Mo^{97}, $\Gamma\leq5\times10^{-4}$ ev, and at a lower limit for the lifetime of this state of 1.5×10^{-12} second. This lifetime is one order of magnitude longer than the one expected from the Weisskopf formula. Thus, the $M1$ transition in Mo^{97} shows the same behavior as the low-energy $M1$'s.

It should be mentioned that the Mo^{97} transition, as well as most of the low-energy transitions measured by the Canadian group, involve a change of two units of orbital angular momentum, whereas the Li^7 gamma ray presumably leads from a $p_{\frac{1}{2}}$ to a $p_{\frac{3}{2}}$ state.

† Assisted by the joint program of the U. S. Office of Naval Research and the U. S. Atomic Energy Commission.
[1] M. Goldhaber and R. D. Hill, Revs. Modern Phys. **24**, 179 (1952).
[2] W. Kuhn, Phil. Mag. **8**, 625 (1929); P. B. Moon, Proc. Phys. Soc. (London) **63**, 1189 (1950).
[3] V. Weisskopf, Phys. Rev. **83**, 1073 (1951).
[4] L. G. Elliott and R. E. Bell, Phys. Rev. **76**, 168 (1949).
[5] R. L. Graham and R. E. Bell, Can. J. Phys. **31**, 377 (1953).
[6] Obtained from Y-12 Plant, Carbon and Carbide Corporation, Oak Ridge, Tennessee.

Reprinted from THE JOURNAL OF CHEMICAL PHYSICS, Vol. 21, No. 8, 1421–1422, August, 1953
Printed in U. S. A.

The "Chemical Knife"; Preservation of Ozone for Thirty-Six Days

H. O. ALBRECHT
Bartol Research Foundation of The Franklin Institute, Swarthmore, Pennsylvania
(Received May 18, 1953)

ABOUT 1933 I noticed more particularly the action of ozone on rubber. The facts are widely familiar, I assume, but seemingly no emphasis to date has been given to a curious aspect of this reaction and its interpretation.

A tube of thick and new rubber broke off where stretched slightly over a metal nipple, in a matter of minutes after producing ozone in the vicinity. This occurred several times before I realized the cause. The broken ends were traversed by a sharp cracks as though slashed by a razor blade, but the rubber was not visibly deteriorated. I later found that a rubber band stretched in the path of a stream of ozonized oxygen (*ca* 8 percent ozone) parted almost instantly, whereas no effect, even superficial, was seen on an unstretched band in so short a time.

An interesting explanation of these effects is "mechanical activation" of the double bonds in the rubber structure at the point of high stress, namely, the bottom of the forming crack. A more orthodox, perhaps equivalent, view is that the "newly formed surface," unprotected by ordinary oxidation or gas absorption, is responsible for this extreme local rate of penetration of a reaction into a solid. The amount of ozone involved is infinitesimal, compared to the conspicuous effect—accurately likened to that of a knife. In either case, the result has some practical (and not always realized) significance in connection with the deterioration of rubber connections, when a Tesla leak detector is used.

Another, unconnected, observation made on ozone at the time, was its stability for thirty-six days at fairly high concentration, in a one-liter sealed Pyrex bulb containing $KMnO_4-H_2SO_4$ solution (same 8 percent ozone in oxygen). The bulb lay in full sunlight during summer weather. I have never heard of ozone being preserved for this length of time and ascribe the stability to the absence of nitrogen oxides, as well as organic matter, because of the $KMnO_4$.

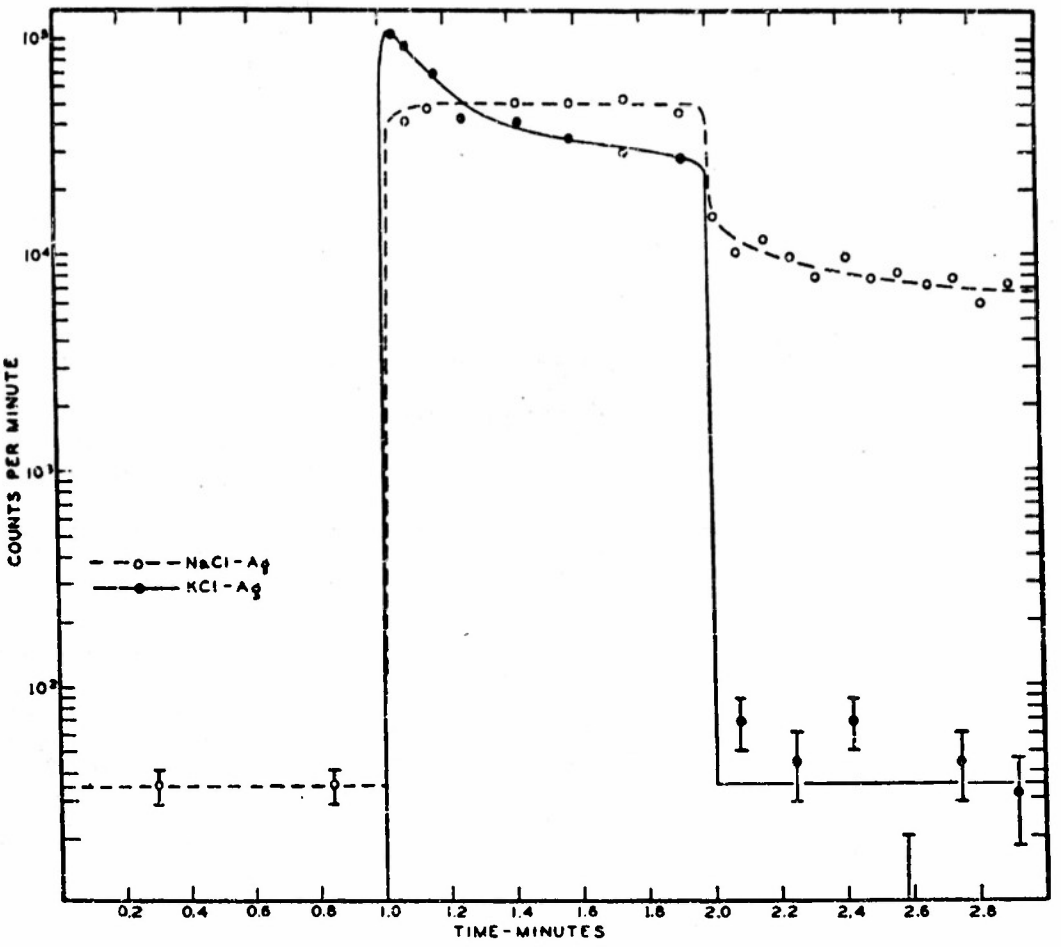

FIG. 1. Photostimulation for one minute of NaCl-Ag and KCl-Ag twenty-four hours after irradiation by three roentgens of x-rays.

counting rate rose to $\sim 10^5$ counts per minute, decreased to 2.5×10^4 counts per minute during one minute of photostimulation, and dropped very nearly to zero when the stimulating light was turned off.

Thirty seconds after the one-minute period of photostimulation, the counting rate arising from NaCl-Ag was 7600 counts per minute, whereas that of KCl-Ag was ~ 35 counts per minute. The large difference in the two curves at $t = 2.5$ min explains why Bittman, Furst, and Kallmann[4] reported the post-stimulation photophorescence of KCl-Ag to be essentially zero which led to the conclusion that only NaCl-Ag exhibits good storage properties. The fact is that KCl-Ag exhibits light storage which can be measured by co-stimulation phosphorescence, but not by poststimulation phosphorescence.

In Fig. 2 is shown a comparison of the co-stimulation phosphorescence of NaCl-Ag and KCl-Ag, the AgCl concentrations being the same as previously given. To obtain the data of Fig. 2, equal volumes of the two materials were irradiated in an x-ray field of intensity twenty roentgens per hour for a period of ten minutes. The irradiated materials were immediately stored in darkness and subsequently stimulated by the one-watt tungsten lamp for a period of six seconds every twenty-four hours. The counting rate during the six-second period of photostimulation is recorded.

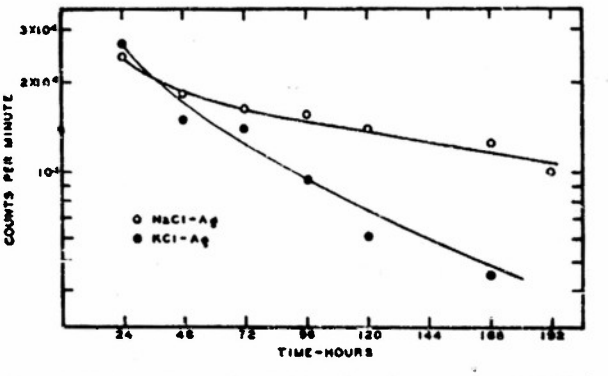

FIG. 2. Decay of co-stimulation phosphorescence of KCl-Ag and NaCl-Ag. The sample of NaCl-Ag was a single crystal (Harshaw).

Note added in proof:—Particular attention should be called to the papers of Mikao Kato, Sci. Papers Inst. Phys. and Chem. Research (Tokyo) 41, 113 (1944); 41, 135 (1944); 42, 35 (1944); 42, 95 (1944). In the fourth publication of the series, he describes many of the storage properties of KCl-Ag and comments on the spectral response of the Geiger counter and its importance in photostimulation studies. Kato's measurements differ from those of the writers in that his means of primary excitation were limited to ultraviolet light. Copies of Kato's papers have been difficult to obtain in the United States and were not available to the writers until after this manuscript had been submitted for publication.

[4] Bittman, Furst, and Kallmann, Phys. Rev. 87, 83 (1952).

Reprinted from THE PHYSICAL REVIEW, Vol. 91, No. 3, 566-567, August 1, 1953
Printed in U. S. A.

The Storage of Energy in Silver Activated Potassium Chloride*

C. E. MANDEVILLE AND H. O. ALBRECHT
Bartol Research Foundation of The Franklin Institute, Swarthmore, Pennsylvania
(Received February 2, 1953; revised copy received April 20, 1953)

Crystals of KCl-Ag and NaCl-Ag have been excited by x-ray irradiation. The photostimulated light yield of the ultraviolet emission band has been observed simultaneously with application of the stimulating near-ultraviolet light. The decay with time of the stored energy in the two phosphors is compared.

THE energy storage properties of some silver activated alkali halides have been discussed in several recent publications.[1,2] The procedure outlined in references 1 and 2 has been to irradiate an excited phosphor with long wave light and observe in a phototube (RCA-1P28) what may be described as a "post-stimulation phosphorescence" of the ultraviolet emission band after the stimulating long wave light has been extinguished. In using the 1P28 as a detector, difficulties are encountered if attempts are made to measure the stimulated emission while the stimulating light is on, because the phototube's spectral response is such as to respond to the stimulating light as well. The stimulated light emitted while the stimulating light is on might be called "co-stimulation phosphorescence." To avoid this problem, the writers have employed photosensitive Geiger counters to detect the stimulated emission. It has long been known[3] that photosensitive Geiger counters can be produced which have an excellent sensitivity at 2500A but no response to near-ultraviolet or visible radiations. Accordingly, in the present investigation, photosensitive Geiger counters have been employed to detect the photostimulated emission of the ultraviolet bands of KCl-Ag and NaCl-Ag, the ultraviolet band of KCl-Ag being centered at 2800A and that of NaCl-Ag at 2500A. Irradiation, storage, and measurements relating to all phosphor samples were carried out at toom temperature (25°C).

To study the photostimulated emission from NaCl-Ag and KCl-Ag, a polycrystalline mass of KCl-Ag (AgCl concentration 0.10 ± 0.02 percent by weight) and a single crystal of NaCl-Ag prepared by The Harshaw Chemical Company (AgCl concentration 0.37 ± 0.06 percent by weight) were irradiated by x-rays of maximum energy 25 kev for ten minutes to receive a dosage of three roentgens. The irradiations were carried out in total darkness, and the materials were stored for twenty-four hours in light-tight containers. At the end of that time, the crystals were each stimulated by a one-watt tungsten lamp at a distance of seven centimeters for a period of one minute. The counting rates of NaCl-Ag and KCl-Ag before, during, and after the one-minute period of photostimulation are shown in Fig. 1. A time of one minute before the stimulating light was turned on was taken arbitrarily as time zero. Prior to stimulation, the slow normal unphotostimulated phosphorescence of NaCl-Ag was $\sim$35 counts per minute, rising immediately to $\sim$50 000 counts per minute in the form of co-stimulation phosphorescence. After one minute of photostimulation, the stimulating tungsten lamp was extinguished, and the luminescence from NaCl-Ag dropped immediately to a post-stimulation phosphorescence count of about 9000 per minute. Thus, photostimulation with the one-watt bulb of NaCl-Ag twenty-four hours after receipt of a dosage of three roentgens gave rise to a co-stimulation phosphorescence 1400 times greater than the residual unphotostimulated phosphorescence (35 counts per minute) existing prior to stimulation, and to a post-stimulation phosphorescence greater than the same quantity by a factor of 257. The similarly exposed KCl-Ag gave no evidence of slow unphotostimulated phosphorescence at 25°C, twenty-four hours after excitation. The counting rate in the photosensitive Geiger counter was only the natural background count. However, upon photostimulation, the

* Assisted by the joint program of the U. S. Office of Naval Research and the U. S. Atomic Energy Commission.
[1] M. Furst and H. G. Kallmann, Phys. Rev. 82, 964 (1951); 83, 674 (1951); Kallmann, Furst, and Sidran, Nucleonics 10, No. 9, 15 (1952).
[2] Bittman, Furst, and Kallmann, Phys. Rev. 87, 83 (1952).
[3] P. B. Weisz, Electronics 19, No. 7, 106 (1946); H. Friedman and C. P. Glover, Nucleonics 10, No. 6, 24 (1952); C. E. Mandeville and H. O. Albrecht, Phys. Rev. 79, 1010 (1950).

Reprinted from THE PHYSICAL REVIEW, Vol. 90, No. 5, 796–803, June 1, 1953
Printed in U. S. A.

Specific Primary Ionization of H_2, He, Ne, and A by High Energy Electrons*

G. W. McCLURE
Bartol Research Foundation of the Franklin Institute, Swarthmore, Pennsylvania
(Received January 28, 1953)

Monoenergetic electrons, magnetically separated from the continuous spectrum of a radioactive β-ray source, are directed through a series of 3 thin-window G-M counters. A measurement of the efficiency of the first counter by the coincidence method yields information from which the specific primary ionization of its contained gas is calculated.

Measurements of H_2, He, Ne, and A over the range of incident electron energies 0.2 to 1.6 Mev have been made and the data compared with the Bethe theory of primary ionization. By adjustment of two constants contained in the theoretical formula, it is possible to fit the data for each of the four gases within the experimental uncertainties. The adjusted formulas yield extrapolated values of the specific primary ionization which are fairly consistent with the work of others at lower and higher energies.

INTRODUCTION

MEASUREMENTS of the specific primary ionization of gases by charged particles have been conducted by a number of investigators[1–7] over a considerable range of incident-particle energies. There have been large discrepancies between the results obtained with different methods of measurement, particularly for electrons in the neighborhood of minimum ionization, and the experimental errors have thus far precluded a critical quantitative comparison between the measurements and the theory.

In view of the many applications of knowledge concerning the ionization of gases in various fields of experimental physics, it was considered worth while to conduct a new set of precise measurements on several gases in the neighborhood of minimum ionization using β-particles from a radioactive source as the primary ionizing radiation. The measurements reported here extend over a sufficient range of energies to make possible a determination of the parameters which enter into the Bethe theory of primary ionization and indicate the degree to which the theory may be relied upon as a tool for extrapolating experimental data.

EXPERIMENTAL PROCEDURE

The experimental procedure consists of measuring the probability that a G-M counter filled with the gas under investigation will be discharged by a β-ray having a known energy and a well-defined path length in the counter. Given the discharge probability (or efficiency) of the counter together with the path length and the gas pressure, one may calculate the specific primary ionization of the contained gas. A discussion of the required calculations will be found near the end of this section of the paper.

The experimental arrangement (as shown in Fig. 1) consists essentially of a 180° β-ray spectrograph (evacuated to 10^{-3} mm Hg) and a set of G-M counters C_1, C_2, and C_3. A radioactive source at S (Pr^{144} in equilibrium with Ce^{144}) gives rise to a continuous spectrum of β-rays ranging in energy from zero to 3 Mev. The series of baffles, B, selects from the continuous spectrum a beam of β-rays with a ± 5 percent energy spread which pass through the counter train via a series of 1-mil aluminum windows W_1, W_2, and W_3. The magnetic field, which determines the momentum of the β-rays entering W_1, is measured by means of a ballistic galvanometer connected to a flip coil F.

The counter C_1 was filled with a gas or mixture of gases whose primary ionization was to be measured. The gas pressure was chosen so that the β-rays in the spectrograph energy range were counted with an efficiency of about 0.5, a condition which results in the least required operating time for determining the primary ionization to a given statistical accuracy. Counters C_2 and C_3 filled with a self-quenching argon-butane mixture served to count the number of β-ray transversals of counter C_1.

The counters were connected to an external circuit which simultaneously recorded the threefold coincidences ($C_1C_2C_3$) and twofold coincidences (C_2C_3). As the walls of C_1 permit the penetration of β-rays only through windows W_1 and W_2, any ray which is to give rise to either type of coincidence must traverse C_1 within the solid angle subtended by the two windows. The efficiency of C_1 for counting rays of this selected group is given by

$$\epsilon=\frac{(C_1C_2C_3)-(C_1C_2C_3)_0}{(C_2C_3)-(C_2C_3)_0}, \tag{1}$$

where the quantities with "0" subscripts represent the cosmic-ray background coincidence rates recorded with the magnetic field of the spectrograph reduced to zero. The background rates were less than 10 percent of the

* Assisted by the joint program of the U. S. Office of Naval Research and the U. S. Atomic Energy Commission.
[1] E. J. Williams and F. R. Terroux, Proc. Roy. Soc. (London) 126, 289 (1929).
[2] P. T. Smith, Phys. Rev. 36, 1293 (1930).
[3] J. T. Tate and P. T. Smith, Phys. Rev. 39, 272 (1932).
[4] W. E. Danforth and W. E. Ramsey, Phys. Rev. 49, 854 (1936).
[5] M. G. E. Cosyns, Nature 138, 284 (1936).
[6] M. G. E. Cosyns, Nature 139, 802 (1937).
[7] F. L. Hereford, Phys. Rev. 74, 574 (1948).

β-ray counting rates during all of the measurements reported here.

It was necessary to operate the counter C_1 as a resistance-quenched counter with all of the gases used in the investigation. As a series resistance of the order of 10^9 ohms was required for proper quenching, the dead time of C_1 was of the order of 10^{-3} sec. In order to obviate the necessity of correcting the measured efficiencies for the dead-time effect, a dc coupled anti-coincidence circuit was introduced between the wire of C_1 and the coincidence selection circuits so as to prevent the recording of any coincidence (C_2C_3) or $(C_1C_2C_3)$ which occurred at a time when the wire potential of C_1 was more than 5 volts below its normal (quiescent) potential. This imposed the condition that counter C_1 be completely recovered from any preceding discharge before a coincidence could be recorded and thus rendered the experimentally determined efficiencies independent of the dead time of C_1.

The background rates used in Eq. (1) to evaluate the efficiencies were corrected to compensate for the fractional inactive time of the recording circuits imposed by the anticoincidence circuit during the β-ray data runs. This correction was accomplished by multiplying the measured background rates by the ratio between the coincidence rates (C_1C_2) measured at each field setting with and without the anticoincidence circuit in operation.

As mentioned above, only those β-rays which traverse C_1 within the solid angle of windows W_1 and W_2 contribute to the measured counting rates. These windows are 0.250 in. in diameter and the plane surfaces on which they are mounted are separated by a distance, $L_0=0.688''$. For β-rays of the energy range considered here, the mean scattering angle in W_1 is sufficiently large that one may consider each point of the window as an isotropic source of rays emanating into the counter. Calculated on this basis, the mean path length L, of rays traveling between windows W_1 and W_2 turns out to be only 1.3 percent greater than the direct pathlength L_0.

A second path-length perturbation arises from a slight, approximately spherical distortion of window W_1, which resulted from subjecting the window to a one atmosphere pressure differential before the counter assembly was attached to the spectrograph. This distortion has the effect of reducing the average path length to a value approximately 0.5 percent less than that calculated on the basis of scattering alone. The combined effects of scattering and window curvature yield a mean path length differing from the value L_0 by less than 0.8 percent. Since the error introduced into the final result by setting the effective mean path equal to L_0 is of the same order of magnitude as the statistical errors, the path-length correction has been neglected in all of the calculation.

Corrections for the energy loss suffered by the β-rays in penetrating the first window were made on the basis

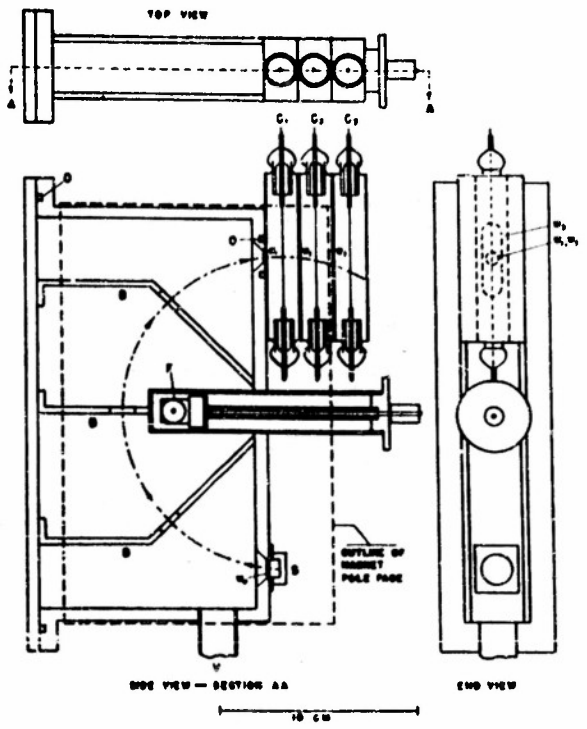

FIG. 1. Apparatus for determining the specific primary ionization of gases. S—beta-ray source; B—spectrograph baffles; F—flip coil for measuring magnetic field; C_1, C_2, C_3—GM counters, W_1, W_2, W_3—0.001 in. Al windows separating counters; V—forepump connection for evacuating spectrograph; O—"O" ring seals.

of the range *vs* energy curves for electrons in Al. For the lowest energy β-rays considered in the present investigation (0.2 Mev), this correction amounts to approximately 9 percent, while for the highest energy rays (1.6 Mev), the correction is approximately one percent.

The statistical distribution of the number of ions produced by monoenergetic rays traversing the well-defined path length between the collimating windows W_1 and W_2 is given by the Poisson law. Accordingly, if x denotes the average number of ionizing collisions per traversal, the probability that no ion pair will be produced in a traversal is equal to e^{-x}. Provided that (1) the counter undergoes a complete discharge whenever at least one free electron is present within its volume, and (2) no secondaries are released from the wall material by the primary rays, the counting efficiency ϵ is

$$\epsilon=1-e^{-x}. \tag{2}$$

The specific primary ionization S (at N.T.P.) is given in terms of x by the formula

$$S=xT/273LP. \tag{3}$$

where L is the path length in cm, P the gas pressure in atmospheres, and T the temperature of the gas in degrees K.

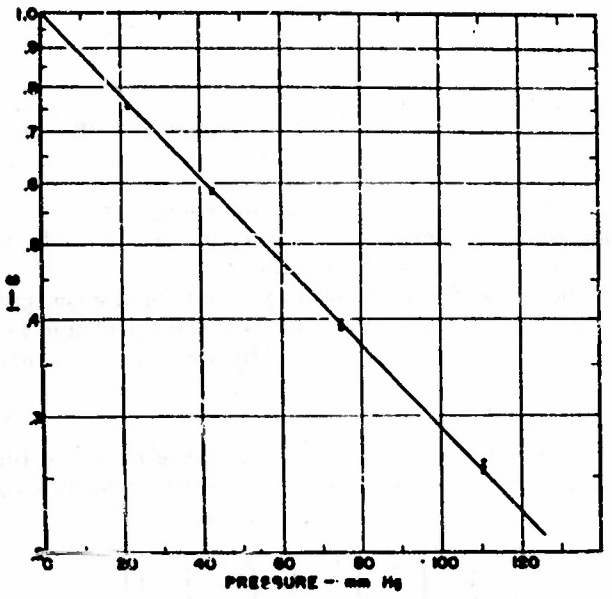

FIG. 2. Variation of the quantity $(1-\epsilon)$ as a function of the pressure of H_2 contained in counter C_1 (0.855 Mev β-rays).

In order to insure the fulfillment of provision (1), the investigation was restricted to gases known to have electron attachment coefficient sufficiently small to be neglected. In addition, care was taken to ascertain that the counter C_1 was operated in a region of its characteristics where increases of from 50 to 100 volts in operating potential yielded no significant change in the measured efficiency.

Spectroscopically pure gases supplied by the Linde Air Products Company were used throughout the investigation. The pressures of gases introduced into the counter C_1 were measured with a mercury manometer constructed of glass tubing of sufficiently large diameter (0.5 in.) to eliminate errors arising from unequal meniscus shapes in the two columns of the manometer. An antiparallax method was used in comparing the heights of the mercury columns with a fixed scale, graduated in mm. Errors in the measured specific primary ionization values, caused by inaccuracies in pressure readings, were less than or equal to the statistical errors.

Counter C_1 exhibited very flat efficiency *vs* voltage curves (slopes less than 1 percent per 100 volts) with pure H_2 fillings but yielded unsatisfactory performance when operated with the rare gases unmixed with a secondary gas component. (With pure rare-gas fillings, the counter broke down into continuous discharge under applied potentials only slightly above the starting threshold.) It was found, however, that the addition of a small percentage of H_2 to any of the rare-gas fillings permitted the counter to function as well as when filled with pure H_2. Therefore, to avoid the difficulties encountered with the pure rare gases, the specific primary ionization measurements on the latter were performed with small partial pressures of H_2 added to C_1. With the mixtures employed, the corrections required to compensate the measurements for the added quantities of H_2 amounted to approximately 10 percent, 16 percent, and 5 percent for He, Ne, and A respectively. The precise percentages, of course, vary slightly with the β-ray energy.

As a test of the over-all reliability of the experimental procedure, a curve of efficiency *vs* pressure was taken on the counter C_1 with H_2 as the filling gas. Figure 2 is a semilogarithmic plot of the measured values of $(1-\epsilon)$ as a function of the hydrogen pressure. It is seen that within the statistical errors the experimental points lie along a straight line which extrapolates to $(1-\epsilon)=0$ at $P=0$ as expected from Eqs. (2) and (3). If secondary electrons from the walls of C_1 contributed any significant amount to the counting rate of C_1, the efficiency *vs* pressure data would be expected to extrapolate to a value $(1-\epsilon)$ less than unity at $P=0$. On the basis of these results, the experimental errors due to wall-effect are considered to be negligible.

EXPERIMENTAL RESULTS

The results of the specific primary ionization measurements on H_2, He, Ne, and A are presented in Table I. The experimental errors indicated in the table are the statistical standard deviations which in all cases are closely comparable with the independent uncertainties associated with the pressure and path-length determinations. The relative magnitude of the specific primary ionization values obtained for any individual gas are considered to be accurate within the statistical errors. Uncertainties in the absolute values, which depend upon the precision of the pressure and path-length determinations, are conservatively estimated at ± 3 percent. Repeat runs on H_2, He, and A, after removing the original gas filling and introducing new fillings of the same pressures, indicated that the measurements were reproducible within the statistical uncertainty.

COMPARISON OF THE EXPERIMENTAL RESULTS WITH THE THEORY

The theory of primary ionization has been treated both classically and quantum mechanically in various degrees of approximation by a number of authors. The most recent and comprehensive treatment of the subject —given by Bethe[8]—yields the following formula for

TABLE I. Measured values of the specific primary ionization of H_2, He, Ne, and A for various β-ray energies.

Energy (Mev)	v/Mc	Specific primary ionization-ions/cm at N.T.P. H_2	He	Ne	A
0.205	0.98	8.45±0.095	7.56±0.16	18.45±0.36	41.7±0.77
0.500	1.71	6.04±0.065	5.58±0.066	13.4 ±0.17	30.5±0.34
0.855	2.49	5.44±0.054	5.08±0.043	12.5 ±0.14	27.7±0.31
1.17	3.15	5.30±0.053	...	...	...
1.55	3.90	5.32±0.059	5.02±0.060	12.4 ±0.13	27.8±0.31

[8] H. A. Bethe, *Handbuch der Physik* (Julius Springer Verlag, Berlin, 1933), Vol. 24, No. 1, p. 515.

the variation of specific primary ionization with the velocity of the incident particle:

$$S=2\pi r_0^2 mc^2 N z^2 \frac{Za}{I_0}\frac{1}{\beta^2}\left[\ln\frac{2mc^2\beta^2}{I_0(1-\beta^2)}+b-\beta^2\right], \quad (4)$$

where S = number of primary ions per cm of path, $r_0=e^2/mc^2$ (classical electron radius), m = electron rest mass, c = velocity of light, N = number of atoms per cc at N.T.P., z = incident particle charge, Z = atomic number of gas, β = ratio of incident particle velocity to the velocity of light, I_0 = ionization potential of the gas, and a, b = dimensionless constants dependent upon the electronic structure of the gas.

For the particular case of atomic hydrogen ($I_0=13.5$ ev, $Z=1$), Bethe has calculated the values of the constants in this equation to be: $a=0.285$, $b=3.04$. For gases other than atomic hydrogen, the calculation of the constants cannot be readily accomplished without introducing rather rough approximations regarding the form of the wave functions of the bound electrons.

In the derivation of Eq. (4) the assumption is made that the incident particle is undeviated by individual collision with the atoms of the gas. This approximation leads to rather large errors at low energies but should not seriously affect the validity of the formula at electron energies greater than a few kv.

TABLE II.

	H_2	He	Ne	A
A	0.356±0.03	0.422±0.038	1.13±0.09	2.37±0.27
C	4.35 ∓0.02	3.98 ∓0.02	9.64∓0.11	21.8 ∓0.20

The form of Eq. (4) indicates that for a given gas, S depends only upon the velocity v and the charge z of the incident ionizing particle. By making the substitution,

$$\beta=(p/Mc)[(p/Mc)^2+1]^{-\frac{1}{2}}, \quad (5)$$

where p is the momentum and M the rest mass of the incident particle, and lumping the constant coefficients in Eq. (4), one obtains the expression:

$$S=A\left\{\left(\frac{p}{Mc}\right)^{-2}\left[\left(\frac{p}{Mc}\right)^2+1\right]\ln\left(\frac{p}{Mc}\right)^2-1\right\}+C\left(\frac{p}{Mc}\right)^{-2}\left[\left(\frac{p}{Mc}\right)+1\right]. \quad (6)$$

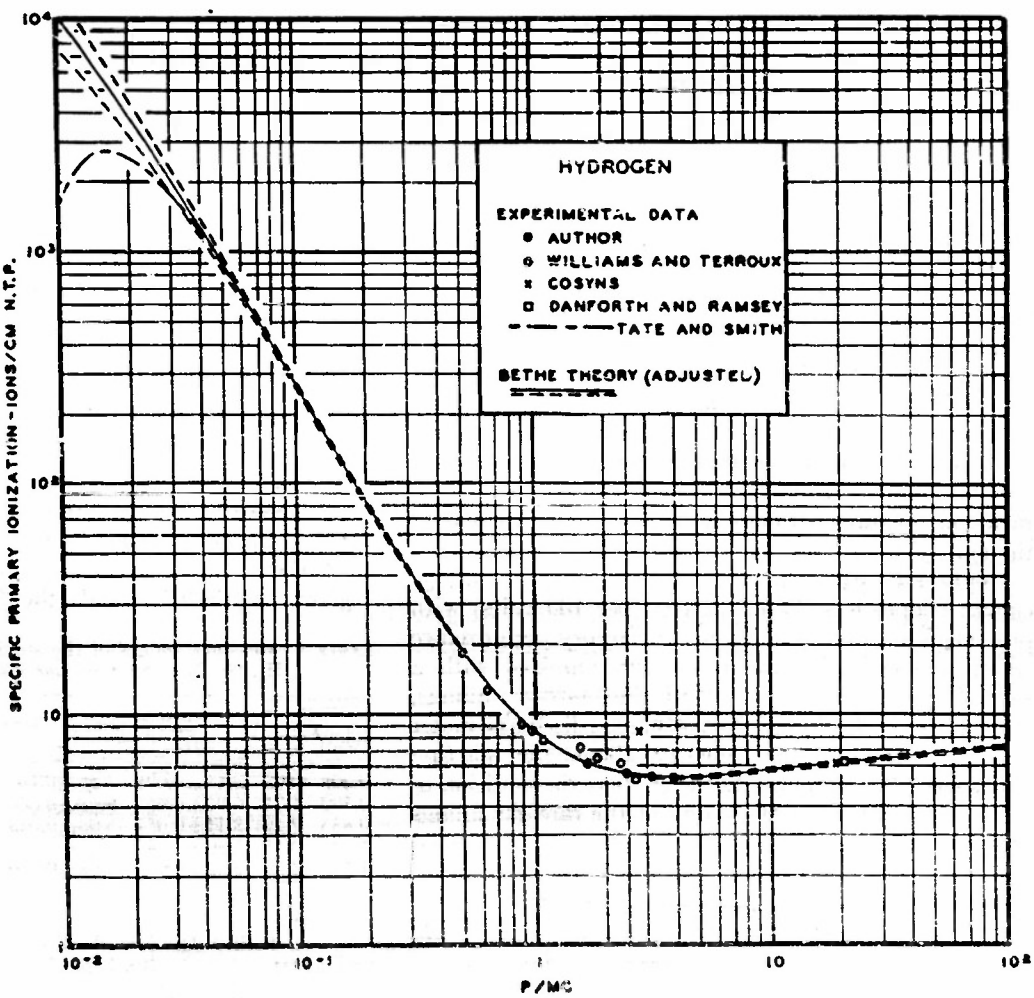

FIG. 3. Experimental results on hydrogen plotted as p/Mc. The data of Williams and Terroux,[1] Tate and Smith,[2] Danforth and Ramsey[4] and Cosyns[5,6] are shown for comparison. The solid curve represents the least-squares fit of the Bethe formula [Eq. (6)] to the present results. The dashed curves neighboring the solid curve are the extremes of the family of theoretical curves which fit all points of the present data within one standard deviation.

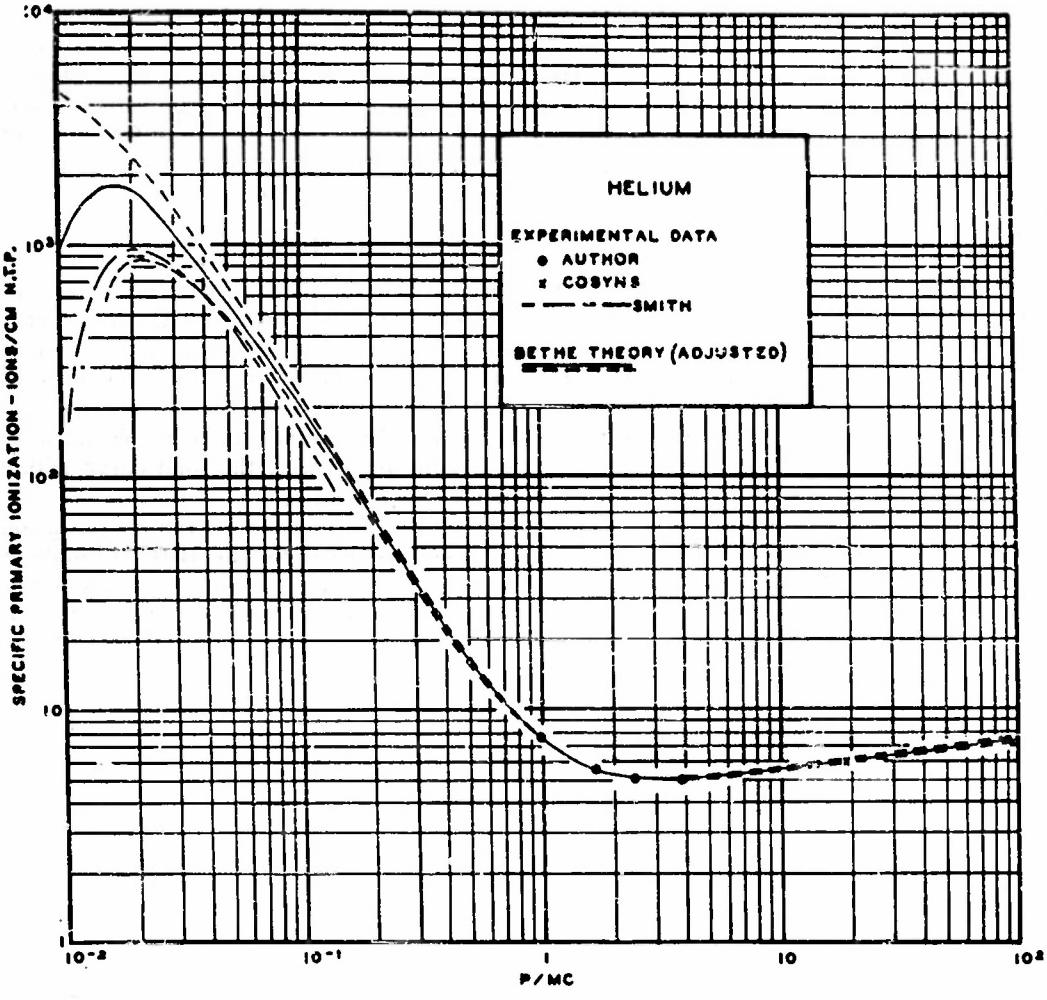

FIG. 4. Experimental results on helium plotted vs p/Mc. The data of Smith[3] and Cosyns[4] are also shown. The same remarks as in the caption of Fig. 3 apply to the solid and dashed curves.

The above form of the Bethe formula is preferred for ease in comparison with the experimental data. In terms of the constants of Eq. (4) the lumped constants A and C in Eq. (6) have the form:

$$A=2\pi r_0^2 mc^2 Nz^2 Za/I_0, \tag{7}$$

$$C=A[b+\ln(2mc^2/I_0)]. \tag{8}$$

In order to compare the theory with the experimental results the constants A and C have been empiricaliy determined for each of the gases investigated so that Eq. (6) yields the best agreement with the experimental results. The values of A and C determined by least squares fits are given in Table II, and plots of Eq. (6) evaluated with the tabulated constants are shown in Figs. 3-6 (solid curves). The dashed curves also shown in the figures indicate the extremes of a family of theoretical curves which fit all of the experimental values determined in the present investigation within one standard deviation. The amounts by which the constants corresponding to the two extreme curves deviate from the least squares values are indicated in Table II by the increments to the right of the $\pm$ and $\mp$ signs. The parameters for one of the extreme curves are obtained by taking the upper signs and those for the other extreme curve by taking the lower signs. It should be noted that the two extreme curves in each of Figs. 3–6 cross over one another in the neighborhood of $p/Mc=2$.

The parameters A and C calculated for atomic hydrogen from Eqs. (7) and (8) using the theoretical values of a and b are $A=0.145$, $C=2.08$. If the above values are multiplied by the factor 2 (to give the effect of doubling the number of atoms/cm³) the resulting constants $A=0.290$ and $C=4.15$ should represent a rather gross approximation to the constants for molecular hydrogen. Comparison with the empirical constants for H_2 given in Table II indicates that the A's agree within 25 percent and the C's within 5 percent. The discrepancy between the A's is not at all surprising in view of the difference in the electronic structures of atomic and molecular hydrogen.

DISCUSSION

(a) Hydrogen

The least squares fit of the Bethe formula (solid curve Fig. 3) to the H_2 data obtained in the present

investigation merges smoothly with the experimental data of Tate and Smith[3] at $p/Mc=0.054$ (electron energy of 750 v) but diverges gradually at lower energies toward primary ionization values in excess of the Tate and Smith values. The experimental points of Cosyns[5] and of Danforth and Ramsey[4] for cosmic-ray mesons (average value of $p/Mc\simeq 19$) agree with the solid curve within the experimental errors. The cloud-chamber data of Williams and Terroux[1] scatter somewhat broadly above and below the curve indicating the presence of relatively large experimental uncertainties, however, the over-all consistency with the present results is quite satisfactory.

Hereford[7] has conducted a low pressure counter study of the primary ionization of H_2 by β-rays and cosmic-ray mesons. These results (not plotted in Fig. 3) are consistent with the other work as regards the ionization of cosmic rays but show considerable discrepancies with the present work in the β-ray energy range. A value obtained by Hereford for a continuous spectrum of β-rays of near-minimum ionization ($2.6<p/Mc<5.8$) is about 15 percent lower than the present data in the same range. On the other hand, a point obtained by Cosyns[6] for 1-Mev electrons ($p/Mc=2.8$) is about 50 percent higher than the present value. The most likely explanation for these discrepancies seems to be that in the earlier low pressure counter work dealing with β-rays the path length was not well defined and that scattering was not adequately treated in calculations of the effective pathlength.

(b) Helium

In the case of helium, there is a rather large discrepancy between the solid curve and the low energy data of Smith.[3] This seems rather surprising in view of the relatively high accuracy with which the formula joins the high energy data with the low energy data for the other gases. The cosmic-ray point obtained by Cosyns[5] for helium agrees with the solid curve within the experimental uncertainties.

The gradual relativistic increase in primary ionization (at high energies) predicted by the Bethe formula is confirmed in both H_2 and He by the consistency of the cosmic-ray data of Cosyns[5] and of Danforth and Ramsey,[4] with the theoretical extrapolation of the β-ray data.

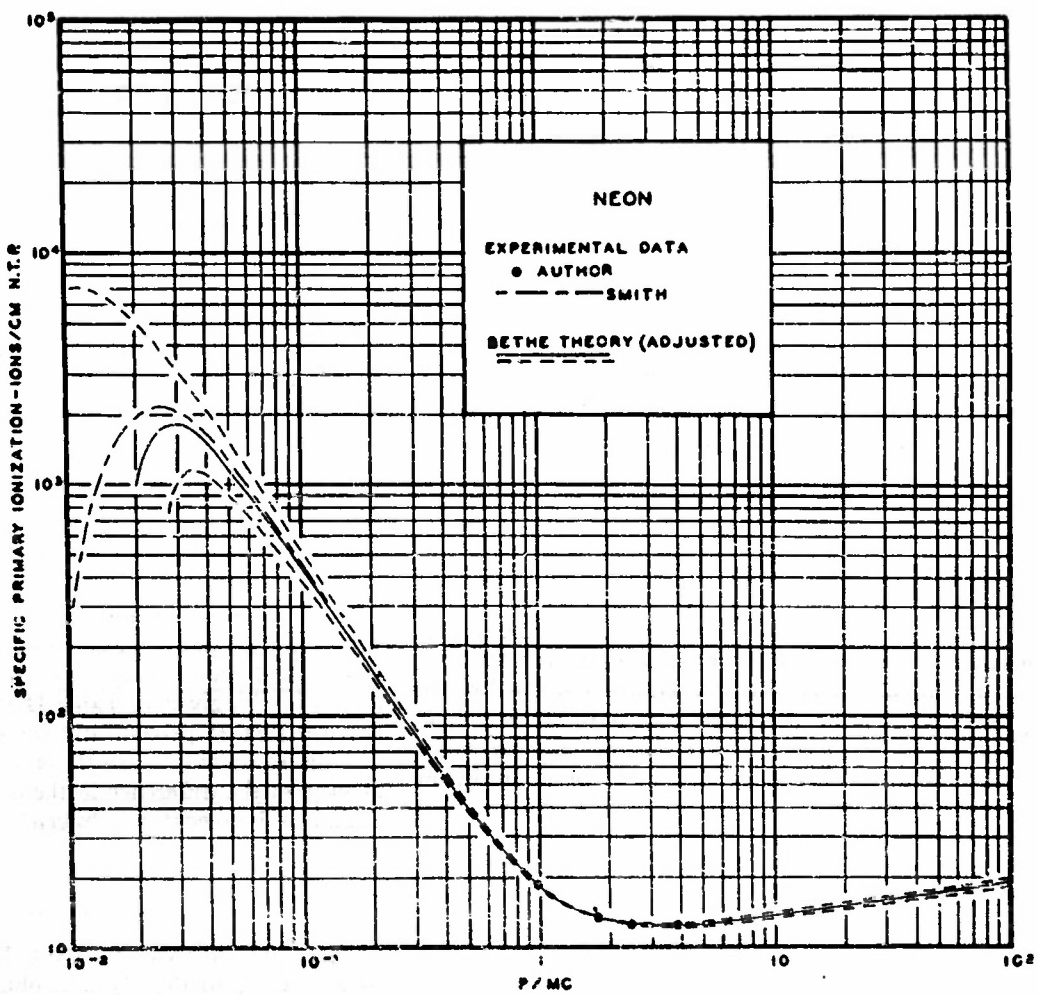

FIG. 5. Experimental results on neon plotted as p/Mc. A plot of Smith's data[3] adjusted as indicated in the text is also shown. The same remarks as in the caption of Fig. 3 apply to the solid and dashed curves.

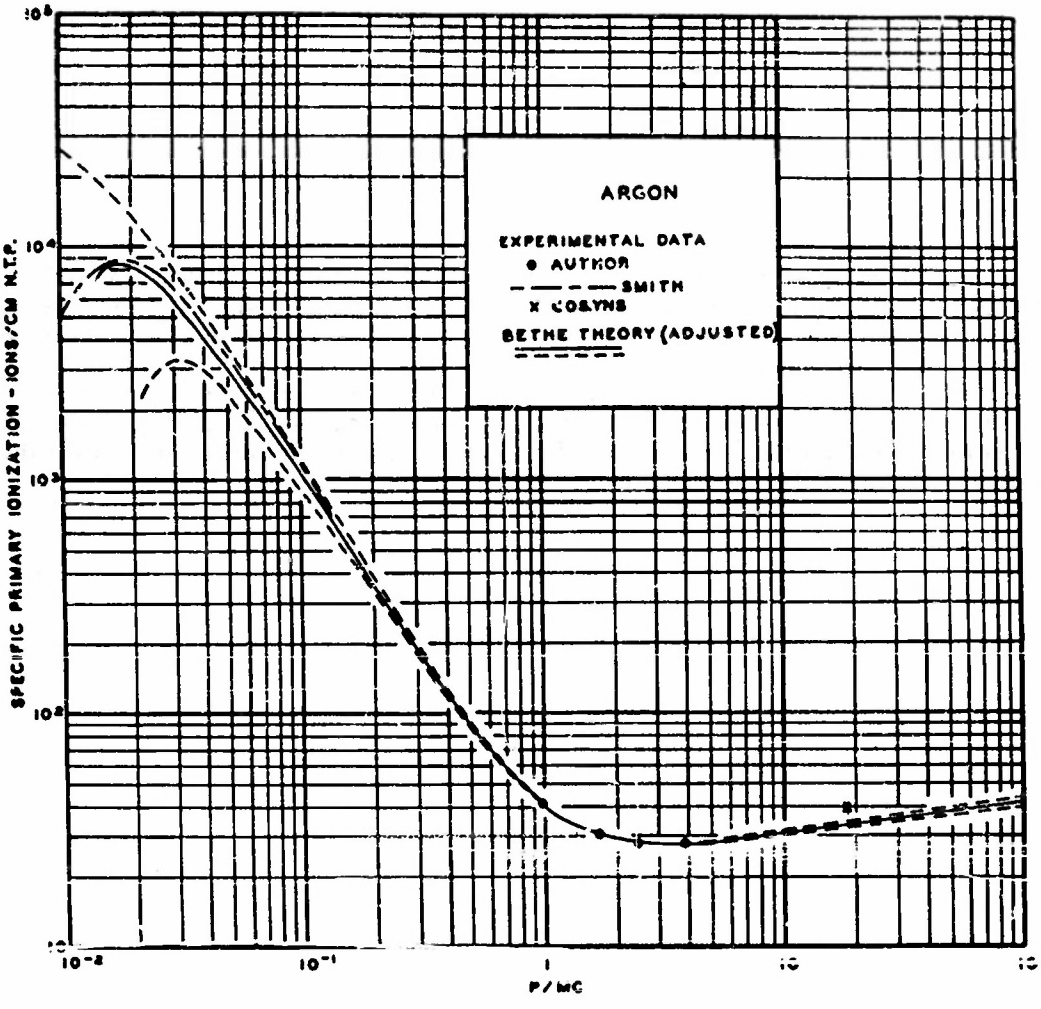

FIG. 6. Experimental results for argon plotted as p/Mc. The data of Smith[3] (adjusted as indicated in the text) and Cosyns[5] are also shown. The same remarks as in the caption of Fig. 3 apply to the solid and dashed curves.

(c) Argon and Neon

In order to compare Smith's results[3] on argon and neon with the present measurements, it is necessary to observe that the quantity measured by Smith is not in general exactly equivalent to specific primary ionization. While the specific primary ionization, S, measured in the present experiment is defined as the number of ionizing collisions per unit path length, the "ionization probability," P, measured by Smith may be defined as the number of electrons released in ionizing collisions per unit of path length. If R denotes the average number of electrons removed from an atom (or molecule) per ionizing collision, we have the relationship

$$S=P/R. \tag{9}$$

The mass-spectrographic measurements of Bleakney[9] show that the $\bar{R}$ values for H_2 and He are equal to unity within approximately one percent for incident electrons in the energy range zero to 500 ev. Consequently, the Smith data for H_2 and He have been plotted directly in Figs. 3 and 4 without compensation for multiple ionization. An analysis of Bleakney's Ne and A data indicate that $R=1.06$ for 500-ev electrons in Ne and $R=1.10$ for 500-ev electrons in A. As the R values for both of the heavy gases vary quite slowly with increasing energy in the range 300 to 500 ev, we have adopted the procedure of extrapolating R as a constant above 500 volts ($p/Mc=0.048$) in transforming the Smith A and Ne data[3] into the curves attributed to Smith in Figs. 5 and 6. The uncertainty as to the accuracy of the transformed curves in the energy range 500 to 4500 ev ($0.048<p/Mc<0.133$) is of little importance in view of a comparable uncertainty in the position of the extrapolated theoretical curve in the low energy region. The fact that the Bethe formula provides the indicated degree of fit over the energy range from approximately 1 kev to 1.6 Mev may be regarded as a substantial verification of the correctness of the form of the theory at energies exceeding 1 kev.

[9] W. Bleakney, Phys. Rev. 36, 1303 (1930); 35, 1180 (1930).

CONCLUSION

The comparison made between the existing experimental results and the adjusted Bethe formula indicate a rather comprehensive agreement over an extremely

large energy range. Although it is unfortunate that the parameters in the Bethe formula have not been calculated from theory for any of the gases investigated here, the formula appears to be a reliable tool for interpolating between and extrapolating beyond measured values of specific primary ionization at energies in excess of a few kev.

At very low energies, there is a systematic departure of the theory from the experimental results, which must be attributed to the weakness of the present theory. The only cases where the Bethe formula extrapolations of the present data are inconsistent are the experimental results of others in the neighborhoods of $p/Mc=0.05$ and $p/Mc=19$ occur in the case of He, where the low energy data of Smith[3] fall below the theoretical curve, and in the case of A where the cosmic-ray point of Cosyns[5] lies above the curve. The decision as to whether these discrepancies are attributable to the theory or to the experimental technique is difficult to make at the present time.

The data obtained in the present investigation, in addition to serving as a useful guide toward further development of the theory of ionization, should be of value both in the design of low efficiency G-M counters and in the analysis of cloud-chamber photographs containing the tracks of fast particles.

Measurements of the specific primary ionization of several other simple gases and of some of the complex organic vapors utilized in G-M counters will be carried out in the near future.

The writer wishes to express his appreciation to Dr. W. F. G. Swann, Director of the Bartol Research Foundation, for several helpful discussions during the course of this work.

Reprinted from THE PHYSICAL REVIEW, Vol. 90, No. 5, 992-993, June 1, 1953
Printed in U. S. A.

The Phosphorescence of Thoria*

C. E. MANDEVILLE AND H. O. ALBRECHT
Bartol Research Foundation, Franklin Institute, Swarthmore, Pennsylvania
(Received April 15, 1953)

WHILE observing luminescent effects resulting from the irradiation of various metallic oxides with nuclear particles, the writers chanced to note a continuous light emission from thoria. This luminescence was detected prior to application of any primary excitants such as alpha-particles, beta-rays, gamma-rays, or ultraviolet light. The property is exhibited by both Norton's reddish arc-melted coarsely crystalline thoria and white pieces of thoria sintered from powdered ThO_2.[1,2] The measurements of light intensity were performed with the use of phototubes RCA-5819 and RCA-1P28 as detectors.

Owing to the natural radioactivity of Th^{232} and its daughter elements, ThO_2 emits ~22 000 α's per gram per second, ~15 000 β's per gram per sec, and ~20 000 γ's per gram per sec. These internally emitted nuclear radiations give rise through self-absorption in the thoria to the observed luminescence which has apparently attained a nearly constant intensity, decaying with the enormous half-period of Th^{232}. When a small piece of crystalline thoria was placed before the slit of a small Hilger quartz spectrograph, no noticeable darkening of the photographic plate was produced after an exposure of two weeks. However, when the crystal was bombarded by ~15 mC of polonium α's, a spectrogram showing an emission band at ~4500A was obtainable within two days. The emission band along with the calibration lines of a mercury arc are drawn in Fig. 1.

A crystal of thoria was irradiated by 15 mC of polonium α's for a period of five minutes. A fast decaying alpha-particle excited phosphorescence, superposed upon the "natural" luminescence, was observed as shown in Fig. 2, curve A. Subtraction of the natural luminescent intensity arising from the internally emitted nuclear radiations yields curve B, the decay curve of the rapidly decaying α-particle induced phosphorescence. Since the curve assumes no constant slope in the time interval covered by the observations, a likely interpretation is that the decay curve is a composite one formed by a superposition of two or more power laws.

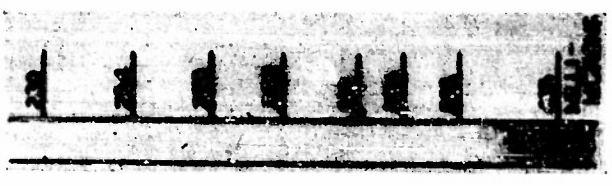

FIG. 1. Luminescent emission of thoria under alpha-irradiation.

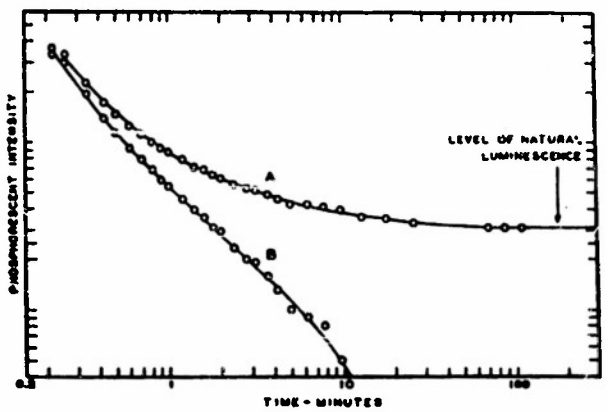

FIG. 2. Decay of the alpha-particle induced phosphorescence of thoria. Curve A is a plot of the observed emission; curve B, phosphorescent decay corrected for the presence of thoria's "natural" luminescence.

Numerous auxiliary experiments were performed to eliminate the possibility that the measured natural luminescence be generated by irradiation of air surrounding the thoria or by bombardment of the glass envelope of the phototube.

It is to be expected that radioactive uranyl salts also possess an intrinsic luminescence. Uranyl nitrate was observed to emit light resulting from interval emission of α-, β-, and γ-rays. Its light emissions seem, however, to be confined to fluorescence or a very short-lived phosphorescence. Measurements commenced a few seconds after cessation of irradiation by polonium alpha-particles and ultraviolet light gave no evidence of any appreciable phosphorescence.

* Assisted by the joint program of the U. S. Office of Naval Research and the U. S. Atomic Energy Commission.

[1] The autoexcited luminescence of *radium* compounds was studied by early investigators. See, for example, J. A. Rodman, Phys. Rev. 23, 478 (1924). References to still earlier measurements are contained in this paper.

[2] The luminescence of ThO_2 activated by Pr, Sm, and Tb has been studied under x-ray, cathode ray, ultraviolet light, and hydrogen flame excitation by F. G. Wick and C. G. Throop, J. Opt. Soc. Am. 25, 37 (1935). These authors do not comment upon any self-induced luminescence nor do they appear to have studied the afterglow in particular. A spectrographic analysis of the thoria employed by the writers showed that Al, Be, Ce, Cr, Cu, La, Si, Ti, Vt, and Zr were all present simultaneously in activator quantities.

Reprinted from THE PHYSICAL REVIEW, Vol. 90, No. 2, 328–329, April 15, 1953
Printed in U. S. A.

Spin and Parity of the 2.3-Mev Excited State of Te^{124}†

FRANZ R. METZGER
Bartol Research Foundation of the Franklin Institute, Swarthmore, Pennsylvania
(Received February 20, 1953)

IT has been reported[1] that the gamma-rays emitted in the disintegration of Sb^{124} do not show any directional correlation. Definite conclusions cannot be drawn from this isotropy as several γ–γ cascades contribute to the observed coincidence rate.

Using pulse-height selectors in both channels, we have investigated the directional correlations of the different cascades separately and report here on the 1.7–0.6-Mev and the 2.06–0.6-Mev cascades.

After a correction for angular resolution, the data on the 1.7–0.6-Mev cascade can be fitted with a distribution $W(\Theta)=1-0.094\times\cos^2\Theta$.

If one assumes spin 0+ for the ground state of the even-even Te^{124} nucleus, the 0.6-Mev excited state has spin 2+.[2] The possible spin combinations are, therefore, 0–2–0, 1–2–0, 2–2–0, 3–2–0, and 4–2–0, all higher spins being excluded by conversion measurements.[3] The assignment 1–2–0 is improbable in view of the absence of a strong crossover transition to the ground state of Te^{124}. A comparison of the theoretical correlations with the experimental points (Fig. 1) eliminates all spin combinations with the exception of 3–2–0. The spin of the 2.3-Mev excited state of Te^{124} is, therefore, taken as 3.

The correlation coefficient $A_2=-0.094\pm0.010$ allows an admixture of at most 10^{-6} parts of quadrupole to the 3–2 dipole transition. In comparison with recently measured $E2$-$M1$ mixtures[4] this $E2/M1$ ratio is off by factors of 10^5 to 10^6. One is therefore inclined to assume that the 3–2 transition in Te^{124} is not $M1$-$E2$, but involves a parity change and is almost pure $E1$. In Sr^{86}, which exhibits a very similar angular correlation, the 3–2 transition is indeed $E1$, as shown by conversion measurements.[5]

Recently a group at Princeton[6] has determined the number of 1.7-Mev conversion electrons to be 1/30 of the number of 0.6-Mev conversion electrons. From measurements with calibrated converters, we estimate the ratio of the intensities of the 1.7-Mev and 0.6-Mev gamma rays as 0.55 ± 0.12. Combining these, one arrives at a conversion coefficient of $(2.6\pm0.7)\times10^{-4}$ for the 1.7-Mev transition. This has to be compared with theoretical values[7] of 2.2×10^{-4} for $E1$ and 5.8×10^{-4} for $M1+10^{-6}E2$. It is therefore concluded that the 1.7-Mev transition in Te^{124} is almost pure $E1$ and that the 2.3-Mev excited state of Te^{124} has spin 3, odd parity.

When measuring the 1.7—0.6-Mev coincidences, one has to accept a contribution of about ten percent from the 2.06—0.6-Mev cascade. In order to insure that the 2.06—0.6-Mev cascade does not alter the 1.7—0.6-Mev data considerably, we investigated the 2.06—0.6-Mev cascade for itself, accepting in one channel only the photoelectron peak of the 2.06-Mev gamma-ray. Although the counting rates were low, it was possible to establish that the 2.06—0.6-Mev cascade shows a correlation of the form $1-0.09\times\cos^2\Theta$ which is practically identical with the 1.7—0.6-Mev correlation. From this, one can conclude that the 2.06—0.6-Mev cascade will not affect the 1.7—0.6-Mev data, and one can furthermore assign spin 2 to the 2.66-Mev level in Te^{124}. In view of the low intensity of the 2.06-Mev transition, no conversion information is available. However, the similarity of the ft values of the two beta-transitions suggests that both states have the same parity, i.e., both are 3 odd.

The assignment of 3— to the two highly excited states in Te^{124} gives some indication as to the spin of the ground state of Sb^{124}, a spin which has been the subject of some speculation in connection with the strong β—γ correlation observed in Sb^{124}. Recently Morita and Yamada[8] have investigated the consequences of the measured β—γ correlation and of the shape of the 2.3-Mev beta-spectrum of Sb^{124}. These authors arrived at 3 as the most probable total angular momentum for the Sb^{124} ground state. The next probable value, 4+, was excluded on the grounds of the relatively low ft value.

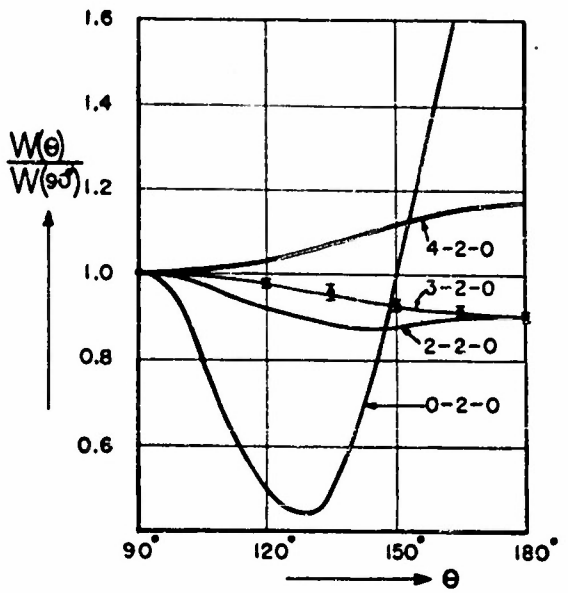

FIG. 1. Directional correlation of the 1.7-0.6-Mev cascade of Te^{124}. The theoretical correlations expected for different spins of the 2.3-Mev state are drawn in for comparison. For the 3–2–0 and 2–2–0 combinations the dipole-quadrupole mixtures were adjusted to fit the experimental $W(180°)/W(90°)$ ratio. For 0–2–0 and 4–2–0 the pure quadrupole-quadrupole correlations are plotted. No mixture is possible for 0–2–0 and only very small admixtures can be expected for 4–2–0.

If the ground state of Sb^{124} were 3—, the beta-transition to the 2.3-Mev excited state of Te^{124} with 3— would be allowed. The experimental logft value, however, is 7.7, which corresponds to a first forbidden transition. It cannot be denied that a logft value of 7.7 could be attributed to an allowed transition ("L forbidden") but this seems at least as artificial as the exclusion of spin 4+ based on a low logft value. The number of observed second forbidden transitions is still very small, and the grouping of the ft values is therefore very uncertain. It might be added that the logft value for the second forbidden beta-transition in Fe^{59}[9] is 10.9, i.e., very close to the value 10.3 for Sb^{124}.

Based on these considerations, we are inclined to make the assignment 4+ rather than 3— to the ground state of Sb^{124}.

† Supported in part by the joint program of the U. S. Office of Naval Research and the U. S. Atomic Energy Commission.
[1] J. R. Beyster and M. L. Wiedenbeck, Phys. Rev. 79, 169 (1950); D. T. Stevenson and M. Deutsch, Phys. Rev. 83, 1202 (1951).
[2] F. R. Metzger, Phys. Rev. 86, 435 (1952).
[3] D. R. Hutchinson and M. L. Wiedenbeck, Phys. Rev. 88, 699 (1952).
[4] M. Glaubman and F. R. Metzger, Phys. Rev. 87, 203 (1952); D. Schiff, thesis, University of Illinois, 1952 (unpublished); R. M. Steffen, Phys. Rev. 89, 665 (1953).
[5] F. R. Metzger and H. C. Amacher, Phys. Rev. 88, 147 (1952).
[6] E. P. Tomlinson, private communication.
[7] Rose, Goertzel, and Perry, Oak Ridge National Laboratory Report ORNL 1023 (unpublished).
[8] M. Morita and M. Yamada, Prog. Theoret. Phys. 8, 449 (1952).
[9] F. R. Metzger, Phys. Rev. 88, 1360 (1952).

Reprinted from THE PHYSICAL REVIEW, Vol. 90, No. 1, 25–28, April 1, 1953
Printed in U. S. A.

The Alpha-Particle Induced Phosphorescence of Silver-Activated Sodium Chloride*

C. E. MANDEVILLE AND H. O. ALBRECHT
Bartol Research Foundation of the Franklin Institute, Swarthmore, Pennsylvania
(Received December 16, 1952)

Using as primary excitants ultraviolet light and polonium alpha-particles, the phosphorescent afterglow of the double banded phosphor, silver-activated sodium chloride, has been measured as a function of the time with photosensitive Geiger counters and photomultiplier tubes. The decay curves of the phosphorescent intensity of the two bands can be represented by appreciably different power laws. Decay slopes greater in absolute magnitude than two on a $\log I - \log t$ plot have been frequently observed.

INTRODUCTION

IN several previous communications,[1,2] the writers have discussed the fluorescence and phosphorescence of NaCl-Ag irradiated by nuclear particles. The earlier reports[1,2] constitute mainly an account of how first phosphorescent emission, and later fluorescent pulses, were detected in photosensitive Geiger counters. In the course of qualitative studies of the phosphorescence of the far ultraviolet band as detected with photosensitive Geiger counters, a marked stimulation of the ultraviolet band by long wave light was noted. The soft radiations from the red and green pilot lights on the control panel of the scaling circuit gave rise to a distinct stimulation of the phosphorescent emission. It was immediately suggested[3] that NaCl-Ag might serve as a dosimeter for nuclear radiation, the phosphorescent yield under photostimulation being a measure of dosage received much earlier. However, the present discussion will concern itself mainly with a study of the normal unstimulated phosphorescence induced in samples of NaCl-Ag by alpha-particles and ultraviolet light.

Since the time of the first reports by the writers,[1–3] the study of the phosphorescence of NaCl-Ag has been extended by Furst and Kallmann[4] and by Bittman, Furst, and Kallmann.[5] The light emission has been shown to occur in two bands[3,4] centered, respectively, at 2500A and 4000A. It has also been known for some time that these two bands are emitted when ultraviolet

* Assisted by the joint program of the U. S. Office of Naval Research and the U. S. Atomic Energy Commission.
[1] C. E. Mandeville and H. O. Albrecht, Phys. Rev. 79, 1010 (1950); 80, 117, 299, and 300 (1950).
[2] H. O. Albrecht and C. E. Mandeville, Phys. Rev. 81, 163 (1951); Rev. Sci. Instr. 22, 855 (1951).
[3] C. E. Mandeville, privately circulated memorandum (September 26, 1950).
[4] M. Furst and H. Kallmann, Phys. Rev. 82, 964 (1951); 83, 674 (1951).
[5] Bittman, Furst, and Kallmann, Phys. Rev. 87, 83 (1952).

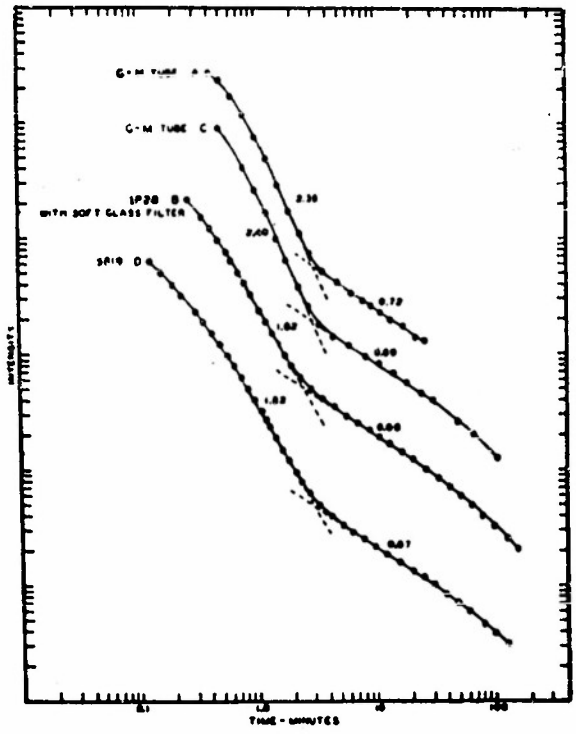

FIG. 1. Phosphorescent decay of NaCl-Ag (Harshaw) irradiated on successive occasions for five seconds at a time by the alpha-particles of polonium. The curves are lettered in chronological order.

light is employed as the primary excitant.[6] A discussion of previous papers on ultraviolet excitation of NaCl-Ag may be found in the aforementioned reference.[6]

PROCEDURE

In the present investigation, the phosphorescence of NaCl-Ag irradiated by alpha-particles and ultraviolet light has been observed, using as detectors photosensitive Geiger counters and photomultiplier tubes RCA-5819 and RCA-1P28. The G-M tubes were constructed with copper cathodes, and the phosphorescent emission was usually introduced through a thin window of Pyrex (3 mg/cm^2) or through a side wall of thickness one millimeter, made of Corning 9741 glass. These tubes exhibited a maximum of spectral response at ~2500A with no detectable response whatever above ~3000A. With the strongest phosphorescent sources used, the counting rates of the photosensitive G-M tubes decreased immediately to cosmic ray background when one millimeter of soft glass was inserted before the counter, indicating only response to the ultraviolet of the short wave band. *Thus, measurements with the G-M tubes constituted observation of the decay of the short wave band alone.*[7] The RCA-5819 photomultiplier was utilized for detection of the phosphorescence of the long wave band. Although these tubes are not expected to respond at wavelengths shorter than 3000A, two millimeters of soft glass were interposed between phosphorescent source and phototube as a precautionary measure for elimination of any last vestiges of response to the short wave band. The dc current flowing in the photomultiplier was taken as a measure of the phosphorescent intensity. The current was measured in a fast galvanometer ($T=4$ sec), and measurements were not commenced until several seconds after cessation of irradiation, so that ballistic corrections were small as shown by calculation in terms of the constants of the galvanometer. The deflection of the galvanometer and the readings of a stop watch were photographed simultaneously with a Sept camera. Measurements with an RCA-1P28 photomultiplier tube were also carried out. This detector is sensitive to light emitted in both bands. The decay curve of the combined emission of both bands is of interest for reasons to be discussed later.

The above discussed detectors can, of course, also be used for the detection of "stored light" released by thermostimulation[8] and photostimulation.[9]

In general, the properties of two types of crystals have been investigated. Single crystals of NaCl+1 percent AgCl were obtained from the Harshaw Chemical Company (hereafter referred to as "Harshaw"), and polycrystalline melts of NaCl+0.5 percent AgCl were prepared at the Bartol Research Foundation (hereafter referred to as "Bartol").

RESULTS

The decay of NaCl-Ag (Harshaw), irradiated for five seconds by a source of twenty-five millicuries of polonium alpha-particles, is shown in Fig. 1. For these measurements the same specimen was bombarded repeatedly, under identical conditions; that is, successive decay curves were taken first in the G-M tube, then in a 1P28 tube with filter, again in the G-M tube, and finally in the RCA-5819 photomultiplier tube. The crystal was completely de-excited between bombardments by photostimulation at the conclusion of each decay curve. Because of the response characteristics of the various detectors as discussed in the preceding section, it is evident that curves A and C give the decay of the short wave band and curves B and D that of the long wave band. All of the curves of Fig. 1 exhibit two distinct slopes on the log-log plot.[10] The short wave band has an early slope of ~(−2.38) followed by a later slope of ~(−0.7). The long wave band decays initially with a slope of ~(−1.83) followed by the later

[6] Etzel, Schulman, Ginther, and Claffy, Phys. Rev. 85, 1063 (1952).

[7] The photosensitivity of the G-M tubes was checked at the beginning and upon completion of each decay curve by means of a standard ultraviolet source. This consisted of an alpha-source bombarding a crystal of fluorite.

[8] H. Friedman and C. P. Glover, Nucleonics 10, No. 6, 24 (1952).

[9] Kallmann, Furst, and Sidran, Nucleonics 10, No. 9, 15 (1952).

[10] It is to be observed that at times less than one minute the decay curves are relatively flat, and the slopes have not as yet assumed in absolute magnitude the value of the exponent of the power law which characterizes the decay. A slope equal in magnitude to the exponent is attained when $At \gg 1$ [see Eq. (2) of the text].

slope of $\sim(-0.7)$. From the curves of Fig. 1, several general conclusions can be drawn:

(1) The absolute value of the decay slopes can be considerably larger than two.

(2) At least two trap depths are involved. The steep initial slope represents the depletion of electrons in traps shallower than the traps related to the slope of $\sim(-0.7)$.

(3) The slope of $\sim(-0.7)$ is not the terminal decay slope of the light emission associated with escape of electrons from the deeper traps. It is an earlier slope which is encountered in a transition region such as that described by Mott and Gurney.[11]

(4) The short and long wave bands decay according to differing power laws in the region below $\sim$5 minutes.

A second Harshaw crystal was irradiated by polonium alphas for five seconds at a time, and decay curves were observed with the use of various detectors as shown in Fig. 2. The results are essentially the same as those of Fig. 1, the short wave band decaying with a steeper slope on the log-log plot than does the long wave band. It is to be noted that the slope of curve *A* is intermediate between the corresponding slopes of curves *B* and *D* (the long wave band alone) and curve *C* (the short wave band). Curve *A*, obtained with no filter before the 1P28, gives the decay of the combined emission of the two bands. To ascertain whether the slower decay [slope $\sim(-0.7)$] offered any explanation for the differing decay slopes of the two bands, the slower decay was extrapolated to small values of the time and subtracted from the total intensity on the interval $0.5\ \text{min}<t<2\ \text{min}$, t being the time. On this time interval, the slope of the difference curve of curve *C* became (-3.00) and that of the difference curve of curve *D* became (-2.16). The apparent difference in the modes of decay was not erased by this operation. The ratio of the slopes remained unchanged. Thus,

$$n_C/n_D = 2.48/1.83 = 3.00/2.16 = 1.35.$$

The decay slopes are thought to have been measured with a probable error of ± 0.05.

The question of whether successive bombardments in some way altered the properties of the crystal come under consideration. The decision was made to observe simultaneously the decay of the two bands resulting from a single irradiation. Accordingly, NaCl-Ag (Bartol) was irradiated for five seconds with polonium alphas. The phosphorescing material was placed between a photosensitive G-M tube and a 1P28 photomultiplier tube. Curves I show the simultaneous decay of the two bands as observed with the 1P28 with filter and with a photosensitive G-M tube. Curves II represent simultaneously observed decay curves using as detectors a G-M tube and the 1P28 without filter. Here again it is clear that the two bands decay with differing power laws and that the decay of the mixture of the two bands has an intermediate slope.[12] It is to be observed that the curves of Fig. 3 assume their maximum negative slopes at times about ten minutes later than do those of Figs. 1 and 2, although the conditions of excitation were identical and the specimen sizes comparable. This difference could be explained by variation of silver content.

DISCUSSION OF RESULTS

Decay slopes greater than two have been previously observed.[13] For example, a slope of -2.09 was reported for ZnS under ultraviolet excitation at 80°C. However, this same decay curve, when examined at a relatively low value of the phosphorescent intensity, begins to exhibit a slope much larger in absolute magnitude than 2. These data are interpreted by Mott and Gurney[11] as evidence for "frozen-in" interstitial ions which serve as luminescence centers.

A similar explanation may also apply to the curves of the present investigation. Let it be assumed that ν interstitial ions are present and that n trapped electrons and n positive holes result from excitation by the alpha-

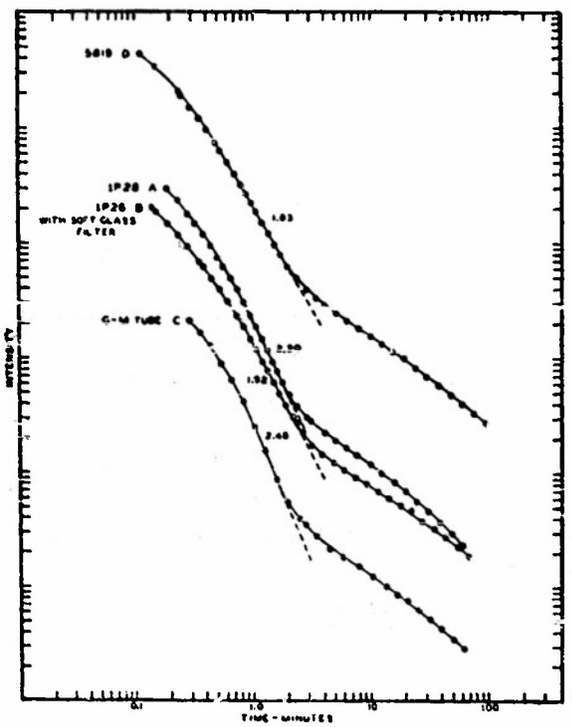

FIG. 2. Phosphorescent decay of NaCl-Ag (Harshaw). The absolute magnitude of the slope of the short wave band observed in the G-M tube is greater than that of the long wave band (5819 and 1P28 with filter). The slope of decay of the two bands combined is intermediate. The curves are lettered chronologically.

[11] N. F. Mott and R. W. Gurney, *Electronic Processes in Ionic Crystals* (Oxford University Press, London, 1948), second edition, p. 215, Fig. 84.

[12] The curves detected in the G-M tubes have been unduly depressed by dead-time loss at times less than one minute. On the interval $1\ \text{min} \leqslant t \leqslant 5\ \text{min}$ where the evaluation of the slope was made, the dead-time loss was negligible.

[13] V. V. Antonov-Romanovsky, Physik. Z. Sowjetunion 7, 366 (1935).

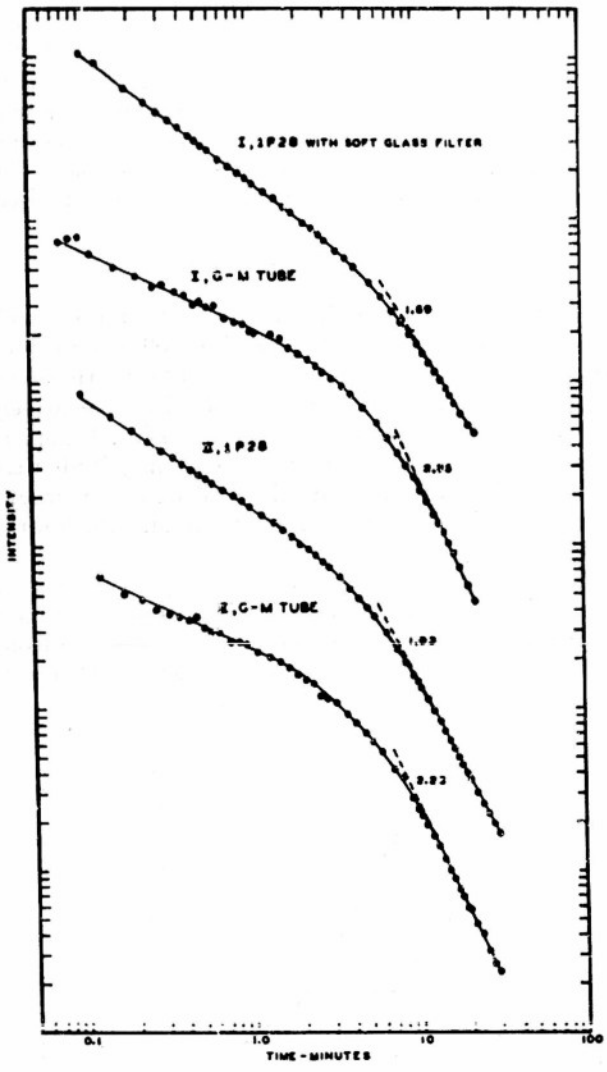

FIG. 3. Phosphorescent afterglow of NaCl-Ag (Bartol) observed simultaneously in G-M tube and photomultiplier.

particles. Then, following Mott and Gurney,[14]

$$dn/dt = -An(n+\nu), \tag{1}$$

where A is a constant. For $n \gg \nu$, the solution of this equation is

$$\frac{dn}{dt} = \left(\frac{dn}{dt}\right)_{t=0} \Big/ (1 + An_0 t)^2. \tag{2}$$

For $n \ll \nu$, the solution is

$$\frac{dn}{dt} = \left[\left(\frac{dn}{dt}\right)_{t=0}\right] e^{-\nu A t}. \tag{3}$$

When the traps are nearly exhausted, at relatively large values of the time, Eq. (1) indicates that a first order process becomes the dominant mode of decay, giving rise through Eq. (3) to slopes on a log-log plot greater than the slope of two which is associated with the normal bimolecular decay of Eq. (2).† For large values of the time, the slope of an exponential process approaches infinity on a log-log plot.

A general conclusion which can be drawn from these measurements is that for a given set of conditions of excitation, the two bands decay according to different power laws. It has been previously shown[6] that the long wave band arises from the presence of paired silver ions in the crystal lattice. It seems, therefore, probable that the trap depth distribution associated with paired silver ions is different from that related to the single silver ions.[15]

ADDITIONAL REMARKS

The decay curves of this paper are representative of about two hundred similar curves which have been recorded in connection with the phosphorescent decay of NaCl-Ag. Although Figs. 1, 2, and 3 refer specifically to the alpha-particle induced phosphorescence, as stated in the introduction, ultraviolet light was also employed as a primary excitant. The decay curves excited by ultraviolet did not differ markedly from those arising from alpha irradiation. Slopes greater in absolute magnitude than two were often encountered.

Although not shown in the accompanying figures, negative slopes having absolute values greater than two were often observed for the decay curves of the long wave band under both ultraviolet and alpha-particle excitation. For one such curve, the "light sum" was calculated for an irradiation with 25 mC of alpha-particles for five seconds. This rough estimate gave a phosphorescence yield in the long wave band of 0.54 photon/alpha on the time interval $5 \text{ sec} \leq t \leq \infty$. Taking into account the presence of the short wave band, a total emission of one or two photons per alpha-particle is suggested. In the course of the present measurements, it was estimated that specimens of approximate dimensions 1 cm×1 cm×0.4 cm were irradiated by $\sim 10^9$ alphas to give a light sum of $\sim 10^9$ photons.

The question arose as to whether the long wave band might be sufficiently intense to photostimulate the decay of the short wave band. Two identical crystals of NaCl-Ag were placed adjacent to each other with one millimeter of soft glass intervening. The long wave emission of one seemed to have no effect on the short wave emission of the other.

The writers wish to express their appreciation for the interest and suggestions of Dr. W. F. G. Swann in connection with these measurements. They wish also to acknowledge very helpful commentary by Dr. Raymond T. Ellickson of the University of Oregon.

[14] See reference 11, p. 212.

† An alternative explanation of the large negative slopes may be related to the storage of electrons in deep traps. Equations (1), (2), and (3) would also apply were there no interstitial ions but n electrons stored in deep traps and n electrons in shallow traps.

[15] See *Preparation and Characteristics of Solid Luminescent Materials; Cornell Symposium of the American Physical Society* (John Wiley and Sons, Inc., New York, 1948) and remarks by Garlick, Prongsheim, and Maurer, p. 397; also statements by Garlick, paper No. 5, p. 111.

reprinted from NUCLEONICS | March 1953, Volume 11, No. 3, Pages 32–35

Extending the Efficient Range of G-M Counters

A two-tube cut-off circuit reduces G-M tube deadtime to 1.5 μsec and permits operation up to 20,000 cps with deadtime losses of only a few per cent. Other methods reviewed are too elaborate, or they correct for deadtime without reducing it

By W. C. PORTER
Bartol Research Foundation of The Franklin Institute
Swarthmore, Pennsylvania

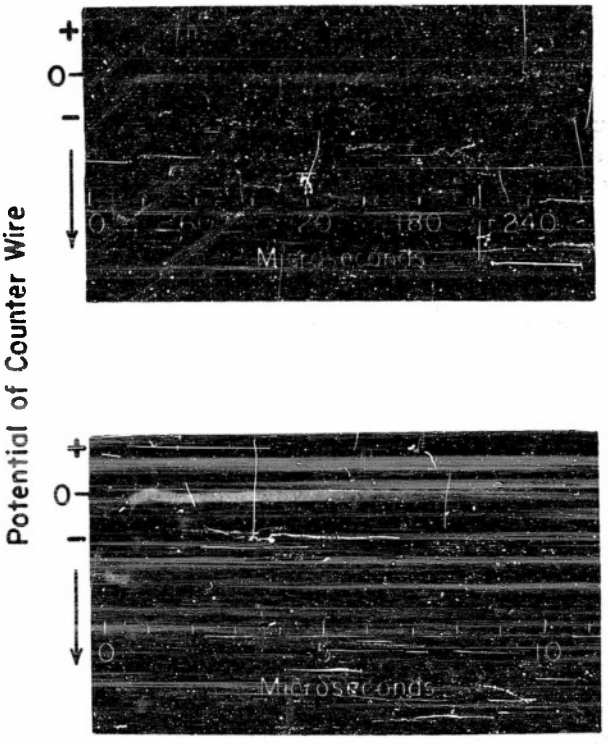

FIG. 1. Oscilloscope sweep triggered by G-M counter. (Top) Stever's method of deadtime presentation under normal operating conditions. (Bottom) With cut-off circuit applied to counter

THE G-M TUBE DEADTIME effect, normally of the order of 10^{-4} sec, has led many investigators to employ more complicated detection instruments.

During the past ten years, numerous methods of reducing deadtime have been developed. In general, the procedures have been either too complicated or have not yielded sufficient improvement to encourage wide application. A "cut-off" circuit has been devised (*1*) which overcomes both of these difficulties and reduces the inoperative time to approximately 1.5 μsec.

To define deadtime and to convey some quantitative insight into its effect on the counting efficiency of a G-M counter, we shall discuss the mechanism of discharge as it is presently understood, and shall review the methods which have been used to achieve improved efficiencies at high counting rates.

Deadtime Discussion

According to the discharge mechanism of G-M counters, first suggested by the work of Ramsey (*2*) and Montgomery and Montgomery (*3*), the active discharge of the tube occurs in about 10^{-6} sec. In many counters, the total transit time of the positive-ion sheath to the cathode is of the order of several hundred microseconds. In general, the voltage pulse initiated by a discharge is characterized by a rapid negative potential change during the period of electron collection, followed by a relatively slow negative continuation induced by the migration of positive ions toward the cathode.

Usually, the *RC* time constant of the external circuit is small compared to the positive-ion collection time. Thus, the central wire reaches a peak negative potential and returns almost to its quiescent voltage long before the ion collection is complete. However, a new discharge does not occur until the positive-ion sheath, which dominates the field around the wire, has migrated enough to allow the field to reach the G-M threshold level.

A new discharge which occurs after the insensitive interval, but before the ions are completely collected, is smaller

in amplitude than one produced when the counter is in its quiescent state because of the reduced field between the wire and the uncollected sheath. The counter response following a discharge is shown in Fig. 1 (top).

Stever's method. Deadtime may be studied with a technique devised by Stever (*4*). A counter discharging at a moderate rate triggers repetitively the sweep of a cathode-ray oscilloscope; the counter output pulses are applied to the vertical-deflection amplifier. The counter dimensions are 6-in. long, 1 in. in diameter, with a 0.003-in.-diameter central wire.

The upper picture of Fig. 1 is a time exposure showing many superimposed sweeps. The vertical descents of the pulses are not visible due to their rapidity. The triggering pulse of each sweep occurs at the extreme left; the pulses farther to the right occur at random times after the sweep-initiating pulses. Each triggering pulse is succeeded by a 100-μsec deadtime period. The randomly occurring pulses following the deadtime interval define an envelope which reaches a constant level at approximately 250 μsec. The increasing size of delayed pulses reflects a dependence of pulse height on the position of the moving positive-ion sheath.

Muehlhause (*5*) has shown that when a counter is discharged within the time required for recovery from a previous pulse, the insensitive time after the secondary pulse is shorter than that following a full sized pulse. The effective deadtime thus depends upon the distribution of time delays between successive discharges.

Correction of constant deadtime. The information gained from a presentation such as Fig. 1 is insufficient to predict the deadtime loss of a counter at arbitrarily high counting rates. Where the deadtime may be considered a constant, a simple expression can be derived for correcting the counting rate of a single counter. If N is the recorded counting rate and N' the rate at which the counter would count if it suffered no deadtime loss, then

$$N' = N/(1 - N\sigma)$$

where σ is the period of time required after a full discharge before the counter is again capable of yielding a pulse large enough to trigger the recording apparatus.

This expression gives N' correct to 1% as long as the probability of an initiating particle entering the counter within the complete recovery time of a previous discharge is less than 0.1. For example, as applied to a typical counter having a deadtime $\sigma = 10^{-4}$ sec and a complete recovery time of 3×10^{-4} sec, the formula would give N' correct to 1% for N up to 300 cps.

To utilize ordinary counters for precise quantitative work at rates higher than a few hundred counts per second, an empirical method of calibration is necessary, using some linear device such as an ionization chamber or a photo-electric cell. Precautions must be taken to avoid statistical uncertainties in the calibrating device.

The effects of deadtime are generally more serious in coincidence arrangements of G-M counters than in the case of single-counter operation. Suppose, for example, each of n identical counters in a coincidence array counts a fraction f of the rays which traverse it. Then the n-fold coincidence efficiency is f^n, which is a smaller value than the individual counter efficiency.

As has been seen in the preceding discussion, the positive ion sheath which remains near the wire after a discharge is the principal factor determining the deadtime of a G-M counter. Consequently, the methods which have been devised to render a counter operable at high rates have been aimed at removing the sheath as rapidly as possible, or limiting the spread of the sheath to a short segment of the wire.

Beaded-Wire Counters

Brodie and Stever (*4*) observed that when beads were placed on a counter wire, the spreading process was limited to a segment of the tube length. With a single bead at the center of the wire, the two halves of the counter could be discharged independently. Apparently little use was made of this observation until Curran and Rae (*6, 7*) made a further study of the recovery properties of beaded-wire counters, and were able to obtain with a 15-bead counter an effective resolving time of $\sim$10 μsec. Parratt, Hempstead and Jossem (*8*) have reported measurements with beaded counters over the range 1–10^5 cps.

An interesting theoretical analysis of counting losses of long beaded X-ray counters was made by Nonaka (*9*). His calculations show that, for a given percentage loss, a long counter having a wire divided by beads into n equal segments should be capable of counting n times the X-ray intensity which an unbeaded counter of the same length could count. It was assumed that the X-ray beam was directed along the axis of the counter, and that the absorbtion of the beam in the gas was small.

Some of the disadvantages which arise with beaded counters are: (1) difficult construction and duplication; (2) poor plateaus as a result of the perturbing effect of the beads upon the electric field near the wire; and (3) an extremely large number of spurious counts. In fact, Parratt *et al.* (*8*) utilize such counts to render the observed counting rate of a beaded counter more nearly proportional to source strength. In virtue of the fact that the number of spurious counts varies with aging, this latter procedure seems of questionable value.

High-Gain Amplifier

At very high radiation intensities, most of the pulses from a G-M counter fall below the level required to trigger an ordinary recording circuit. It was shown by Trost (*10*) that the integrated pulse current in counter tubes continues to increase far beyond the "choking" region for counting with an ordinary circuit.

Muehlhause and Friedman (*5*) furthered the work of Trost by using a high-gain video amplifier of 0.01-volt sensitivity. Their work indicates that the effective deadtime varies with overvoltage and with counting rate. Their range of deadtimes (at low rates) varied from about 500 μsec, near the Geiger-Müller threshold, to about 150 μsec near the limit of the plateau. With a fixed overvoltage, the effective deadtime varied from 220 μsec, at 100 cps, to nearly 10 μsec at 60,000 cps. Thus, the maximum counting rate of a typical G-M counter may be pushed to 100,000 cps by providing sufficient pulse amplification, but the gain in resolving power up to 10,000 cps is relatively slight.

Circuit Control

Neher and Harper (*11*) first successfully increased the working rate of counters electronically. Their circuit was a simple one. The initial voltage developed by a counter when applied to this circuit resulted in a reduction of

potential to a point below the starting value. For each pulse, this reduction was sustained until the original working potential could be restored without subsequent breakdown. A time in excess of 10^{-4} sec was usually required.

The circuit was intended for non-self-quenching mixtures which in normal use gave inoperative times from 10^{-3} to 10^{-2} sec, and were workable only at very low rates. The limitation for such mixtures is the time required to eliminate all particles capable of releasing electrons from the gas or from the cathode—a period which may be longer than the time required to sweep positive ions to the cathode.

Self-quenching counter. The self-quenching counter greatly extends the possibilities of circuit control of deadtime. In such counters, processes occur which greatly reduce the probability of ejection of electrons from the cathode at the time of arrival of the positive-ion sheath. Furthermore, de-excitation of gas atoms excited to metastable states is greatly accelerated, so that the wire potential may be restored to normal very soon after the start of a discharge without danger of initiating spurious counts.

Since the deadtime in a self-quenching counter is determined solely by the time which the sheath requires to reach the critical radius, Simpson (*13*) reasoned that a reversal of potentials would draw the sheath back to the wire—and in a time considerably less than the normal deadtime. Following this collection, the usual working voltages could be restored. His procedure led to a minimum insensitive time of 2.0×10^{-6} sec, reducing the normal deadtime by a factor of five.

The elaborate circuit used to achieve these large short-time alterations in potential discouraged wide use of the original procedure. However, Simpson's work introduced a basic idea and stimulated other investigators to seek simplification.

Flip-flop circuit. Hodson (*15*) achieved a great simplification of Simpson's procedure when he was able to reverse the sign of counter potentials using a two-tube flip-flop circuit in place of the nine-tube arrangement. He observed an insensitive time of 3.0×10^{-5} sec.

The work of both Simpson and Hodson was dominated by the idea that the reduction in deadtime was due to a rapid collection of positive ions. However, it was becoming increasingly obvious that some of the improvement afforded by the potential-reversing circuits arose from an interruption of the spreading of the discharge along the wire—a real quenching of active ionisation. Hodson, in a later private communication to Smith (*14*), suggested that such a quenching must have occurred. Smith estimated that the spreading was limited to about 40% of the length of a 60-cm counter, and referred to further work by Hodson which displayed the same deadtime reduction when the potential across a counter was reduced only 250 volts.

The trend for reducing the deadtime now was to limit the discharge before it had spread the entire length of the wire. Elliot (*16*), using a two-tube multivibrator arrangement, succeeded in limiting the discharge to 25% of the length in a 60-cm tube, and Collinge (*16*) later limited the spreading of the discharge to 5 cm or less in a 30-cm tube. Unfortunately, Collinge's circuit involved a large number of tubes and his minimum deadtime was not under 2.0×10^{-5} sec. Neither of the last two investigators made use of a reversing potential, and both achieved their reduction of insensitive time solely by interrupting the ionising process.

Fixed deadtime. In another approach to the problem, den Hartog and Muller (*17*) developed an ingenious arrangement which externally fixed the deadtime, setting it at a value in excess of the total collecting time of the ions. Although a counter tube is thus inoperative for a relatively long time, the circuit provides a meter which indicates directly the percentage of sensitive time for each counting rate. Den Hartog and Muller state that corrected rates up to 20,000 cps were successfully handled with this circuit.

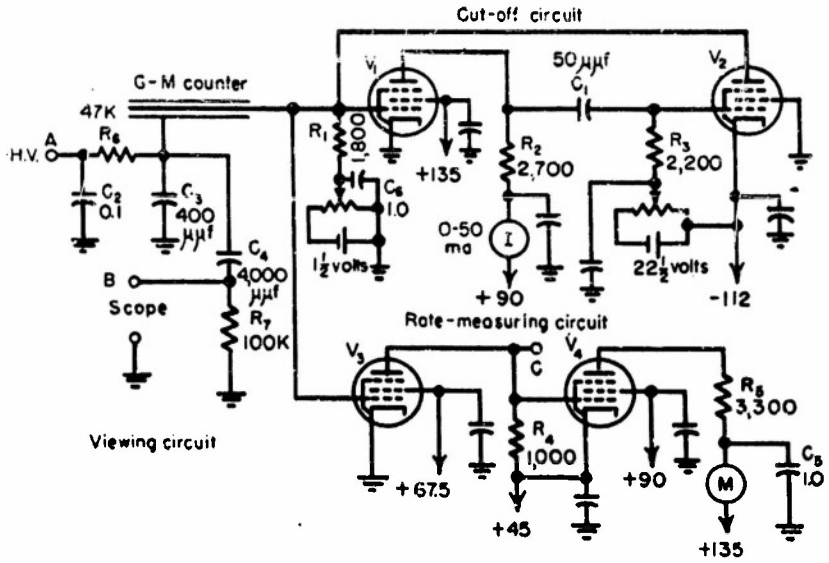

FIG. 2. Two-tube cut-off circuit with rate-measuring circuit for high speeds

In one specific instance, a 12-mm-diameter counter with an active length of 30 cm was used. With an incident radiation of 20,000 cps, the counter was operative for 15% of the time. Thus, only 3,000 cps were actually recorded. While use is not made of the fact to achieve short deadtimes, this circuit also interrupts spreading and confines the active discharge to 4 cm along the counter wire.

Cut-Off Circuit

Ramsey, in 1949 (unpublished), succeeded in confining the discharge to 1 cm of the wire length in a 20-cm tube, and thus achieved a drastic increase in operating speeds.

Porter and Ramsey (*1*) were able to simplify the procedure and confine the discharge equally well with a two-tube feed-back arrangement. They made a deliberate effort to limit the spreading process in order to increase speed and life. Previous studies by Ramsey (*18*) on current time and spreading velocity suggested that, with the argon-ether

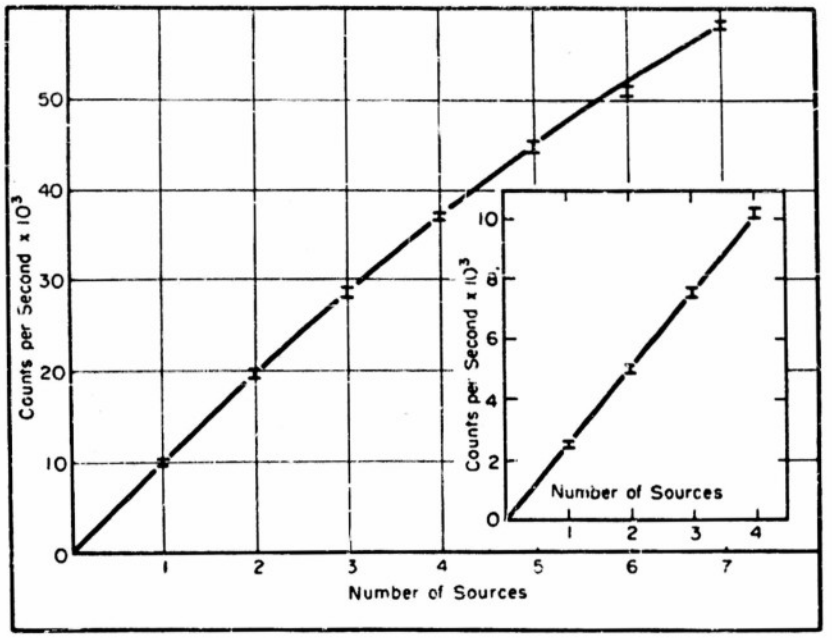

FIG. 3. Counting rates obtained by placing sources to yield 10,000 cps each. Inset curve obtained by placing sources to yield 2,500 cps each

and argon-butane mixtures used, such a simplification might be possible.

By working within 30 volts of the potential characterized by pulse equalization, and minimizing stray capacitances, Porter and Ramsey were able to achieve an insensitive time of 1.5 μsec. An examination of the charge distribution indicated that active ionization had been confined to 1 cm of the tube length.

Circuit operation. Figure 2 shows the two-tube cut-off circuit with a rate-measuring arrangement used for high speeds. All tubes are 6AK5's and all unlabeled by-pass capacitors are 0.0025 μf.

When the pulse from a G-M counter has developed approximately 0.2 volts across R_1, the pulse is amplified enough in V_1 to cause the grid of V_2 to come from below cut-off bias; hence the plate current of V_2 adds to the voltage drop of R_1—a cumulative action which proceeds until V_1 is cut-off. The grid of V_2 starts to recover rapidly by virtue of the short time constants involved. As the grid of V_2 recovers, the plate current of V_2 decreases until the voltage drop across R_1 is less than the cut-off bias of V_1. The resulting negative pulse on the plate of V_1 abruptly returns the grid of V_2 below its cut-off value. The time required for an entire cycle of the circuit operation is approximately 1.5 μsec. After this period, the circuit is again ready to accept a new pulse.

Continuous oscillographic observations of both wire and cylinder were made at all rates. This examination of the wire potential indicated a pulse form controlled by the feed-back circuit, and independent of counting rate up to rates as high as 200,000 cps. It also demonstrated that the normal operating voltage is restored in about 7.5×10^{-7} sec.

Measurements of charge on the cylinder, with and without the circuit operating, indicated that this cut-off procedure reduced the charge to that which would be observed in a tube 1 cm in length. Further discussion of the charge distribution as observed with a tube made with a segmented cathode can be found elsewhere (*1*). Figure 1 illustrates the difference between the usual deadtime picture using Stever's original procedure, and the picture obtained when the cut-off circuit is in operation.

Effect of radiation intensity. To obtain information on the variation of the counting rate of a circuit-controlled counter as a function of the relative intensity of incident radiation, the following procedure was used.

Each of seven radioactive sources was so placed in relation to the counter that a counting rate of 10,000 cps was obtained; the position of each source was carefully marked. Then, starting with one source and adding one source at a time in its marked position, the counting rates corresponding to one, two, three and so on up to seven sources were recorded. In this way, the main plot shown in Fig. 3 was obtained. A thin-walled glass counter, 20 cm long and 0.9 cm in diameter, with a 0.003-in.-diameter wire was used. The inset curve was gotten in a similar manner, with four sources located in relation to the counter so that each source gave a counting rate of 2,500 cps.

The indicated uncertainties in the measured counting rate represent the approximate fluctuations observed on the meter in the integration circuit. A straight line can be drawn through the origin and all of the points on the low-counting-rate curve. All of the rates indicated in this figure are far above those for which the average investigator would trust his counter if used under normal operating conditions.

This circuit has been used successfully at this laboratory with gas mixtures of argon-ether (6.5:1) at approximately 5.5-cm-Hg pressure; argon-butane (6:1) at approximately 8.5 and at 12-cm Hg; and argon-alcohol (4:1) at 8.0-cm Hg. With any of these mixtures and a photon source of radiation, the reduction in pulse height at the cylinder indicated that the discharge had been limited to 1 cm of the total length of the counter. How the circuit will work with other mixtures and with other pressures is not yet known.

* * *

The author wishes to express his appreciation to Dr. W. F. G. Swann, Director of The Bartol Research Foundation, Dr. G. W. McClure and Mr. W. E. Ramsey for many helpful discussions and advice. This work was assisted by the joint program of the ONR and the AEC.

BIBLIOGRAPHY

1. W. C. Porter, W. E. Ramsey, *J. Franklin Inst.* **254**, 153 (1952)
2. W. E. Ramsey, *Phys. Rev.* **67**, 1022 (1940)
3. C. G. Montgomery, D. D. Montgomery, *Phys. Rev.* **57**, 1030 (1940)
4. H. G. Stever, *Phys. Rev.* **71**, 38 (1942)
5. C. O. Muehlhause, H. Friedman, *Rev. Sci. Instr.* **17**, 506 (1946)
6. S. C. Curran, E. R. Rae, *Rev. Sci. Instr.* **18**, 871 (1947)
7. S. C. Curran, E. R. Rae, *J. Sci. Instr.* **24**, 253 (1947)
8. L. G. Parratt, C. F. Hempstead, E. L. Jossem, *Rev. Sci. Instr.* **23**, 1 (1952)
9. I. Nonaka, *J. of the Phys. Soc. of Japan* **7**, No. 1. (1952)
10. A. Trost, *Z. Physik* **117**, 257 (1941)
11. H. V. Neher, W. W. Harper, *Phys. Rev.* **49**, 940 (1936)
12. J. A. Simpson, Jr., *Phys. Rev.* **66**, 39 (1944)
13. A. L. Hodson, *J. Sci. Instr.* **25**, 11 (1948)
14. P. B. Smith, *Rev. Sci. Instr.* **19**, 453 (1948)
15. H. Elliot, *Proc. Phys. Soc. London* **62**, 369 (1949)
16. R. Collinge, *Proc. Phys. Soc. London* **63B**, 15 (1950)
17. H. den Hartog, F. A. Muller, *Physica* **16**, 17 (1950)
18. W. E. Ramsey, *Phys. Rev.* **83**, 242 (1951)

Printed in U.S.A.

Reprinted from THE PHYSICAL REVIEW, Vol. 89, No. 3, 559-561, February 1, 1953
Printed in U. S. A.

Gamma-Radiations from Zr^{95} and Nb^{95}†

C. E. MANDEVILLE, E. SHAPIRO,‡ R. I. MENDENHALL, E. R. ZUCKER,§ AND G. L. CONKLIN
Bartol Research Foundation of the Franklin Institute, Swarthmore, Pennsylvania

(Received October 14, 1952)

By employing lead absorption, coincidence counting techniques, and scintillation spectrometry, it has been shown that each beta-ray of Nb^{95} is followed by a gamma-ray of energy 0.76±0.02 Mev and that most of the beta-rays of the parent element Zr^{95} are followed by a single gamma-ray at 0.73±0.02 Mev. A disintegration scheme is proposed.

INTRODUCTION

IT has been shown that the 65±2 day Zr^{95} and the 35±1 day Nb^{95} are formed in several different nuclear reactions.[1]

In a magnetic spectrograph,[2] the energies of the gamma-rays emitted by Zr^{95} have been measured at 0.73 Mev (93 percent) 0.23 Mev (93 percent), and 0.92 Mev (7 percent). Approximately two percent of the beta-ray disintegrations of Zr^{95} have been shown to terminate at a 90-hour metastable level[3] of the residual nucleus, radioactive Nb^{95}. The energy of the isomeric transition has been measured as 0.216 Mev[4] and 0.24 Mev.[5] The radiation is totally converted. The energy of the relatively hard abundant gamma-ray of Zr^{95} has also been measured as 0.708 Mev.[4]

Spectrometric measurements have yielded quantum energies of 0.75 Mev,[6] 0.758 Mev,[4] and 0.77 Mev[7] for the single gamma-ray of Nb^{95}, the 35-day daughter element. The energy of this gamma-ray was also measured as 0.92 Mev by the method of coincidence absorption.[8] In these latter measurements, the gamma-ray which appeared to have an energy of 0.92 Mev was found in both the zirconium and niobium fractions. However, the beta-gamma coincidence rate of Zr^{95} was such as to suggest that on the average, each beta of Zr^{95} is followed by less than 0.3 Mev of gamma-ray energy. When a carefully purified source of Nb^{95} yielded a beta-gamma coincidence rate sufficiently large to account for the presence of the hard gamma-ray thought to be of energy 0.92 Mev, it was concluded that the presence of this gamma-ray in the zirconium fraction arose from an incomplete chemical separation, and that it is actually only associated with the daughter element. Because of the various conflicting reports concerning the gamma-radiations, the properties of $Zr^{95}-Nb^{95}$ have been re-investigated.

PROCEDURE AND RESULTS

A source of $Zr^{95}-Nb^{95}$ was produced in the fission process at the Oak Ridge pile. Pure separated sources of Zr^{95} and Nb^{95} were prepared repeatedly by Steinberg's oxalate procedure.[9] The gamma-rays of Nb^{95}, Zr^{95}, and $Zr^{95}-Nb^{95}$ were absorbed in lead as shown in Fig. 1. From the slopes of the curves it is evident that the gamma-rays emitted by the three different radioactive sources are essentially the same in energy. No evidence appears on any of the absorption curves to suggest the presence of any gamma-rays of lower energy and comparable intensity. Repeated chemical separations always gave absorption curves similar to those of Fig. 1. The quantum energy taken from the slope of the curve is 0.80±0.05 Mev.

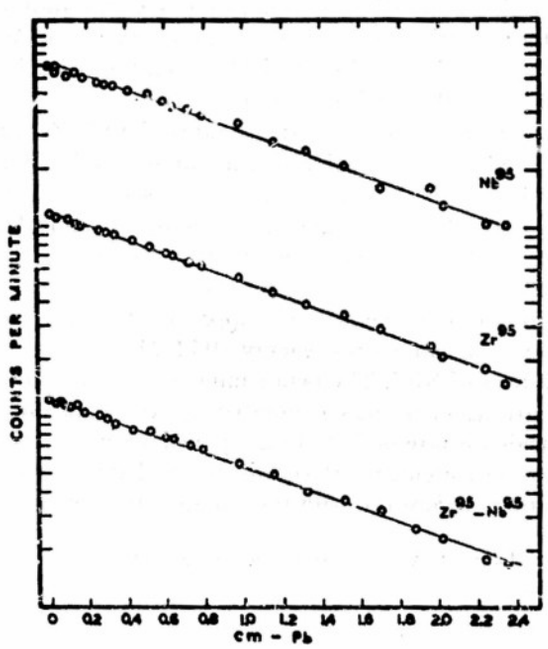

FIG. 1. Absorption in lead of the gamma-rays of Nb^{95}, Zr^{95}, and $Zr^{95}-Nb^{95}$.

† Assisted by the joint program of the ONR and AEC.
‡ At present at Tracerlab, Inc., Boston, Massachusetts.
§ Frankford Arsenal, Philadelphia, Pennsylvania.
[1] Sagane, Kojima, Miyamoto, and Ikawa, Phys. Rev. 57, 1180 (1940); B. L. Goldschmidt and J. Perlman, *Radiochemical Studies: The Fission Products* (McGraw-Hill Book Company, Inc., New York, 1951), Paper No. 34, National Nuclear Energy Series, Plutonium Project Record, Vol. 9, Div. IV; Brady, Engelkemier, and Steinberg, Papers 85 and 88; L. Jacobson and R. Overstreet, Paper 91. The volume in which these latter references may be found will hereafter be referred to as NNES 9.
[2] V. A. Nedzel, NNES 9, Paper 87.
[3] D. W. Engelkemier and E. L. Brady, NNES 9, Paper 92; E. P. Steinberg, NNES 9, Paper 93.
[4] G. E. Hudgens and W. S. Lyons, Phys. Rev. 75, 206 (1949).
[5] J. S. Levinger, NNES 9, Paper 94.
[6] W. Rall and R. G. Wilkinson, Phys. Rev. 71, 321 (1947).
[7] V. A. Nedzel, NNES 9, Paper 90.
[8] C. E. Mandeville and M. V. Scherb, Phys. Rev. 73, 1434 (1948).
[9] E. P. Steinberg, NNES 9, Paper 243.

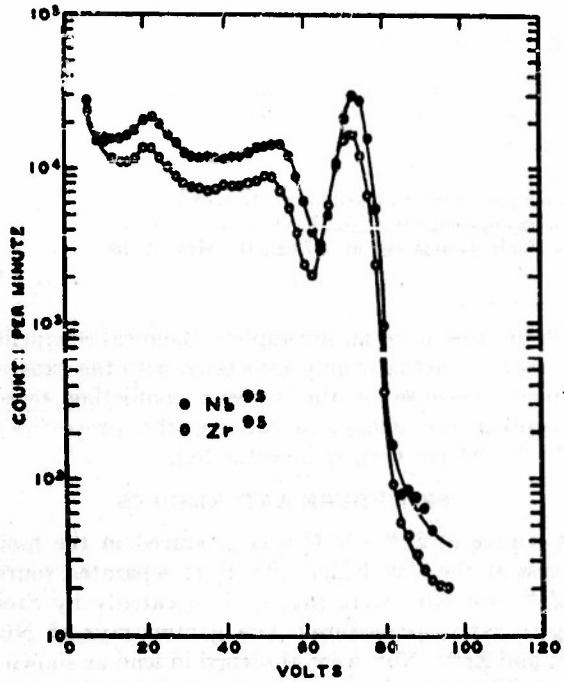

FIG. 2. Pulse-height distribution of gamma-rays from Zr^{95} and Nb^{95} on NaI(Tl).

With the aid of a scintillation spectrometer, the photoelectric lines of the gamma-rays of freshly separated Zr^{95} and Nb^{95} were observed in a crystal of NaI(Tl). The pulse-height distributions are shown in Fig. 2, where it is clear that the gamma-ray of Nb^{95} is somewhat more energetic than that of Zr^{95}. Calibration of the spectrometer with the gamma-rays from Au^{198}, Na^{22}, Cs^{137}, Sc^{46}, and Co^{60} yielded quantum energies of 0.73 ± 0.02 Mev and 0.76 ± 0.02.

The beta-gamma coincidence rates of Nb^{95}, Zr^{95}, and $Zr^{95}-Nb^{95}$, as a function of aluminum absorber thickness before the beta-ray counter, are shown in Fig. 3. It is evident that the average value of the coincidence rate is approximately the same in the three cases, confirming that most of the beta-rays of Zr^{95} are followed, on the average, by approximately the same amount of gamma-ray energy (0.71 Mev) as are the beta-rays of Nb^{95}. The beta-gamma coincidence counting arrangement was calibrated by the beta-gamma coincidence rate of Sc^{46}. In a separate group of coincidence measurements at certain selected thicknesses of absorbers before the beta-ray counter, the amounts of gamma-ray energy per beta-ray of Table I were obtained.[10,11]

TABLE I. Average gamma-ray energy per beta-ray.

Radionuclide	Absorber thickness	Gamma-ray energy (Mev)
Nb^{95}	5 mg/cm²	0.71±0.09
Zr^{95}	40 mg/cm²	0.67±0.08
$Zr^{95}-Nb^{95}$	40 mg/cm²	0.73±0.09

THE DISINTEGRATION SCHEME

The 1.0-Mev beta-spectrum of Zr^{95} ($\Delta j=2$, yes!)[12] terminates at the 90-hr level of $Nb^{95}(p_{1/2})$;[13] so the orbital of the last odd nucleon of Zr^{95} is taken to be $d_{5/2}$. Log ft[14] for the more abundant beta-spectrum of Zr^{95} is 6.62, permitting the interpretation that the spec-

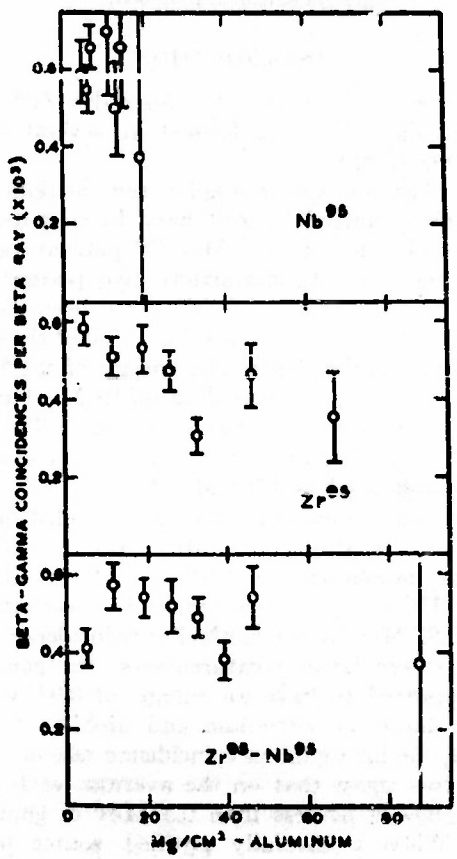

FIG. 3. Beta-gamma coincidence rate of Nb^{95}, Zr^{95}, and $Zr^{95}-Nb^{95}$ as a function of aluminum absorber thickness before the beta-ray counter.

[10] The present coincidence rates and associated gamma-ray energies are in contradiction with the previous report (reference 8) that the beta-rays of Zr^{95} are coincident with less than 0.3 Mev of gamma-ray energy. The earlier results must be ascribed to the presence of unidentified impurities having relatively low beta-gamma coincidence rates.

[11] When a radionuclide is grown from a parent element of comparable half life, it can be shown that if a chemical separation is effected at a considerable length of time after onset of growth, the disintegration rates are in the ratio of

$$C_D/C_P=\lambda_D/(\lambda_D-\lambda_P),$$

where the subscripts P and D refer to parent and daughter, and the λ's are the decay constants. For the 65-day Zr^{95} and the 35-day Nb^{95}, this ratio is 3.16 ± 0.2. In the present investigation the ratio of the gamma-ray activities was observed in both scintillation counters and Geiger counters and found to be 2.2 ± 0.1 confirming a good separation if the gamma-radiations of the parent and daughter are essentially the same.

[12] Mayer, Moszkowski, and Nordheim, Revs. Modern Phys. 23, 315 (1952).

[13] M. Goldhaber and A. W. Sunyar, Phys. Rev. 83, 906 (1951).

[14] A. M. Feingold, Revs. Modern Phys. 23, 10 (1951).

trum may be once forbidden ($\Delta j=0, \pm 1$, yes!) or l-forbidden ($\Delta j=1$, no!, $\Delta l=2$). According to the former classification, the excited level at 0.73±0.02 Mev in the residual nucleus Nb^{95}, could have the orbital $p_{3/2}$, $f_{5/2}$, or $f_{7/2}$. Were it either of the first two values, a relatively intense gamma-ray of energy ~0.5 Mev would be expected to appear among the radiations of Zr^{95}, emitted in the transition between the level at 0.73±0.02 Mev and the 0.21-Mev metastable level of the 90-hr Nb^{95} (see Fig. 4). Only in the case of $f_{7/2}\rightarrow g_{9/2}$ does the probability of a transition to the ground state of Nb^{95} exceed that of a transition to the metastable level ($f_{7/2}\rightarrow p_{1/2}$). Since no gamma-radiation at 0.5 Mev is observed, the most likely of the three orbitals associated with the assumption of a once forbidden transition is $f_{7/2}$.

If an l forbidden beta-transition is assumed, the orbital assignment of the 0.73±0.02 Mev level is uniquely $g_{7/2}$. The transition $g_{7/2}\rightarrow g_{9/2}$ is, of course, far more probable than $g_{7/2}\rightarrow p_{1/2}$. Since the $f_{7/2}$ shell closes at 28 nucleons, the $g_{7/2}$ subshell, closing at 58 nucleons, is favored.

From shell model considerations and the conversion coefficients of the 0.76±0.02 Mev gamma-ray of Nb^{95}, it has been previously shown[15] that the decay of Nb^{95} to Mo^{95} can be characterized by $g_{9/2}\rightarrow g_{7/2}\rightarrow d_{5/2}$.

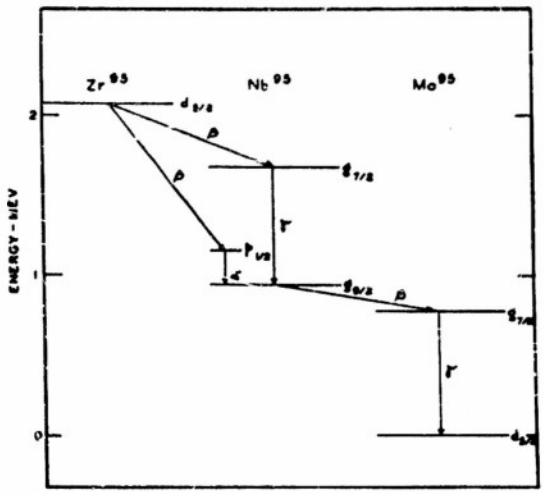

FIG. 4. Disintegration scheme of $Zr^{95}-Nb^{95}$.

[15] C. Y. Fan, Phys. Rev. 87, 252 (1952).

Reprinted from JOURNAL OF THE FRANKLIN INSTITUTE,
Vol. 254, No. 5, November, 1952
Printed in U. S. A.

RADIATIONS FROM Zr^{97} AND Nb^{97} *

BY

C. E. MANDEVILLE,[1] E. SHAPIRO,[1] R. I. MENDENHALL,[1] E. R. ZUCKER [2] AND G. L. CONKLIN [1]

ABSTRACT

$Zr^{96}O_2$ (isotopic concentration 90 per cent) was irradiated by slow neutrons in the Oak Ridge pile. The half-period of the niobium daughter element, chemically separated from zirconium, was found to be 72.1 ± 0.7 min. and that of Zr^{97} to be 17.0 ± 0.2 hr. By aluminum absorption and Feather analysis, maximum beta ray energies of 2.50 Mev and 1.40 Mev were measured for parent and daughter element, respectively. Lead absorption of the quantum radiations of the equilibrium mixture indicated a gamma ray at 0.74 Mev as well as a softer component. Coincidence absorption yielded a maximum gamma ray energy of 1.42 Mev. The beta-gamma coincidence rate of Nb^{97} was constant, independent of the beta ray energy and of such magnitude as to suggest that each beta ray is followed on the average by 0.7 Mev of gamma ray energy. The beta-gamma coincidence rate of the equilibrium mixture showed that the hard beta rays of Zr^{97} proceed directly to the metastable state of Nb^{97}. Very few beta rays of Zr^{97} are in immediate coincidence with any gamma radiation.

INTRODUCTION

The properties of the 17-hr. Zr^{97} and of its daughter element, the 70-min. Nb^{97}, have already been the subject of considerable investigation (1–5).[3] Absorption techniques have been employed to show that the beta rays of Zr^{97} have a maximum energy of 2.2 Mev and those of Nb^{97} a maximum energy of 1.4 Mev (3). The gamma rays of either isotope were measured by lead absorption to be approximately 0.8 Mev (3), and it was concluded that in the case of both actitivies, each beta ray is accompanied on the average by one gamma ray. Subsequent spectrometric measurements (5) have yielded beta ray energies of 1.91 ± 0.02 Mev and 1.267 ± 0.02 Mev and gamma ray energies of 0.747 ± 0.005 Mev for Zr^{97} and 0.665 ± 0.005 Mev for Nb^{97}. The gamma ray at 0.747 ± 0.005 Mev was shown to be emitted from an isomeric level in Nb^{97} of half period 60 sec. (5).

In the present investigation, $Zr^{96}O_2$ (isotopic concentration 90 per cent in Zr^{96}), obtained from the Y-12 plant, Carbide and Carbon Chemicals Division, Union Carbide and Carbon Corportion, Oak Ridge, Tennessee, was irradiated by slow neutrons in the Oak Ridge pile. The

* Assisted by the joint program of the ONR and the AEC.

[1] Bartol Research Foundation of The Franklin Institute, Swarthmore, Pa.
[2] Frankford Arsenal, Philadelphia, Pa.

[3] The boldface numbers in parentheses refer to the references appended to this paper.

radioactive materials were received within twenty-four hours after cessation of irradiation and chemical separations were immediately commenced.

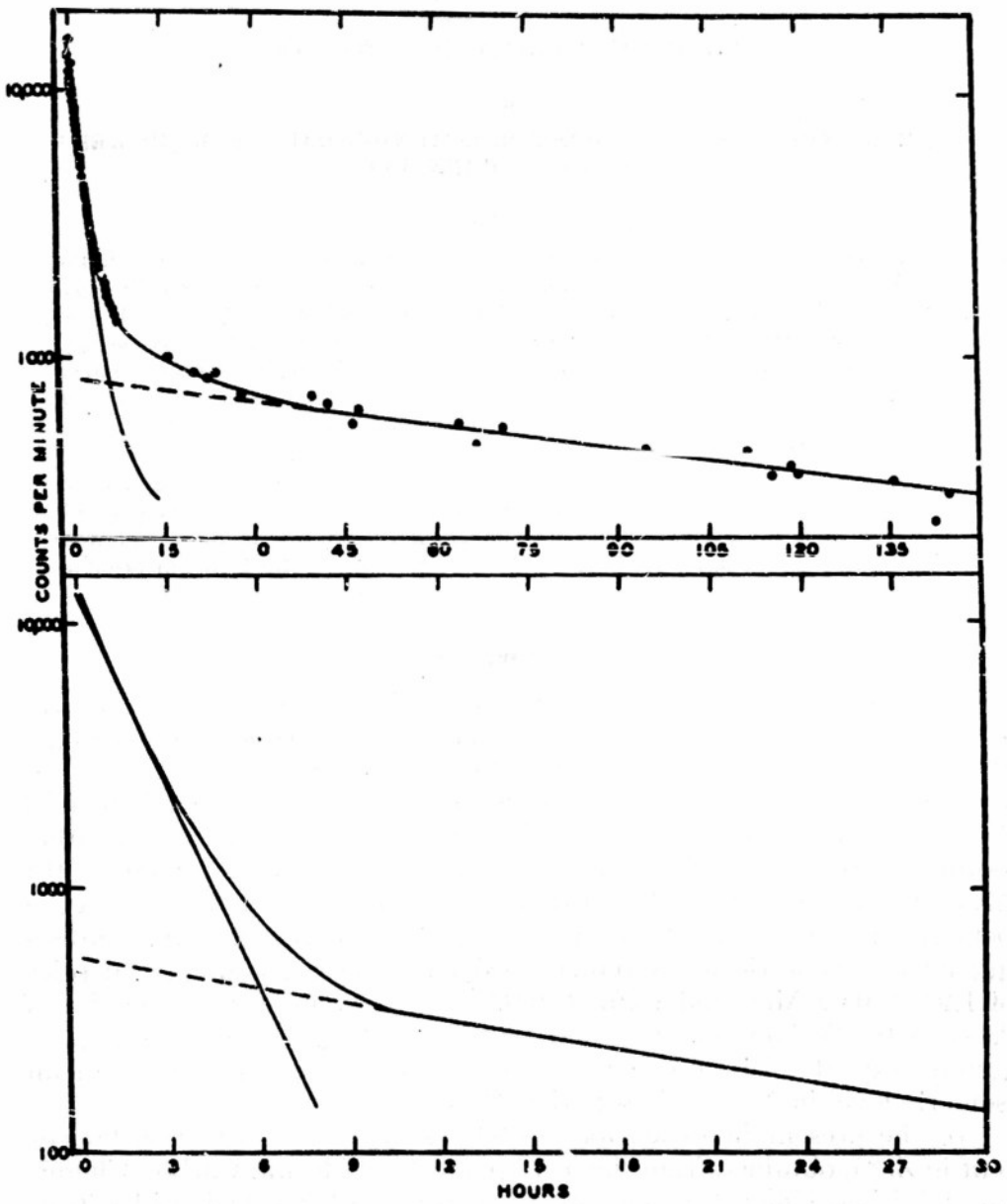

FIG. 1. Decay of the 72-min. Nb^{97}.

The slow neutron irradiated zirconium dioxide was dissolved by potassium pyrosulfate fusion. The separation of the niobium daughter activity from zirconium was effected by the use of Steinberg's "oxalate" procedure (6). A crystalline precipitate, presumably potassium acid

oxalate, formed on addition of excess oxalic acid to the aqueous solution of the fusion mixture. An assay, made after centrifugation, showed that most of the activity remained in solution. The centrifugate was poured off and retained. The activity carried with the precipitate was

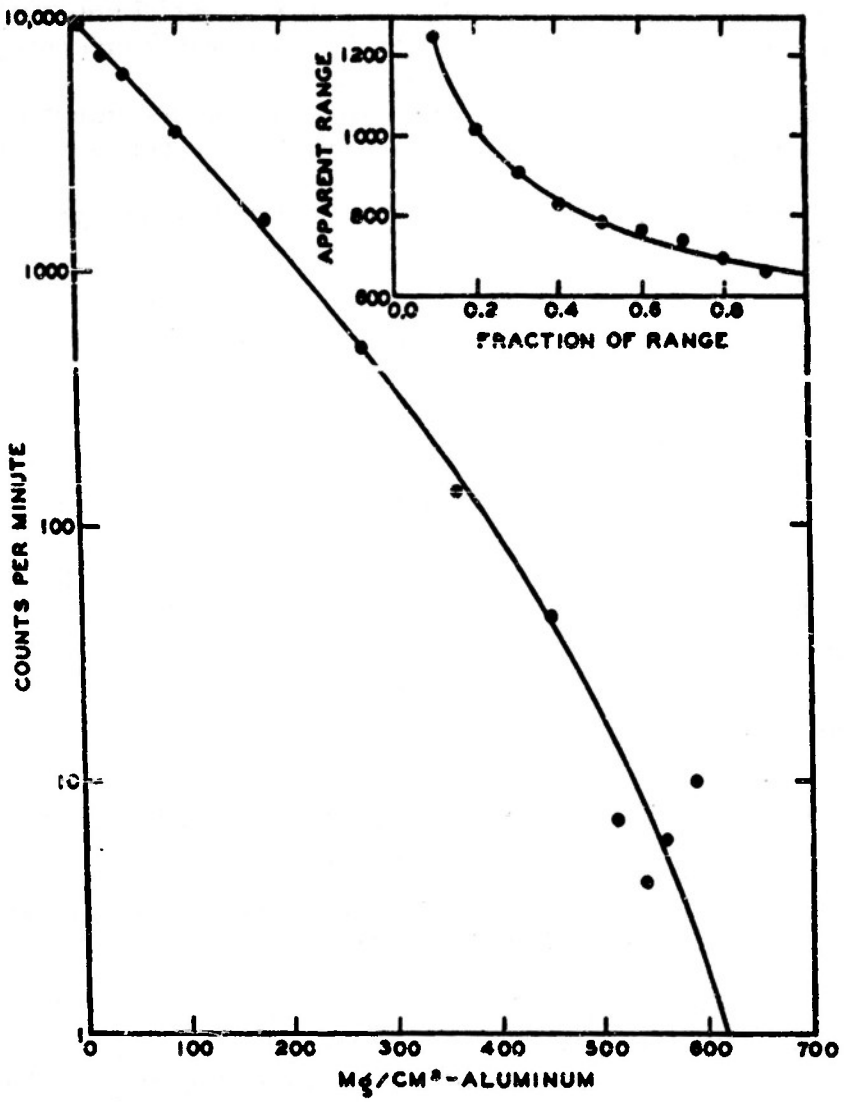

FIG. 2. Absorption in aluminum of the beta rays of Nb^{97}.

recovered by dissolving the precipitate in hot water, recrystallizing it from cold water, centrifuging, and combining the centrifugates. The separation outlined above was carried out on several successive occasions to supply fresh sources of Nb^{97}.

Nb^{97}

The decay of Nb^{97}, freshly separated from its parent element, was followed for ten half-periods, and the half-period, taken from the slope of the decay curve was found to be 72.1 ± 0.7 min. This value is to be compared with previously reported values of 68 min. (7) and 75 min. (2). These decay curves are shown in Fig. 1. The 72-min. activity is present along with a trace of the 17-hr. Zr^{97} and other unidentified impurities of longer half-periods.

The beta rays of Nb^{97}, freshly separated from its parent element, were absorbed in aluminum as shown in Fig. 2. The points of this curve

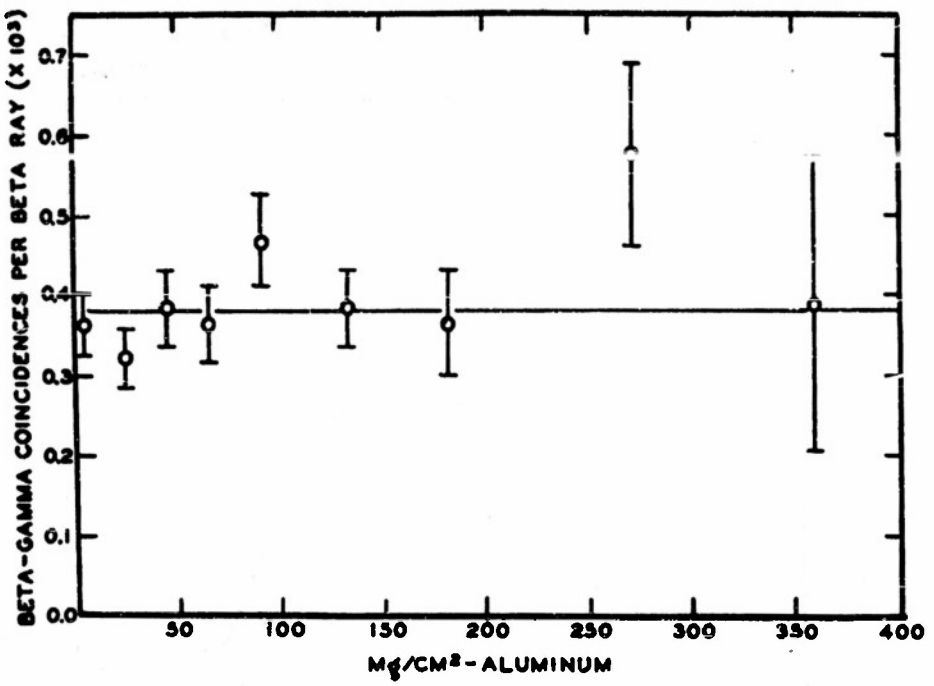

FIG. 3. Beta-gamma coincidence rate of Nb^{97} as a function of the surface density of aluminum placed before the beta ray counter.

were corrected for radioactive decay of the short lived activity during the course of the measurements. A Feather plot (8) of these data, also shown in Fig. 2, gave a maximum beta ray energy of 1.40 Mev, in agreement with the earlier measurements.

A third source of Nb^{97} was prepared to obtain the beta-gamma coincidence rate of Fig. 3. It is seen to be constant, independent of the beta ray energy, suggesting that the beta ray spectrum of Fig. 2 is a simple one. Calibration of the beta-gamma coincidence counting arrangement by the beta-gamma coincidence rate of Sc^{46} showed that each beta ray of Nb^{97} is followed, on the average, by 0.7 Mev of gamma

ray energy. Each point of Fig. 3 was, of course, properly corrected for decay of the source.

Zr^{97}

The radioactive decay of Zr^{97}–Nb^{97} was followed for ~200 hr. and the resulting half-period for the parent element, Zr^{97}, was calculated to be 17.0 ± 0.2 hr., in agreement with earlier measurements (2,3). The decay curve of the equilibrium mixture of the two radio-elements is shown in Fig. 4. The 17-hr. period is seen to be present along with some relatively long period impurities which were not identified.

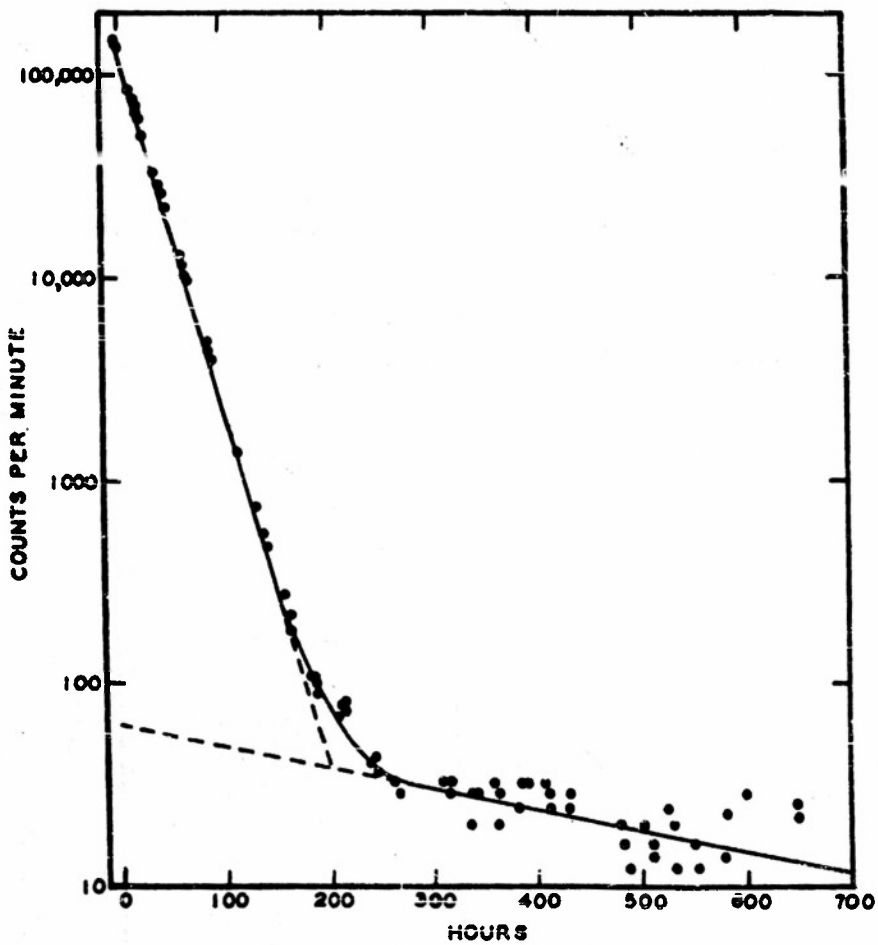

FIG. 4. Decay of the 17-hr. Zr^{97}.

The beta rays of the equilibrium mixture of the two activities was absorbed in aluminum. The assumption was made that at zero absorber thickness, half of the counting rate could be assigned to the beta rays of the 72-min. Nb^{97} and half to Zr^{97}. Assuming this equality of contribution at zero absorber thickness, the beta spectrum of Nb^{97} was

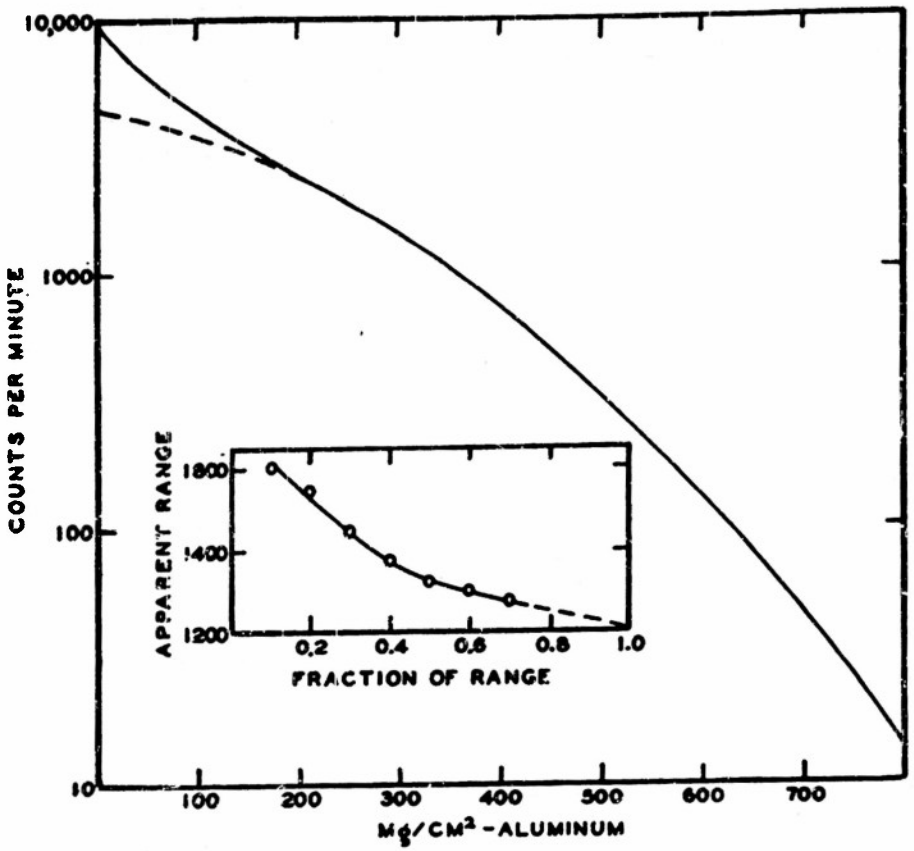

FIG. 5. Beta spectrum of Zr^{97}. This is a "difference" curve, obtained by subtracting the spectrum of Nb^{97} from that of Zr^{97}–Nb^{97}.

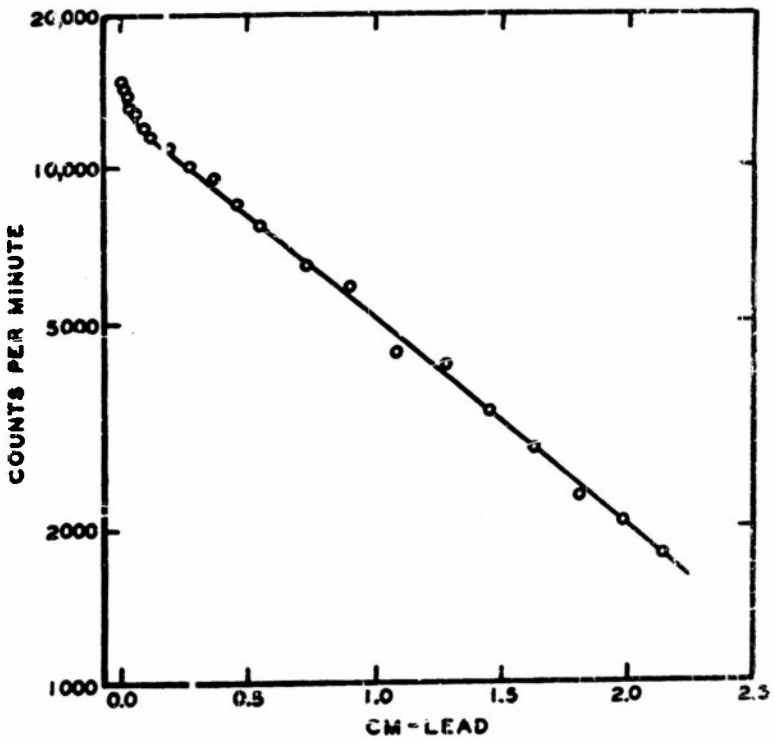

FIG. 6. Absorption in lead of the quantum radiations of Zr^{97}–Nb^{97}.

subtracted from the beta spectrum of the equilibrium mixture to give a difference spectrum of maximum energy 2.50 Mev. A semi-logarithmic plot of these beta rays also showed that a softer spectrum (end point 200 mg./cm.^{2}) is also present in the decay of Zr^{97}. These absorption data are plotted in Fig. 5.

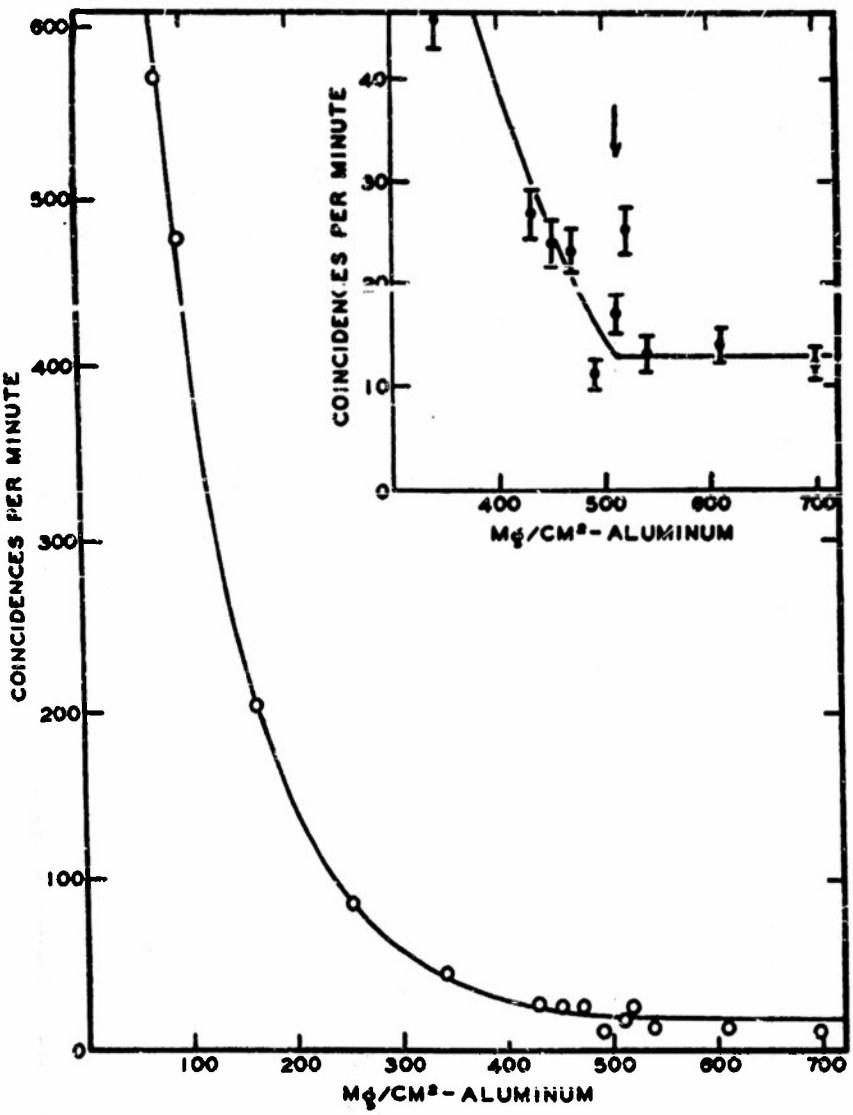

FIG. 7. Coincidence absorption of the secondary electrons of the gamma rays of Zr^{97}

The gamma rays of the equilibrium mixture of the two activities was absorbed in lead as shown in Fig. 6, and the quantum energy taken from the slope of the curve was found to be 0.74 Mev. From the initial points of the curve, it is evident that a softer component is also present.

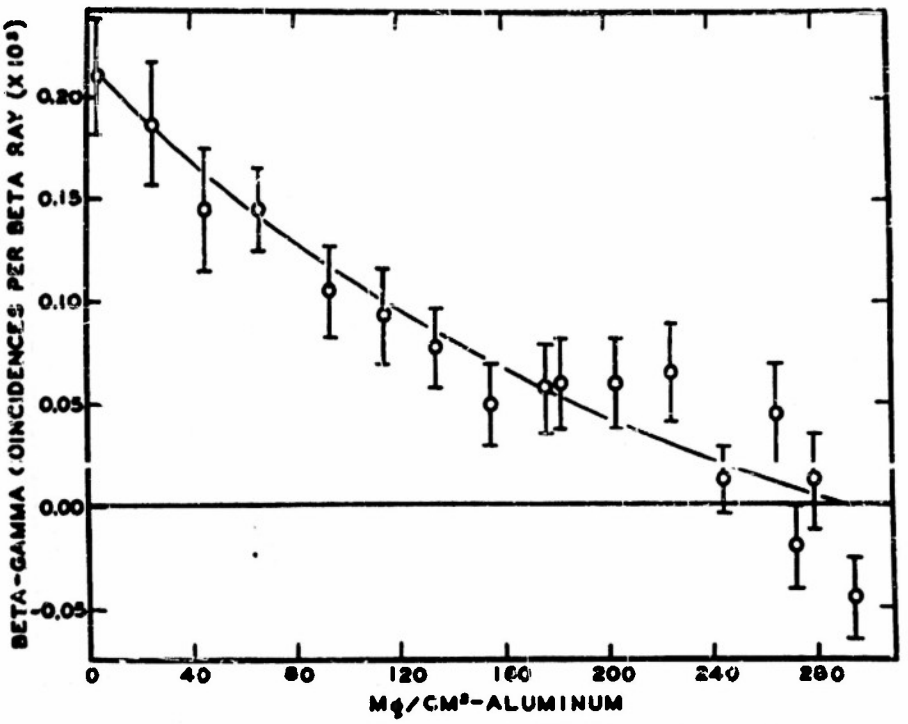

FIG. 8. Beta-gamma coincidence rate of Zr^{97} and Nb^{97} in equilibrium.

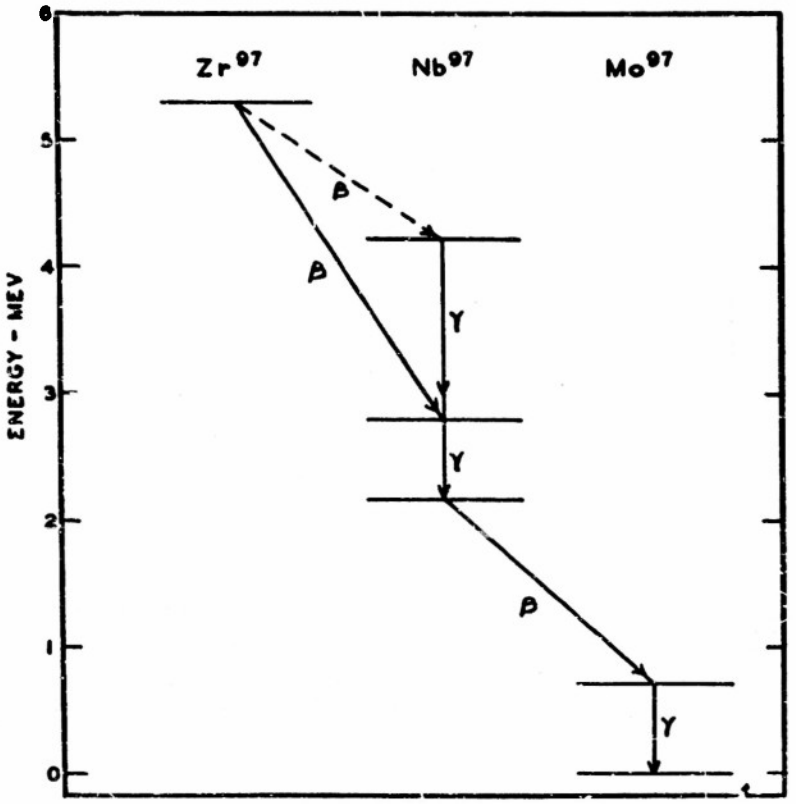

FIG. 9. Disintegration scheme for $Zr \xrightarrow{97\beta} Nb \xrightarrow{97\beta} Mo^{97}$.

To measure the energy of the most energetic gamma-ray emitted in the decay of Zr^{97}-Nb^{97}, a source was placed on an aluminum block before two coincident thin-walled G-M tubes. A coincidence absorption curve of the secondary electrons ejected from the aluminum block is shown in Fig. 7. The end point of the distribution corresponds, according to a previously published calibration curve (9), to a quantum energy of 1.42 Mev. Since the beta-gamma coincidence rate of Nb^{97} showed that its beta spectrum is simple and followed by about 0.7 Mev of gamma ray energy, and since the 1.42 Mev radiation does not appear on the lead absorption curve of Fig. 6, it is concluded that the 1.42 Mev quanta are of low intensity and are emitted by Zr^{97}, coupled, perhaps, with the softer component of the complex beta spectrum of Fig. 5.

The beta-gamma coincidence rate of Zr^{97} and Nb^{97} in equilibrium is shown in Fig. 8, where it is seen to decrease rapidly to zero, well before the end point of the hard beta spectrum of Zr^{97} is reached. This curve is interpreted to represent absorption of the beta-gamma coincidence rate of Fig. 3 in the presence of the harder beta rays of Zr^{97}, which are not in immediate coincidence with any gamma rays. The essential features of the coincidence curve of Fig. 8 have been previously observed (5), and the lack of coincidences has been interpreted to show that most of the nuclear beta rays of Zr^{97} proceed to the 60-sec. isomer (5) of Nb^{97}. The measurements of this paper confirm this analysis.

CONCLUSIONS

The absorption and coincidence data of the preceding sections, combined with those of the earlier measurements (1–5), give the disintegration scheme of Fig. 9.

Acknowledgment

The writers wish to acknowledge the kind interest of Dr. W. F. G. Swann, Director of the Bartol Research Foundation.

REFERENCES

(1) SAGANE, KOJIMA, MIYAMOTO, AND IKAWA, *Phys. Rev.*, Vol. 57, p. 1179 (1940).
(2) A. V. GROSSE AND E. T. BOOTH, *Phys. Rev.*, Vol. 57, p. 664 (1940).
(3) S. KATCOFF, AND B. FINKLE, Paper 83, Book 2, Coryell and Sugarman, *Radiochemical Studies: The Fission Products* (McGraw-Hill Book Co., Inc., New York, New York), p. 705.
(4) O. HAHN AND F. STRASSMAN, *Naturwiss.*, Vol. 29, p. 285 (1941).
(5) BURGUS, KNIGHT, AND PRESTWOOD, *Phys. Rev.*, Vol. 79, p. 104 (1950).
(6) E. P. STEINBERG, Paper 243, Book 3, Coryell and Sugarman, *Radiochemical Studies: The Fission Products* (McGraw-Hill Book Co., Inc., New York, New York), p. 1495.
(7) G. E BOYD, communication to Seaborg and Perlman, *Rev. Mod. Phys.*, Vol. 20, p. 585 (1948).
(8) N. FEATHER, *Proc. Camb. Phil. Soc.*, Vol. 30, p. 599 (1938).
(9) C. E. MANDEVILLE AND M. V. SCHERB, *Phys. Rev.*, Vol. 73, p. 1434 (1948).

Reprinted from THE PHYSICAL REVIEW, Vol. 88, No. 3, 554–555, November 1, 1952
Printed in U. S. A.

Gamma-Rays from Sn^{125}†

C. E. MANDEVILLE, E. SHAPIRO, R. I. MENDENHALL, E. R. ZUCKER,* AND G. L. CONKLIN
Bartol Research Foundation of the Franklin Institute, Swarthmore, Pennsylvania

(Received June 23, 1952)

An inner beta-spectrum at ~0.5 Mev, coincident with gamma-radiation, constitutes 10±2 percent of the total beta-radiation of the 10-day Sn^{125}. The gamma-rays have a maximum energy of 1.67±0.10 Mev.

THE ten-day activity in tin has been assigned[1] to Sn^{125}. Spectrometric measurements[2] have yielded maximum beta-ray energies of 2.37±0.02 Mev and 0.40±0.01 Mev. The spectrum of lower energy was estimated to contain five percent of the total beta-radiation. A search was made for the gamma-radiation which should accompany the beta-rays of the inner group, but because of low intensity, none was detected by the spectrometric method. It was mentioned, however, that absorption measurements in lead indicated the "possible presence" of a gamma-ray at 1.5 Mev.

During the past four years, four different quantities of metallic tin, two isotopically concentrated in Sn^{124} and two of naturally occurring tin, have been irradiated in the Oak Ridge pile.[3] The following chemical procedure has been followed. Irradiated metallic tin was dissolved in HCl and carrier Sb and Te solutions were added. Metallic Te precipitated at once, and Sb was precipitated as a metal by addition of powdered Fe to the hot 6*N*—HCl solution. Sn and some Fe were precipitated from the filtrate by addition of metallic zinc. This precipitate was dissolved by HCl, oxidized with H_2O_2, and Sn and Fe were separated by addition of NaOH to excess to form soluble Na_2SnO_3 and insoluble $Fe(OH)_3$. The filtrate was acidified with HCl, then made slightly ammoniacal, precipitating $SnO_2 \cdot xH_2O$ which was ignited to SnO_2.

A gamma-ray at 1.7 Mev was noted in the tin fraction in 1948 but was dismissed as the intense hard gamma-ray of Sb^{124}. More recently this gamma-ray has been observed in a coincidence absorption counting arrangement, and the quantum energy has been measured as 1.67±0.10 Mev. This coincidence absorption curve (Fig. 1) of the secondary electrons of the gamma-ray was observed repeatedly for forty days, and the ordinate values were observed to decay with a half-life of ten days.

A source of the ten-day tin was placed in a beta-gamma coincidence counting arrangement, and beta-

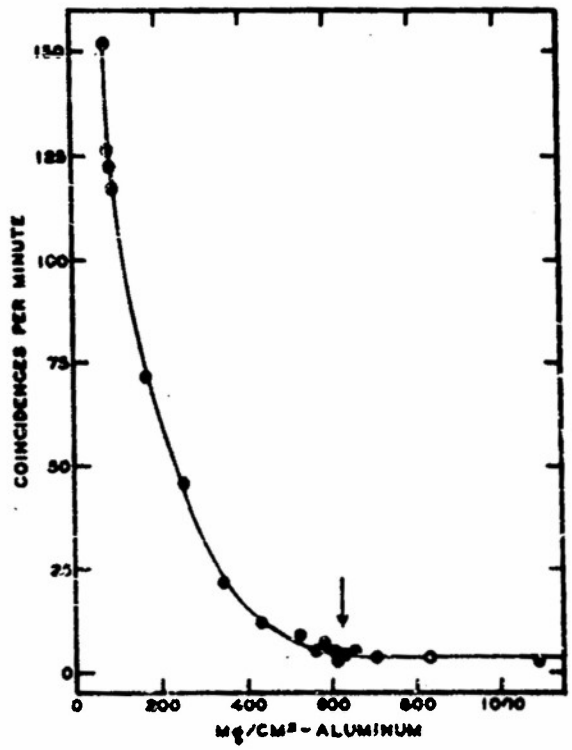

FIG. 1. Coincidence absorption of the secondary electrons of the gamma-rays from Sn^{125}.

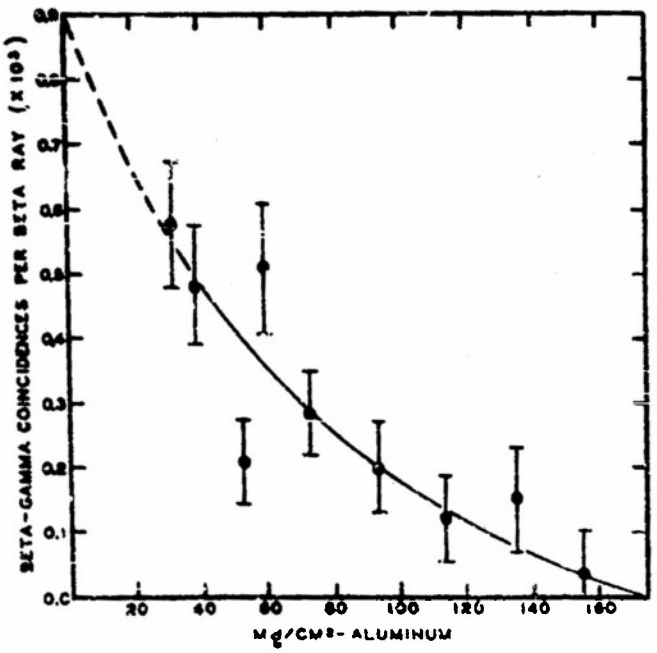

FIG. 2. Beta-gamma coincidence rate of Sn^{125} as a function of the surface density of aluminum before the beta-ray counter.

† Assisted by the joint program of the ONR and AEC.
* Frankford Arsenal, Philadelphia, Pennsylvania.
[1] J. C. Lee and M. L. Pool, Phys. Rev. 76, 606 (1949).
[2] R. W. Hayward, Phys. Rev. 79, 409 (1950).
[3] Isotopically concentrated Sn^{124} supplied by Y-12 Research Laboratory, Carbide and Carbon Chemicals Division, Union Carbide and Carbon Corporation, Oak Ridge, Tennessee.

gamma coincidences were measured as a function of aluminum absorber thickness before the beta-ray counter. The data are shown in Fig. 2 where the beta-gamma coincidence rate is seen to decrease to zero at 180 mg/cm² of aluminum, indicating an inner beta-ray group at ~0.5 Mev. These beta-gamma coincidences were observed to decay over a period of 40 days with the 10-day period. On calibration of the beta-gamma coincidence counting arrangement with the beta-gamma coincidence rate of Sc^{46}, the beta-gamma coincidence rate of Fig. 1 indicated, on extrapolation to zero absorber thickness, that the gamma-ray at 1.67 Mev is coincident with 10±2 percent of the beta-rays of the 10-day Sn^{125}.

The 15-day Sn^{117m}, a possible contaminant, has been observed to decay with the emission of γ-rays at 159 kev and 162 kev in cascade, and $\gamma-e^-$ coincidences have been noted.[4] In the present measurements, sufficient lead was placed before the gamma-ray counter to reduce the intensity of a gamma-ray of energy 160 kev by a factor of four. However, the beta-gamma coincidence rate of Fig. 2 remained unchanged, further confirmation of the assignment of the coincidences to Sn^{125}.

Measurements by Boyd and associates[5] at Oak Ridge, employing a scintillation spectrometer, yield a quantum energy of ~1.9 Mev for this gamma-ray.

Note added in proof.—The orbital of the 60-day level in Te^{125} is $h_{11/2}$. The beta-spectrum of Sb^{125} terminating at that level obeys the selection rule $\Delta I = 2$, yes!, suggesting that the ground state of Sb^{125} is $g_{7/2}$. Since the 2.4-Mev spectrum of Sn^{125} is of the form[3] $\Delta I = 2$, yes!, an orbital of $h_{11/2}$ is predicted for the ground state of Sn^{125}. For the inner spectrum of Sn^{125}, log ft is 7.2 ($\Delta I = 0$, !, yes!). No satisfactory orbital assignment appears to be available for the 1.67-Mev level in Sb^{125}, suggesting excitation of the nuclear core so that the single particle model breaks down, or that the harder beta-spectrum leads to a metastable level in Sb^{125} rather than to the ground state.

[4] J. W. Mihelich and R. D. Hill, Phys. Rev. 79, 781 (1950).

[5] *Nuclear Data*, National Bureau of Standards Supplement 2 to Circular 499 (1951).

Distribution List

Professional

Dr. W. F. G. Swann, Director, Bartol Research Foundation of the Franklin Institute, Swarthmore, Pennsylvania

Professor C. C. Lauritsen, Department of Physics
California Institute of Technology, Pasadena, California

Professor C. D. Anderson, Department of Physics
California Institute of Technology, Pasadena, California

Professor R. B. Brode, Department of Physics
University of California, Berkeley 4, California

Professor E. O. Lawrence, Radiation Laboratory
University of California, Berkeley 4, California

Professor J. R. Richardson, Department of Physics
University of California (Los Angeles) Los Angeles 24, California

Professor E. C. Creutz, Department of Physics
Carnegie Institute of Technology, Schenley Park, Pittsburgh 13, Pennsylvania

Dr. M. A. Tuve, Department of Terrestrial Magnetism
Carnegie Institute of Washington, Washington, D. C.

Dr. R. S. Shankland, Case Institute of Technology
Department of Physics, University Circle, Cleveland 6, Ohio

Professor S. K. Allison, Institute of Nuclear Studies
University of Chicago, Chicago, Illinois

Professor J. Rainwater, Columbia University,
Nevis Cyclotron Laboratories, P. O. Box 117,
Irvington-on-Hudson, New York

Professor R. R. Wilson, Laboratory of Nuclear Studies
Cornell University, Durham, North Carolina

Professor W. M. Nielsen, Department of Physics
Duke University, Durham, North Carolina

Dr. Guy Suits, Research Laboratory, General Electric Company
Schenectady, New York

Dr. Kolman Kay, Department of Physics,
George Washington University, Washington, D. C.

Professor E. P. Hincks, Department of Physics
Harvard University, Cambridge, Massachusetts

Director, Nuclear Laboratory, Harvard University,
Cambridge, Massachusetts

Professor F. W. Loomis, Department of Physics,
University of Illinois, Urbana, Illinois

Professor A. C. G. Mitchell, Department of Physics,
Indiana University, Bloomington, Indiana

Professor J. A. Van Allen, Department of Physics,
State University of Iowa, Iowa City, Iowa

Professor J. D. Stranathan, Department of Physics,
University of Kansas, Lawrence, Kansas

Professor J. M. Cork, Department of Physics,
University of Michigan, Ann Arbor, Michigan

Professor W. E. Hazen, Department of Physics,
University of Michigan, Ann Arbor, Michigan

Professor J. H. Williams, Department of Physics,
University of Minnesota, Minneapolis, Minnesota

Professor E. P. Ney, Department of Physics,
University of Minnesota, Minneapolis, Minnesota

Professor Truman S. Gray, Servo-Mechanisms Laboratory,
Massachusetts Institute of Technology,
Cambridge 39, Massachusetts

Professor J. R. Zacharias, Laboratory of Nuclear Science and
Engineering, Massachusetts Institute of Technology,
Cambridge 39, Massachusetts (2)

Professor S. A. Korff, Department of Physics,
New York University, University Heights, New York 53, New York

Professor B. Waldman, Nuclear Physics Laboratory,
University of Notre Dame, Notre Dame, Indiana

Professor J. N. Cooper, Department of Physics,
Ohio State University, Columbus 10, Ohio

Professor W. E. Stephens, Department of Physics,
University of Pennsylvania, Philadelphia 4, Pennsylvania

Professor A. J. Allen, Department of Physics,
University of Pittsburgh, Pittsburgh, Pennsylvania

Professor G. T. Reynolds, Department of Physics,
Princeton University, Princeton, New Jersey

Professor M. G. White, Department of Physics,
Princeton University, Princeton, New Jersey

Professor Laticia del Rosario, Department of Physics,
Gobierno De Puerto Rico, Universidad De Puerto Rico,
Rio Piedras, Puerto Rico

Professor K. Lark-Horovitz, Department of Physics,
Purdue University, Lafayette, Indiana

Professor T. W. Bonner, Department of Physics,
Rice Institute, Houston, Texas

Professor R. E. Marshak, Department of Physics,
University of Rochester, Rochester, New York

Professor Charles A. Whitmer, Chairman,
Department of Physics, Rutgers University,
New Brunswick, New Jersey

Professor E. L. Ginzton, Microwave Laboratory,
Stanford University, Palo Alto, California

Professor F. Bloch, Department of Physics,
Stanford University, Palo Alto, California

Professor J. D. Trimmer, Department of Physics,
University of Tennessee, Knoxville, Tennessee

Professor A. L. Hughes, Department of Physics,
Washington University, St. Louis, Missouri

Professor R. D. Sard, Department of Physics,
Washington University, St. Louis, Missouri

Professor J. H. Manley, Department of Physics,
University of Washington, Seattle 5, Washington

Dr. J. W. Coltman, Research Laboratories, Westinghouse
Electric Corporation, East Pittsburgh, Pennsylvania

Professor R. G. Herb, Department of Physics,
University of Wisconsin, Madison 6, Wisconsin

Professor W. W. Watson, Department of Physics,
Sloane Physics Laboratory, Yale University,
New Haven, Connecticut (2)

Governmental

Chief of Naval Research, Att: Nuclear Physics Branch
Department of the Navy, Washington 25, D. C. (2)

Director, Naval Research Laboratory
Att: Technical Information Officer, Washington 25, D. C. (6)

Commanding Officer, Office of Naval Research
Chicago Branch Office, 10th Floor, John Crerar Library Bldg.,
86 East Randolph Street, Chicago 1, Illinois

Commanding Officer, Office of Naval Research
San Francisco Branch Office, 1000 Geary Street,
San Francisco, California

Commanding Officer, Office of Naval Research
New York Branch Office, 346 Broadway,
New York 13, N. Y.

Commanding Officer, Office of Naval Research
Pasadena Branch Office, 1030 East Green Street,
Pasadena 1, California

Commanding Officer, Office of Naval Research,
Navy No. 100, Fleet Post Office, New York, New York

Office of Technical Services,
Department of Commerce, Washington 25, D. C.

Superintendent, Nucleonics Division, Naval Research Laboratory
Anacostia, Washington, D. C.

Chief of the Bureau of Ships, Att: Code 390,
Department of the Navy, Washington 25, D. C.

Chief of the Bureau of Ships, Att: Code 330
Department of the Navy, Washington 25, D. C.

Chief of the Bureau of Ordnance, Att: Rem
Department of the Navy, Washington 25, D. C.

Chief of the Bureau of Ordnance, Att: Re9a
Department of the Navy, Washington 25, D. C.

Chief of the Bureau of Aeronautics, Att: RS-5
Department of the Navy, Washington 25, D. C.

Chief of the Bureau of Aeronautics, Att: Technical Library
Department of the Navy, Washington 25, D. C.

Commanding Officer, Naval Radiological Defense Laboratory
San Francisco Naval Shipyard, San Francisco 24, California

Armed Services Technical Information Agency
Documents Service Center, Knott Building,
Dayton 2, Ohio (5)

Chief of Naval Operations, Att: Op 36.
Navy Department, Washington 25, D. C.

Commander, U. S. Naval Ordnance Test Station
Technical Library, Inyokern, China Lake, California

Commanding General, Air Force Cambridge Research Center
Att: Geophysics Research Library, 230 Albany Street,
Cambridge 39, Massachusetts

Senior Scientific Advisor,
Office of the Under Secretary of the Army
Department of the Army, Washington 25, D. C.

Director, Research and Development Division
General Staff, Department of the Army, Washington 25, D. C.

Chief, Physics Branch, U. S. Atomic Energy Commission,
1901 Constitution Avenue, N. W., Washington 25, D. C.

U. S. Atomic Energy Commission, Att: Roland Anderson
Patent Branch, 1901 Constitution Avenue, N. W.,
Washington 25, D. C.

U. S. Atomic Energy Commission, Library Branch
Technical Information Division, ORE
P. O. Box E, Oak Ridge, Tennessee

Oak Ridge National Laboratory, Att: Central Files
P. O. Box P, Oak Ridge, Tennessee

Oak Ridge National Laboratory, Att: Head, Physics Division
P. O. Box P, Oak Ridge, Tennessee

Brookhaven National Laboratory, Att: Dr. S. C. Stanford
Research Library, Upton, L. I., New York

Argonne National Laboratory, Att: Hoylande D. Young,
P. O. Box 5207, Chicago 80, Illinois

Document Custodian, Los Alamos Scientific Laboratory
P. O. Box 1663, Los Alamos, New Mexico

Technical Information Group, General Electric Company
P. O. Box 100, Richland, Washington

Carbide and Carbon Chemical Div. (K-25 Plant)
Plant Records Department, Central Files (K-25)
P. O. Box P, Oak Ridge, Tennessee

Carbide and Carbon Chemical Div. (Y-12 Plant)
Central Reports & Information (Y-12)
P. O. Box P, Oak Ridge, Tennessee

Ames Laboratory, Iowa State College,
P. O. Box 14A, Station A, Ames, Iowa

Knolls Atomic Power Laboratory, Att: Document Librarian
P. O. Box 1072, Schenectady, New York

Mound Laboratory, Att: Dr. M. M. Haring
U. S. Atomic Energy Commission
P. O. Box 32, Miamisburg, Ohio

Sandia Corporation, Sandia Base
Att: Mr. Dale N. Evans, Classified Document Division,
Albuquerque, New Mexico

U. S. Atomic Energy Commission
Att: Div. of Technical Information & Declassification Service,
New York Operations Office, P. O. Box 30,
Ansonia Station, New York 23, New York

National Bureau of Standards Library
Room 203, Northwest Building, Washington 25, D. C.

Mr. Leonard Eyges, Scientific Attache, American Embassy,
24 Rue Gabriel, Paris, France

Director, Office of Ordnance Research
2127 Myrtle Drive, Durham, North Carolina

Commanding General, Air Research and Development Command
Att: RDRRP, P. O. Box 1395, Baltimore 3, Maryland

Foreign

Doctor Cesar Lattes, Scientific Director
Brazilian Center of Physical Research,
Rio de Janeiro, Brasil